

LOW FLOW SIMULATION OF THE ILLINOIS RIVER USING
A CONCEPTUAL HYDROLOGIC MODEL

By

RONALD CREIGHTON MARTIN

Bachelor of Arts

Ohio State University

Columbus, Ohio

1964

Submitted to the Faculty of the Graduate College
of the Oklahoma State University
in partial fulfillment of the requirements
for the Degree of
MASTER OF SCIENCE
May, 1975

Thesis
1975
M382 l
cop. 2

SEP 12 1975

LOW FLOW SIMULATION OF THE ILLINOIS RIVER USING
A CONCEPTUAL HYDROLOGIC MODEL

Thesis Approved:

Richard M. Davies

Thesis Adviser

A. F. Gaudy

Don F. Kincannon

N. N. Durbin

Dean of the Graduate College

916385

ACKNOWLEDGEMENTS

I would like to express my sincere appreciation to Dr. Richard N. DeVries, my principal adviser, for his encouragement, interest, advice, instruction, professional approach, and friendship extended throughout my period of graduate study. I also wish to extend my sincere thanks to Dr. Don F. Kincannon and Dr. Anthony F. Gaudy, Jr. for their consideration and instruction throughout the year.

My wife, Linda, deserves extra special thanks for the understanding and encouragement she has given during my graduate studies, as well as for the numerous extra burdens she has had to bear while I have been in this program.

Mr. "Jack" Yates deserves special thanks for extending to me the hospitality of his office, the Tulsa River Forecast Center (RFC), and the use of its facilities.

Special thanks also to "Tony" Haffer of the Tulsa RFC for the considerable time and effort he has expended helping me with the computer work.

Special thanks also to David M. Morris for telling me about Oklahoma State University and the fine program available here.

TABLE OF CONTENTS

Chapter	Page
I. INTRODUCTION	1
II. LITERATURE REVIEW	3
Hydrologic Cycle	3
Interception	3
Infiltration	5
Depression Storage	8
Overland Flow	8
Current Streamflow Forecasting Models	8
Rainfall-Runoff - Unit Hydrograph Model	9
Empirical Low Flow Techniques	18
Recession Analysis	18
Stage or Discharge Relationships	20
Conceptual Hydrologic Models	20
Streamflow Synthesis and Reservoir Regulation (SSARR) Model	20
U. S. Department of Agriculture Hydrological Laboratory (USDAHL) Model	24
U. S. Geological Survey Watershed Model	28
Stanford Watershed Model IV (SWM IV)	29
Interception	32
Impervious Area	34
Infiltration	34
Overland Flow	36
Soil Moisture	38
Interflow	38
Groundwater	38
Evapotranspiration	41
Channel System	43
Snowmelt	45
National Weather Service River Forecast System (NWSRFS)	45
Differences From SWM IV	45
Mean Basin Precipitation (MBP)	51
Streamflow	59
Potential Evapotranspiration (PE)	60
Sacramento Model	62
Incident Surfaces	62
Upper Zone	64
Lower Zone	64
Evaporation and Evapotranspiration	66

Chapter	Page
Routing	68
Channel Storage	68
Model Accuracy	68
III. MODEL SELECTION AND BASIN DESCRIPTION	69
Model Selection	69
Basin Description	69
Illinois River near Watts, Oklahoma	70
Illinois River near Tahlequah, Oklahoma	72
IV. RESULTS AND DISCUSSION	73
Calibration of the NWSRFS	73
Raw Data	75
MBP Computation Procedure	76
Station Weight Computation	76
MBP Computation for Each Basin	78
Potential Evapotranspiration (PE) Computation	80
Streamflow Computation	80
Combined Data Tape	82
Channel Time Delay Histogram	82
Selection of Initial Parameter and Soil Moisture Values and the Effect of Changes Leading to the Final Values	84
Parameter A	84
CB	87
CC	88
EHIGH	88
ELOW	88
EPXM	90
GAGEPE	92
GWSI	93
KGS	93
KS1	93
KV	94
K1	94
K24EL	94
K24L	95
K3	95
LIRC6	96
LKK6	96
LZSI	97
LZSN	97
NEP	98
NDUR	98
POWER	98
RESI	98
SCEPI	99
SGWI	99

Chapter	Page
SRC1	99
SRGX1	99
STHIGH	99
STLOW	100
UZSI	100
UZSN	100
LAG	101
Discussion of the Calibration	103
V. CONCLUSIONS	108
VI. SUGGESTIONS FOR FUTURE STUDY	109
A SELECTED BIBLIOGRAPHY	110
APPENDIX	112

LIST OF TABLES

Table	Page
I. Normalized Weights for Each Grid Point	54
II. Grid Point Weights for the Various Stations . . .	55
III. Grid Point Weights Used to Compute Thiessen Weights	55
IV. MBP Area Assignments and Histograms for Watts and Tahlequah	80
V. Initial and Final Parameter Values	85
VI. Typical Initial Parameter Values and Ranges . . .	86
VII. Initial CB Values	87
VIII. Initial ELOW Values	90
IX. Initial EPXM Values	91
X. Example of Change in Layer Bias Due to Increase in EPXM	91
XI. Example of Change in Monthly Bias Due to Increase in EPXM	92
XII. Initial KGS Values	93
XIII. Initial K3 Values	95
XIV. Initial LZSI Values	97
XV. Model Fit by Flow Intervals for Tahlequah - Water Years 1964-1971	103
XVI. Model Fit by Flow Interval for Watts - Water Years 1964-1971	104

LIST OF FIGURES

Figure	Page
1. Simplified Hydrologic Cycle	4
2. Rainfall Distribution	7
3. Rainfall-Runoff Relation	10
4. Rainfall Runoff Relation Using Soil Moisture Conditions as a Parameter	12
5. Computation and Plotting of the Antecedent Precipita- tion Index	13
6. Operational Rainfall-Runoff Relation	17
7. Hydrograph Components	19
8. Stage-Stage Relation	21
9. Storage/Flow Relation for Simple Recession	25
10. Land Phase of the USDAHL Conceptual Hydrologic Model	26
11. Soil Moisture Flow Chart for the USDAHL Model	27
12. Stanford Watershed Model IV	33
13. Infiltration Division	35
14. Soil Moisture Ratio (LZS/LZSN) versus Percent of Infiltration Entering Groundwater	40
15. Simplified Model of Outflow From Groundwater Storage	42
16. Channel Time-delay Histogram for the Illinois River near Watts, Oklahoma	44
17. Flowchart of Soil Moisture Accounting Portion of the National Weather Service River Forecasting System	48
18. b versus LZS/LZSN for Various Values of POWER for CB = 0.1	49

Figure	Page
19. A Grid Superimposed on a Basin	52
20. The Four Quadrants Surrounding Precipitation Station A	57
21. A Simplified Flow Chart of the Land Phase of the Sacramento Model	63
22. Overall View of the Sacramento Model	65
23. Recession Plot for the Sacramento Model	67
24. Illinois River Basin	71
25. Grid Placement for Basin Gridding	77
26. Grid Placement for Precipitation Station Coordinates	79
27. MBP Zones	81
28. Evapotranspiration Curve	89

CHAPTER I

INTRODUCTION

As man continues to expand his level of activity in the flood plains of his rivers and streams, the potential for damage both to the works of man and to the stream itself continues to increase. Man realized early in his history the benefits of settling near a river, and soon thereafter learned of the disadvantages (floods, etc.). Not wanting to be deprived of these benefits, man soon began to build levees to protect himself and his property from floods. Today, flood protection measures may be generally classified in one of two ways: flood protection structures (such as levees and dams) or flood forecasting. These help protect man from the river, but they don't protect the river from man. To protect the rivers, Congress has enacted laws; governmental agencies have been established and standards have been set. A goal has been set for our country (1,p.1) "...it is the national goal that the discharge of pollutants into the navigable waters be eliminated by 1985..." but that is the future.

As desirable as zero pollutant discharge may be, a realistic appraisal shows that this country is a long way from meeting such a standard. For at least the reasonably near future, the natural assimilative capacities of our bodies of water will continue to be utilized for further degradation of the wastes from man's activities.

Perhaps the most important characteristic of a river that

determines its assimilative capacity is the volume of flow in the river. In evaluating the assimilative capacity of a stream, statistically-derived low-flow analyses such as the 7-day, 10-year return period, low flow are used. Such analyses give an indication of what the low flow has been, but these historical methods suffer from the limitation of describing only what has happened at some time in the past; they ignore the fact that new weather and streamflow record values are frequently set and that the minimum flows on record are probably higher than will occur in the future. They are also inadequate for describing what will actually occur tomorrow, next week, or next month. To evaluate the effect of new developments properly, changes in the watershed or climatic regime, or the daily effect of old pollutant sources, it is necessary to be able to forecast the low flows that will actually occur.

The purpose of this report is to describe the use of a conceptual hydrologic model to simulate the streamflow in a natural basin (with emphasis on the low flows).

CHAPTER II

LITERATURE REVIEW

Hydrologic Cycle

All true forecasting techniques attempt to predict the water level or flow at some desired point by simulating, however grossly, all or a portion of the hydrologic cycle. Therefore, it is appropriate to review the hydrologic cycle briefly (Figure 1) prior to discussing different forecasting methods.

Interception

Before reaching the ground, precipitation may either evaporate or be intercepted by vegetation or other objects such as rocks or buildings and held in interception storage. Once in interception storage, the precipitation either remains there until it evaporates or it is blown to the ground by wind or displaced by subsequent precipitation. Interception does not completely stop once the storage becomes full, but continues at a reduced rate throughout the storm due to evaporation. Generally, as the wind speed increases, storage decreases and evaporation increases. Although the amount of interception storage varies seasonally (with the type and density of vegetation), it is fixed at any given time. The reduction of runoff due to interception storage is more significant (and apparent) for small storms and for the very beginning of larger storms.

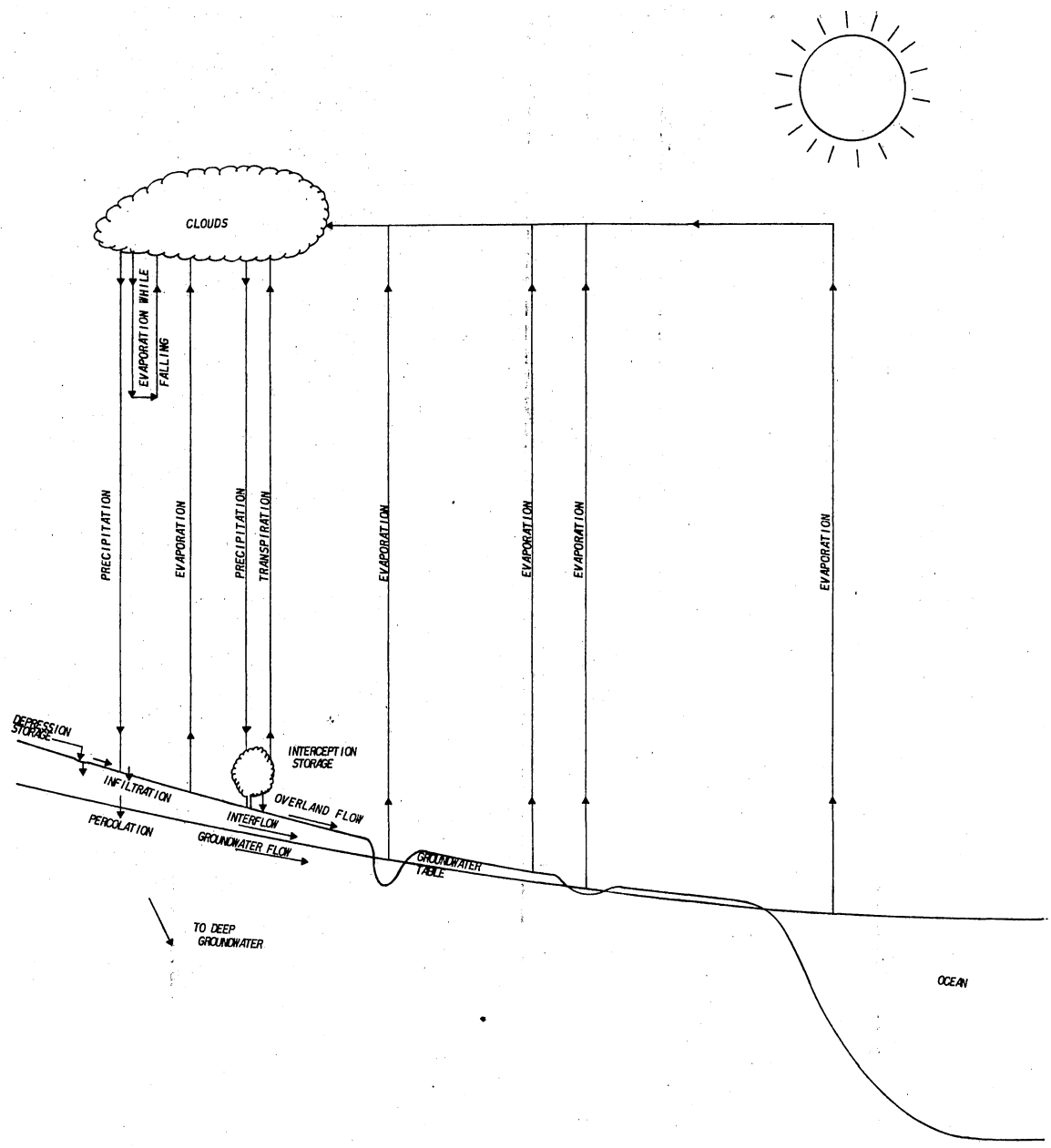


Figure 1. Simplified Hydrologic Cycle

than for the whole of a large storm, because the interception storage capacity decreases in significance as the total amount of precipitation increases. Since interception storage represents a large percentage of the numerous small storms throughout a year, it may represent a significant amount of the annual precipitation for a basin. In a well developed forest or other dense cover, interception can easily be 25 percent of the annual precipitation (2).

The water that actually reaches the ground may infiltrate into the soil, be held on the surface as depression storage; it may travel to a channel as overland flow and become surface runoff; or it may evaporate.

Infiltration

Infiltration occurs when water passes through the soil surface and into the soil itself, while the movement of water within the soil itself is called percolation. Percolation moves the water away from the soil-air interface and permits infiltration to continue. Infiltration is the result of two processes:

1) movement of water under gravitational force into the soil through large openings or channels, and

2) capillary action

Most of the water infiltrates through the gravity channels and then spreads out within the soil by capillary action, although capillary action causes some water to infiltrate over the entire wetted soil surface.

The maximum infiltration rate is called the infiltration capacity. Although it is limited primarily by the soil permeability, the porosity of the soil, and the amount of large gravity channels, it also varies

with the soil moisture, rainfall rate, soil type, vegetation, and season. The infiltration capacity varies considerably over the typical watershed. This can be illustrated by a plot of the cumulative frequency distribution of the infiltration capacity of the basin (Figure 2). This is the curve that would result from the plotting of a large number of simultaneous infiltrometer measurements. Such a curve is valid only at a given point in time, or for a short time interval, because the infiltration capacity changes with time. It is interesting to note that Neal (4) has found that the most significant factor affecting the infiltration capacity during the first twenty minutes of rainfall is the initial soil moisture (infiltration capacity varies inversely with the soil moisture). However, some types of soil may even repel water until they are thoroughly wet. Very large drops tend to pack the soil surface and reduce the initial infiltration rate, until the soil surface is covered with a sheet of water. In general, the infiltration rate varies directly with the rainfall rate until the two rates are equal, although the infiltration rate tends also to decrease as a storm progresses due to the increase in soil moisture. At rainfall rates above the infiltration capacity, the infiltration rate does not increase.

After infiltration, the water may remain in storage near the surface where it will stay until it is returned to the atmosphere by evapotranspiration; it may move laterally through the upper layers of soil to a channel as interflow; it may move downward to the water table, become part of the active groundwater flow and flow to a channel, or it may penetrate farther and become part of deep (inactive) groundwater storage.

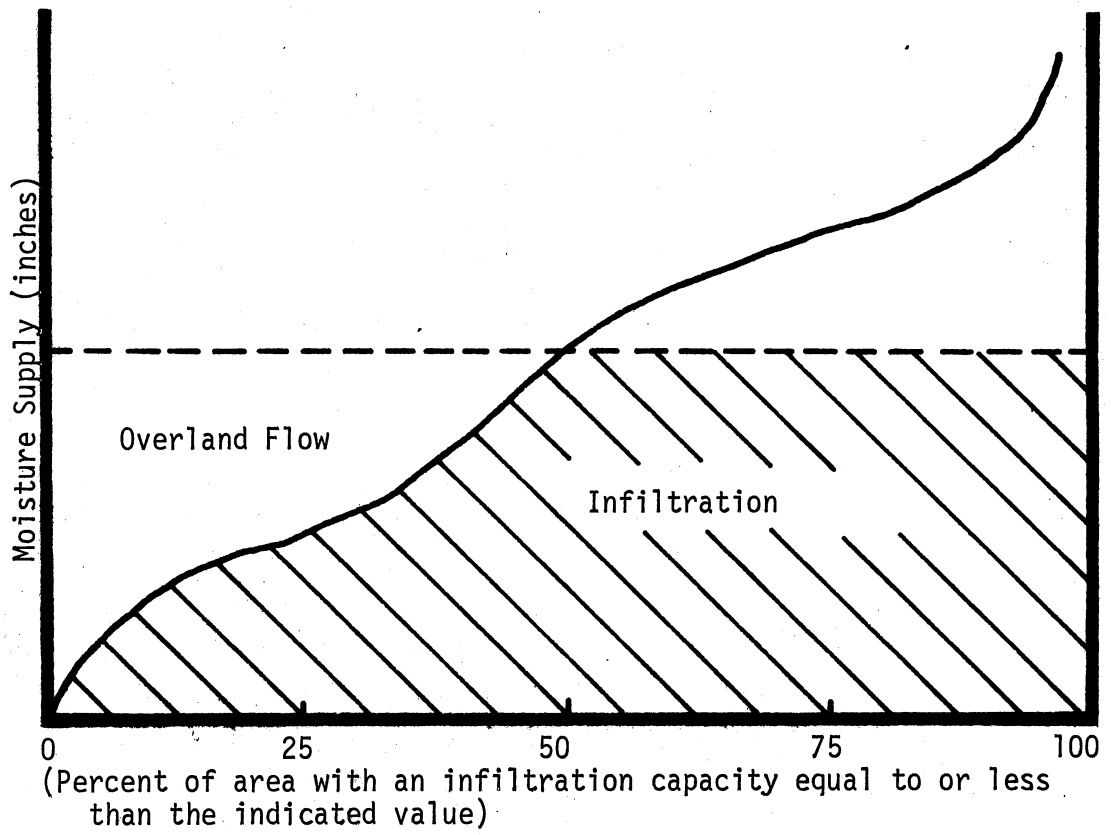


Figure 2. Rainfall Distribution

Source: (17) p. 12

Depression Storage

Depression storage occurs in closed drainages which may vary in size from soil particles to ponds covering several acres. When the rainfall rate exceeds the infiltration capacity, depression storage accumulates the excess rainfall. As the smaller depressions become full, overland flow begins to occur and either flows into larger depressions or to a channel. Evaporation and infiltration continue during each phase. As with interception storage, depression storage affects small storms and the initial portions of larger storms mainly, although the total depression storage capacity is much greater than the total interception storage capacity. The primary factors affecting depression storage are soil surface roughness, topography of the basin, and man's alterations to the basin. The storage capacity of depressions within a basin varies inversely with the surface slope.

Overland Flow

Soon after the rainfall rate exceeds the infiltration capacity, a thin sheet of water builds over the soil surface and forms a temporary storage called surface detention. Overland flow is the movement of water in surface detention. The portion of overland flow that is not lost to evaporation or infiltration will flow into a channel.

Current Streamflow Forecasting Methods

Even today, many river forecasts are made using a combination of strictly empirical relationships, an "artistic" swag of a pencil, a few educated guesses, a good imagination, a little knowledge and,

at times, a generous amount of luck. This is a result of a lack of technology, a lack of money, and insufficient desire to change. The lack of technology has been overcome.

Forecasting techniques consist of two components:

- 1) a method of computing the runoff from the local area, and
- 2) a method of routing flow through the reaches.

If the area of forecasting is to be regarded as a professional field with roots in scientific soil, it is apparent that it will have to forsake the strictly empirical approach and fully embrace techniques that at least attempt to duplicate or simulate each of the physical processes in the hydrologic cycle. Although the knowledge was adequate to model portions of the cycle for a basin, the computational load to do this for a whole basin would have been an overwhelming task prior to the advent of large digital computers. Thus, techniques were developed that grossly reproduced portions of the hydrologic cycle. The rainfall-runoff relationship used with a unit hydrograph illustrates this approach quite well.

Rainfall-Runoff - Unit Hydrograph Model

This type of model varies from a simple plot of rainfall versus runoff to rather complicated multi-variable procedures. They may be derived by mathematical regression analysis and involve the solving of equations, or they may involve graphical coaxial correlation techniques such as have been used successfully by the National Weather Service for flood forecasting throughout the county (2)(3). A simple rainfall versus runoff plot will yield adequate results on an annual basis, but for daily computations it is completely inadequate (Figure 3). However,

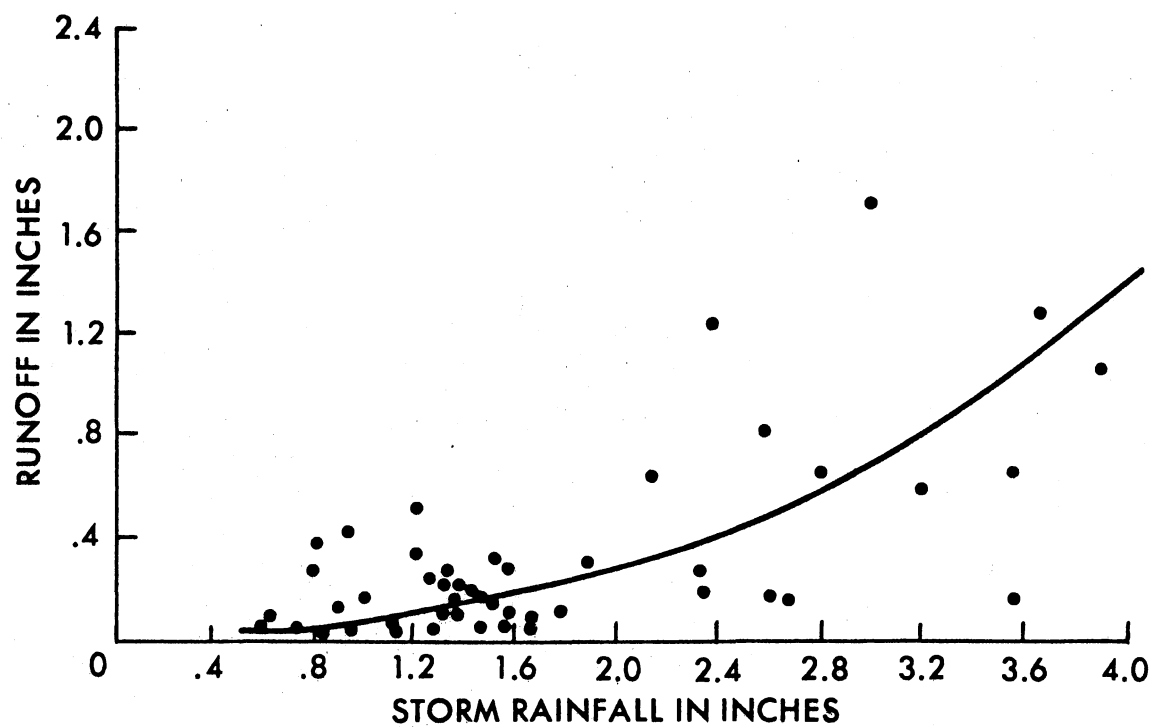


Figure 3. Rainfall-Runoff Relation

Source: (8), p. 41

reasonably good results have been obtained by use of more involved coaxial relationships that include an index to the precipitation that has fallen in the recent past (Antecedent Precipitation Index or API), time of year, storm duration, and the amount of precipitation that fell during the storm (mean basin precipitation in inches). Such a technique yields the direct storm runoff in inches, which can be converted to a hydrograph by use of a unit hydrograph.

One of the earlier attempts to improve the accuracy of the rainfall-runoff relationship involved the inclusion of a qualitative evaluation of the current soil moisture conditions (Figure 4). Even though this is an improvement, it places too great a burden on the judgement of the individual forecaster. To make the scheme more objective, variables such as the number of days since the last rainfall were introduced, but this did not account for the rainfall intensity. Gradually, these ideas led to adoption of a somewhat more sophisticated system for indexing the soil moisture conditions. It included the time since the last rainfall as well as the amount of the storm rainfall. This is known as the Antecedent Precipitation Index (API), and can be expressed by the following equation

$$API = C_1 P_1 + C_2 P_2 + C_3 P_3 \dots + C_n P_n$$

where C_n is a constant and P_n is the precipitation that fell n days before day 0. However, for routine daily forecasting, this was rather cumbersome to use, so it was assumed that C decreased logarithmically, and the equation was transformed to

$$API_t = (API_0)k^t$$

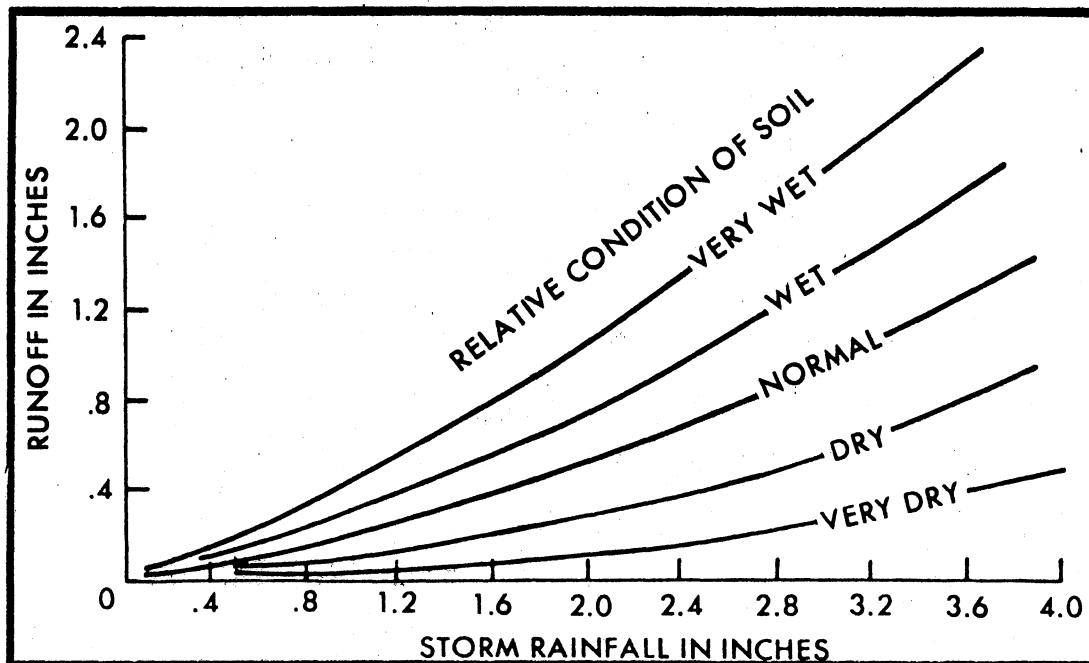


Figure 4. Rainfall-Runoff Relation Using Soil Moisture Conditions as a Parameter

Source: (8), p. 41

where t is the number of days since day 0, and k is a recession factor. In actual use, the API was computed daily, thus t was equal to 1. Therefore, the form of the equation becomes

$$API_1 = k(API_0)$$

Thus, the API for today equals the API for yesterday, multiplied by k (which is normally assumed to be 0.90, but may vary from 0.85 to 0.95). If any precipitation fell during the past twenty-four hours, it is then added to the API value just computed, and this becomes the API for today (Figure 5). This is given by the following form of the equation

$$API_1 = k(API_0) + P$$

where P is the precipitation during the past twenty-four hours. Since k is assumed to equal 0.90 unless there is unmistakable evidence to the contrary, the form of the equation normally used is

$$API_1 = API_0 - 0.1(API_0) + P$$

which is a very simple calculation. When starting to compute the API, satisfactory values may be obtained by initializing the API at 1.0 inch about two months prior to the storm under consideration, and then working forward.

Obviously, most of the weight is given to precipitation which occurred most recently, with little weight given that which occurred more than thirty days ago. Due to its ease of calculations, objectivity, and fairly good results, it has been a rather popular and widely used index.

The recession coefficient, k , used in the API computation,

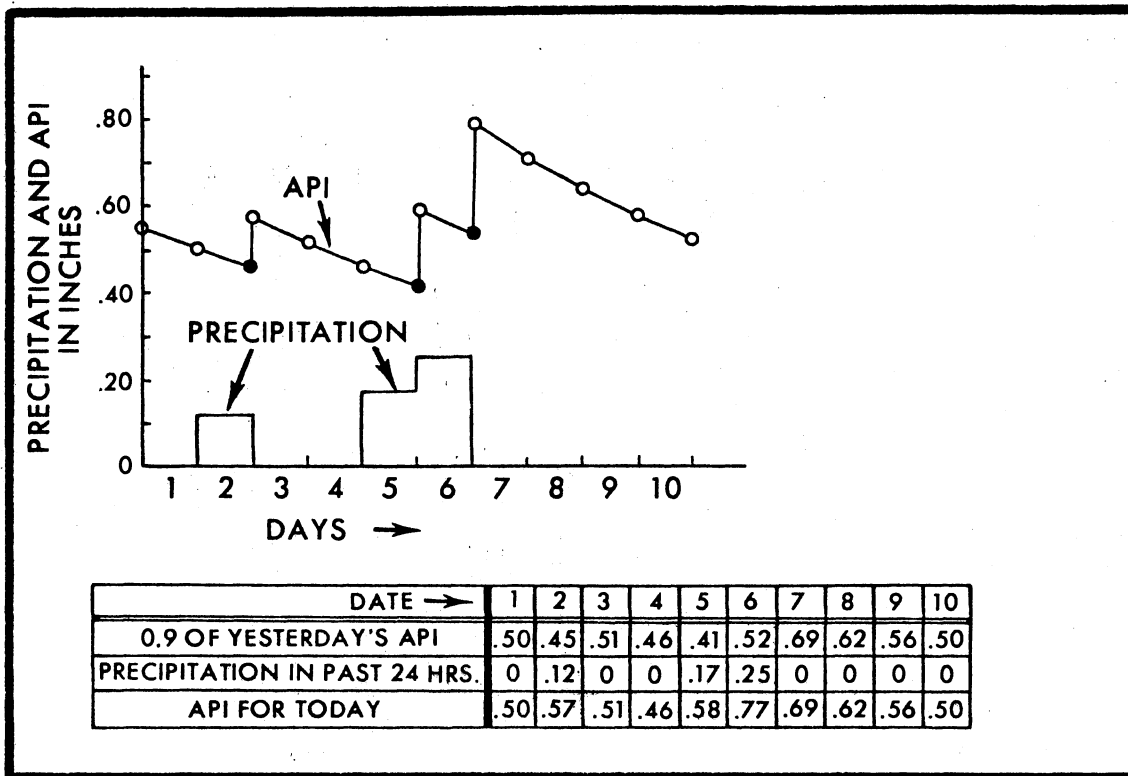


Figure 5. Computation and Plotting of the Antecedent Precipitation Index

Source: (8), p. 45

represents the loss of soil moisture from a basin, and thus is a function of the physiological, climatological, and vegetative characteristics of the basin. Since k has to account for basin characteristics that vary seasonally, it was necessary to introduce a seasonal correction factor in the form of the week of the year. Although this assumes that climatic conditions are the same each year (which is certainly not true), it is a valid enough assumption for practical use.

Thus far there is rainfall, API, and time of year to use in deriving a correlation with runoff. One additional variable normally used in the correlation is the storm duration, which is important because the losses in a short storm are less, and thus more direct and surface runoff result. Determining the storm duration for a short, distinct storm is not too difficult, but it can become quite complicated for long, drawn-out storms. Richards (8) suggested:

One approach, when six-hourly precipitation amounts are available currently, is to take the sum of all six-hourly periods with 0.20 inch or more precipitation plus half the sum of intervening periods with less than 0.20 inches. This approach assumes that when 0.20 inch or more occurs in six hours, the effective duration is six hours; when less than 0.20 inch occurs, the effective duration is three hours (p. 14).

The principal data requiring manipulation is the precipitation data. Some type of mean basin precipitation (MBP) must be determined. Various methods are available such as the arithmetic mean, Thiessen polygons, grid-weighting, or the isohyetal method. Although the isohyetal method is the most accurate method, it requires the knowledge and subjectivity of a skilled analyst, and thus does not meet the criterion of objectivity. The choice would then be between the Thiessen polygons or the grid-weighting method, both of which can be accurate as well as objective. A description of these methods and their use can be found

in references (2), (3), (8), and (9).

Since this model forecasts only direct runoff (not groundwater flow), it is necessary to separate the storm hydrograph into direct runoff and groundwater flow for the correlation analysis. Linsley (2) (3) describes several methods of hydrograph separation, but the most important thing is to select one technique and stay with it during development and use of the model.

Having the five variables, it now remains to develop a correlation among these variables. Various numerical methods of correlation analysis are available as part of most computer libraries and these take the pain out of the procedure. However, the older method of correlation is the coaxial graphical correlation analysis (2)(3)(8). The complexity of this can be seen in Figure 6. Suffice it to say that the graphical method works, but it is a rather tedious process whose accuracy depends largely on the experience, knowledge, and artistic skill of the analyst (8).

To use the graphical method, after it has been developed, enter with the API, move left to the proper week of the year curve then down to the proper storm duration, then right to the storm precipitation, and then up to the storm runoff. After the direct runoff for the storm has thus been determined, it can be distributed in time by use of the appropriate unit hydrograph, which is the hydrograph of one inch of direct runoff from a storm of specified duration for a specified basin area. Unit hydrograph theory and derivation are adequately explained in standard references (2)(3). The groundwater flow is then added to the direct runoff; the total runoff thus determined being the forecast for either a headwater basin or for the local area of a reach. This

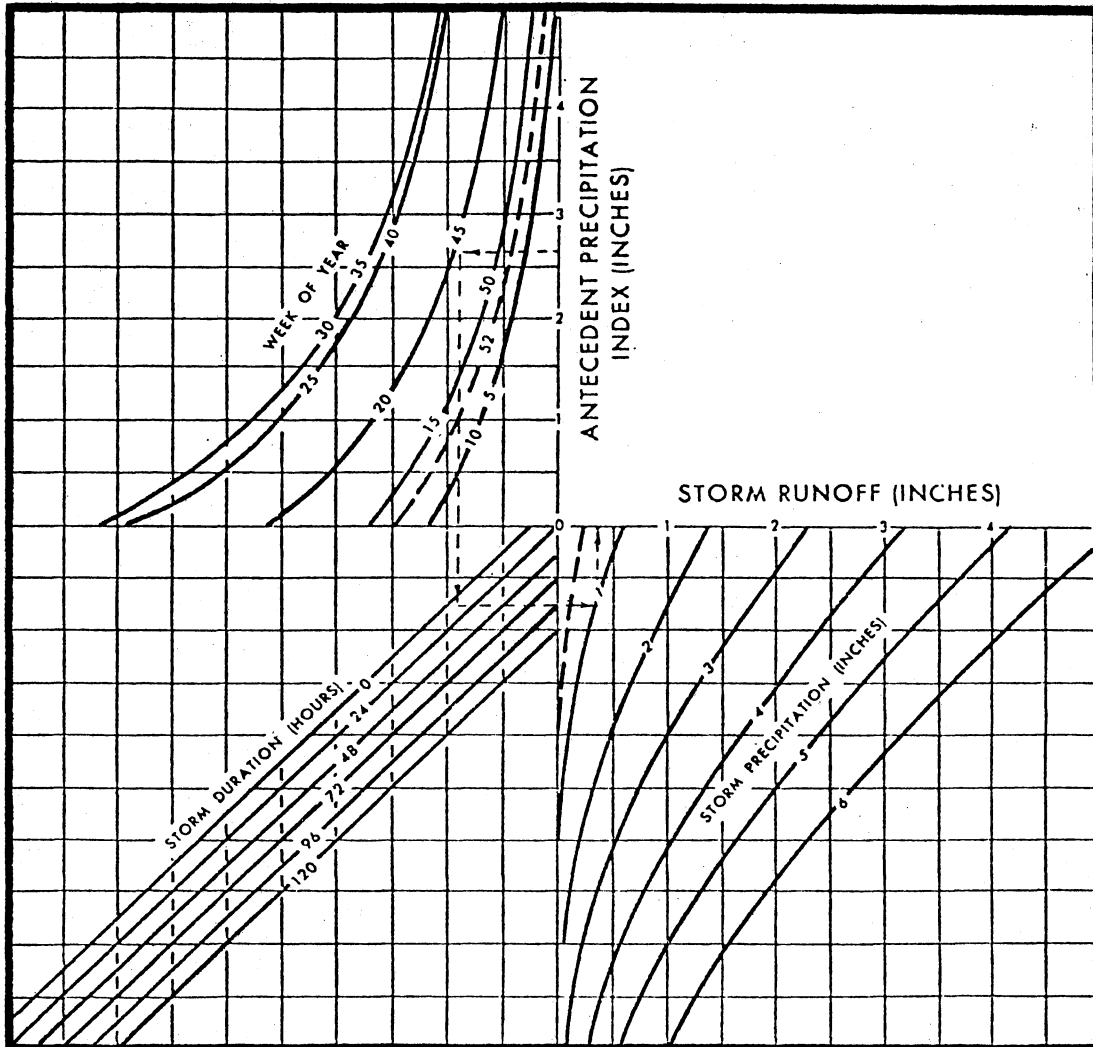


Figure 6. Operational Rainfall-Runoff Relation

Source: (8), p. 47

flow can then be routed downstream using a routing technique such as variable K & L (K is a reach storage coefficient, L is lag), or one of the other routing methods commonly used.

The API technique has served well in the past, but it suffers from the fact it is really only a correlation of results, not a duplication or even an approximation of the physical processes actually occurring in the basin. It is only an index to these processes. It should be remembered, however, that this technique was developed when forecasters did not have large digital computers at their disposal as is the case today.

Empirical Low Flow Techniques

Recession Analysis

This method may be used when a stream is falling and on the recession limb of its hydrograph (Figure 7). This is the only method being discussed that cannot be used for forecasting the entire hydrograph. The preparatory step for this method is to analyze past observed recession curves, and from that data develop either a graphical or mathematical expression (usually some form of exponential function) that describes the recession curves for the basin. If no significant precipitation has fallen and the stream is in recession, the operational step consists of entering the derived curve or expression with the current discharge and extrapolating the recession from the current observation over the desired time period using the curve or expression. If significant precipitation has fallen or the stream is not in recession, this method cannot be used. If the recession curve does not vary much from

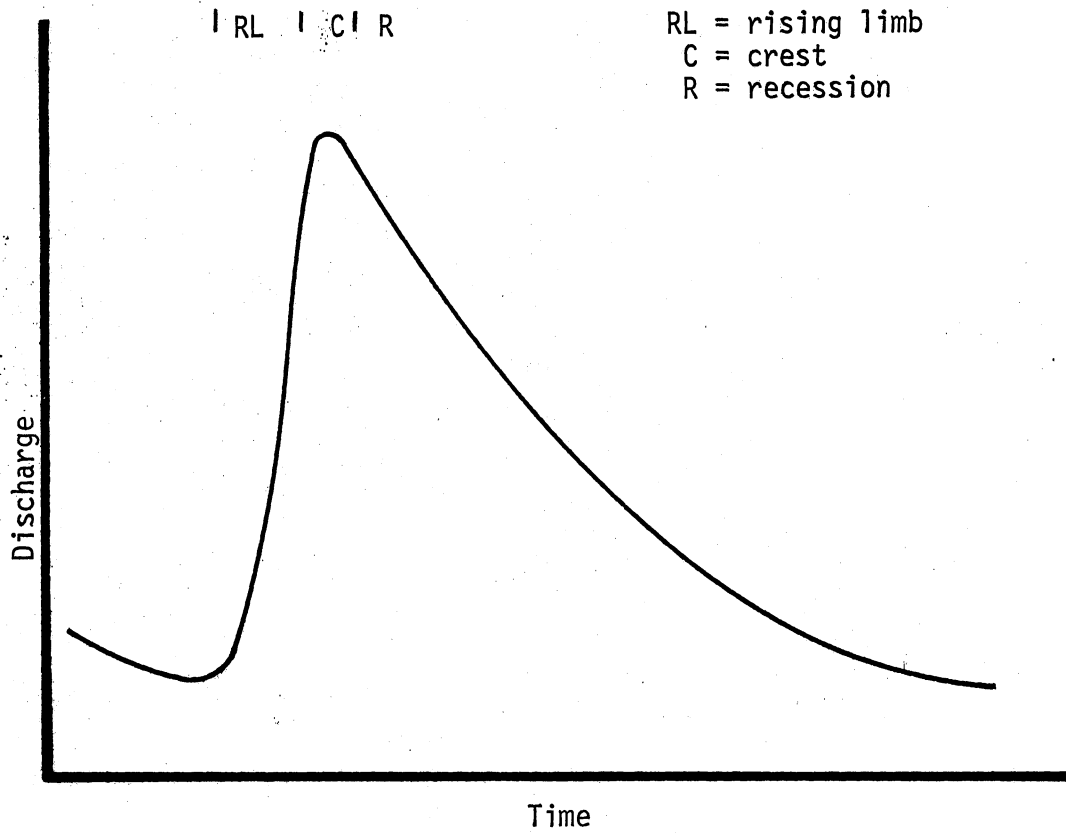


Figure 7. Hydrograph Components

season to season, this method can give an accurate forecast.

It would seem that this method's principal use is as a quick interim method to use while developing a more sophisticated method, or if the value of the forecast does not warrant a better method.

Stage or Discharge Relationships

One of the oldest methods of forecasting is by use of a stage-versus-stage relationship. This is simply a historical relationship of the stage of an upstream station versus the stage at a downstream station at a later time (Figure 8). When done carefully, this can be a useful and reasonably accurate technique for a short range forecast. It is especially useful on large rivers which do not fluctuate rapidly and where the local runoff is negligible in comparison to the flow in the river (such as the Mississippi River), and for streams that are not rated but on which stage measurements are taken regularly. Difficulties may occur with this method as a result of not considering precipitation, differences in storage for rising and falling stages, and unstable channel bottoms, but used with care and understanding, it can be a very useful technique.

Conceptual Hydrologic Models

Streamflow Synthesis and Reservoir Regulation

(SSARR) Model

The original version of the SSARR model was a streamflow synthesis model developed in 1957. Its primary purposes were to simulate snow-melt runoff and provide high flow forecasting capabilities for the

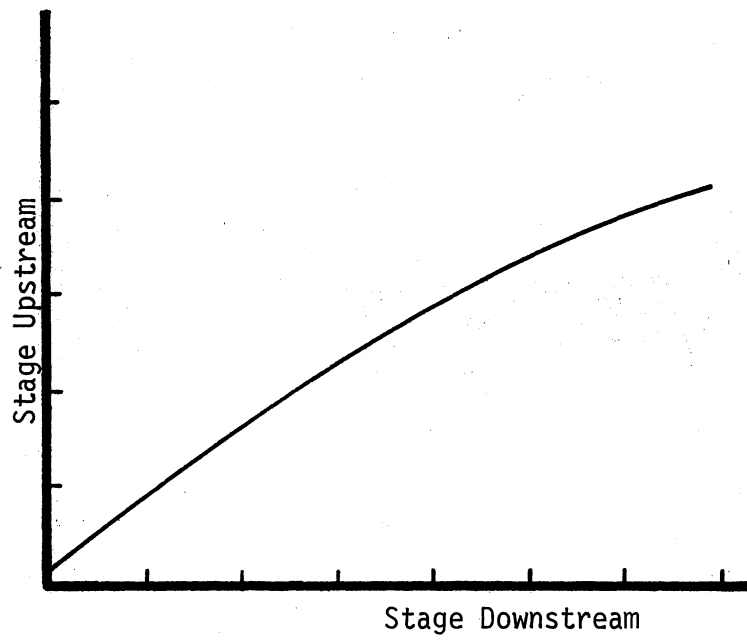


Figure 8. Stage-Stage Relation

Columbia River Basin. By 1960, it had grown into a general streamflow synthesis model, and by 1968, it had evolved into a full hydrologic synthesis and reservoir regulation model.

This model is able to simulate the responses of land surfaces, reservoirs, and streams to both rain and snowfall. It uses multi-variable relationships in the form of tables to represent physical relationships. The storage effects are synthesized by use of multi-phase lake routing. Channel backwater effects are simulated by use of a three-variable table that relates discharge to two water surface elevations along a stream channel. It can also simulate irrigation diversions and return flow as well as local area inflows. A brief overview of the model's function follows.

After the mean basin precipitation (MBP) is calculated, it is used to compute the total runoff by use of a rainfall-runoff relation that gives percent runoff as a function of a soil moisture index (SMI). This relation allows part of the incident precipitation to go to runoff, while the rest goes into soil moisture storage, which is depleted only through evapotranspiration. Computation of the SMI is illustrative of the simplicity of the land phase of this model

$$SMI_2 = SMI_1 + (\text{RAINFALL-RUNOFF}) - K(\text{ET})$$

where K is a constant, and ET = evapotranspiration (monthly average). The SMI is calculated on a time period which is variable from 0.1 to 24 hours. The total runoff is then divided according to set rules among baseflow, subsurface flow, and surface flow for temporal distribution. Each component is routed individually through a series of linear reservoirs and then combined to give the total basin discharge.

Snowmelt is accounted for as a function of temperature and the heat content of the precipitation. Temperature varies by elevation layers according to a set temperature lapse rate.

One feature of the SSARR model that is not found on the other models is a self-adjusting feature. Since the average reporting network does not always provide adequate data to properly define the actual precipitation distribution, differences between the observed and simulated flows do occur. As this difference may cascade downstream, the simulation can sometimes attain bad values through no deficiency of the model itself. The model assumes that this difference is due either to

- 1) the amount of precipitation being wrong, or
- 2) the time of the precipitation being wrong.

Prior to the forecast time, the model computes a period of antecedent conditions, if the discharge computed at the end of this period (that is, the beginning of the forecast period) does not match the observed flow with specified limits, the model adjusts the moisture input and recomputes the antecedent condition. The model continues to iterate this adjustment-recomputation procedure until the values are within set limits. Manual adjustment is also possible if the automatic adjustment is inadequate.

Calibration of the model is accomplished through trial and error adjustment of parameters representing soil moisture, evapotranspiration, depression storage, surface storage, subsurface storage, groundwater storage, infiltration to each of the aquifer zones, time delay (represented by storage and flow relationships in each zone), and channel storage effects. A total of fourteen input parameters is required.

The SSARR model has been applied mainly to relative large basins

with a reasonable degree of success. Its usefulness for small basins and low flows is not known.

U. S. Department of Agriculture Hydrological
Laboratory (USDAHL) Model

The USDAHL model was developed using data from a 2.37 square mile experimental watershed at Coshocton, Ohio. Simulations were originally made on a single storm basis and later expanded to synthesize a period of continuous record.

The baseflow analysis upon which this model is based was derived from the plotting of basin storage versus discharge (Figure 9). The curve could be approximated by five straight lines which then represented the five flow regimes of the system's land phase. The slope of each section is the storage coefficient (K) for each flow regime (K_1 = overland flow; K_c = channel storage; K_2 = quick-return flow (inter-flow); K_3 = delayed return flow; and K_4 = prolonged-return flow). Not all regimes need be present for a given storm.

The land phase of the model functions in the following general manner. Input precipitation either flows laterally as overland flow (OF), or is infiltrated into the soil's uppermost reservoir (Figures 10 and 11), from which it either flows as quick-return flow (QRF), or seeps downward into the next reservoir. It either flows out of this zone as delayed-return flow (DRF) or seeps downward into the saturated zone which is depleted by prolonged-return flow (PRF). The response of the OF and surface runoff is modified by division of the basin into three soil types based on elevation: upland, hillside, and bottomland. The flow is envisioned as flowing from upland to hillside to bottomland,

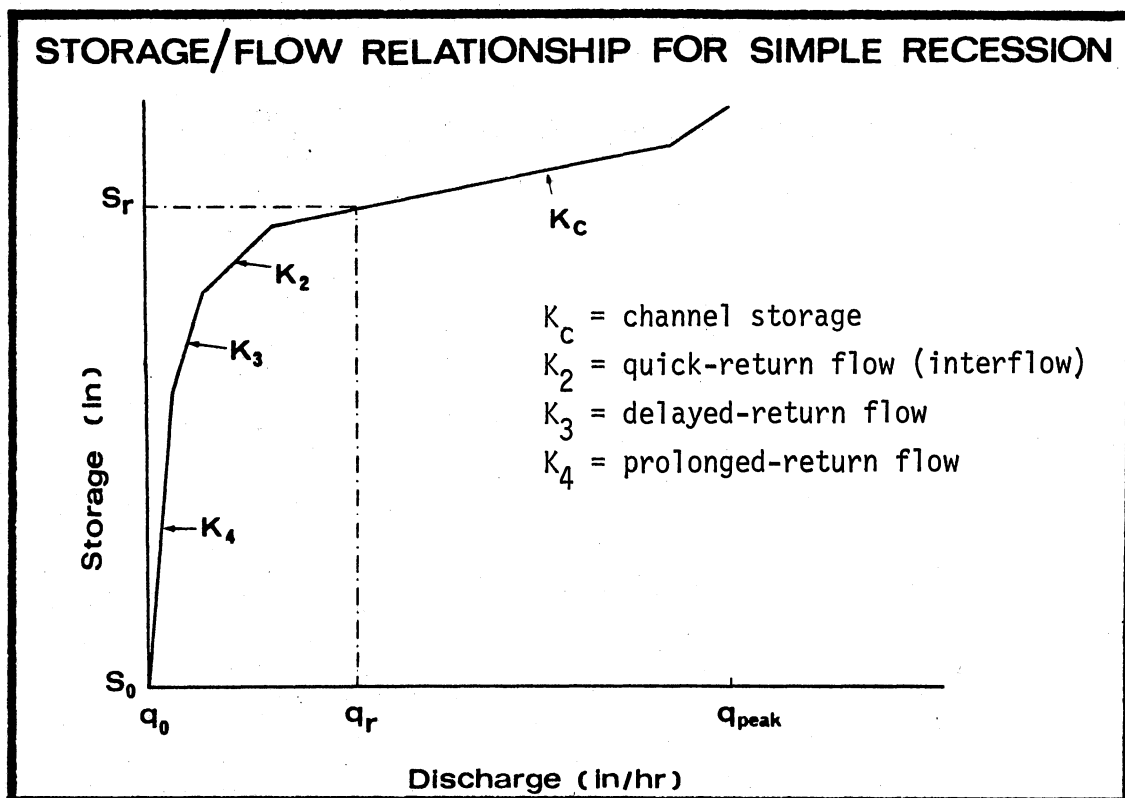


Figure 9. Storage/Flow Relation for Simple Recession

Source: (11)

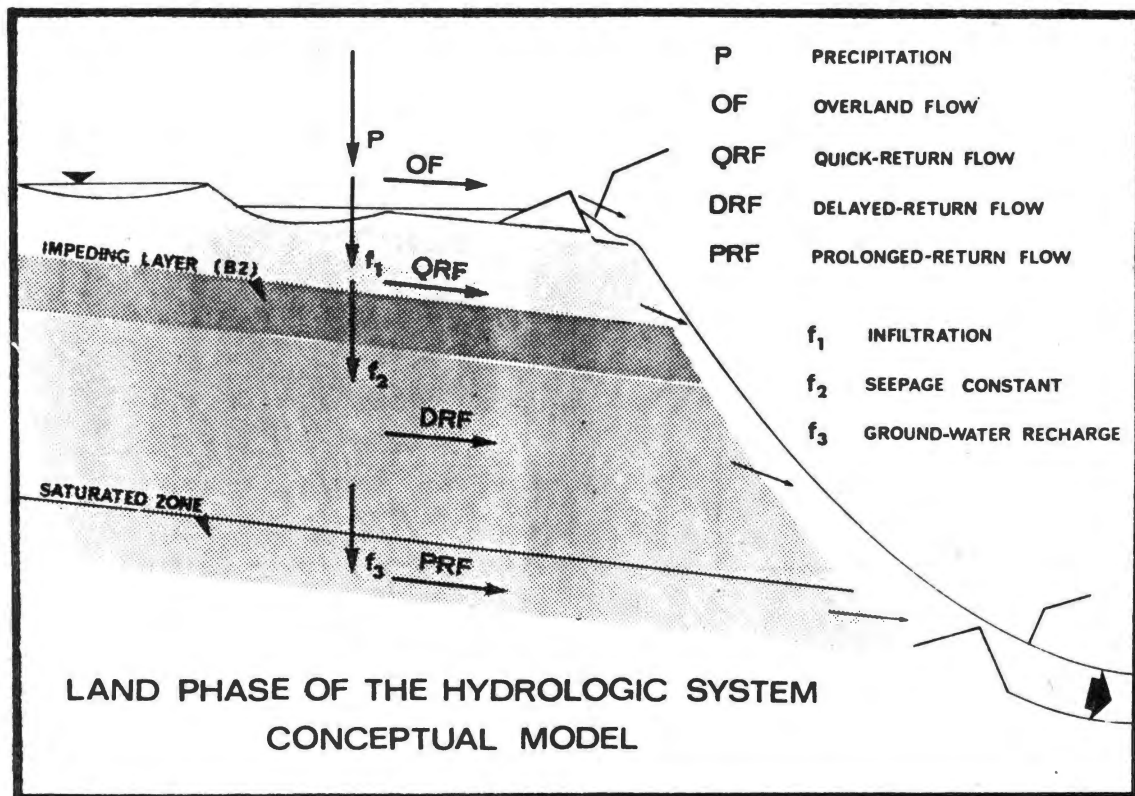


Figure 10. Land Phase of the USDAHL Conceptual Hydrologic Model

Source: (11)

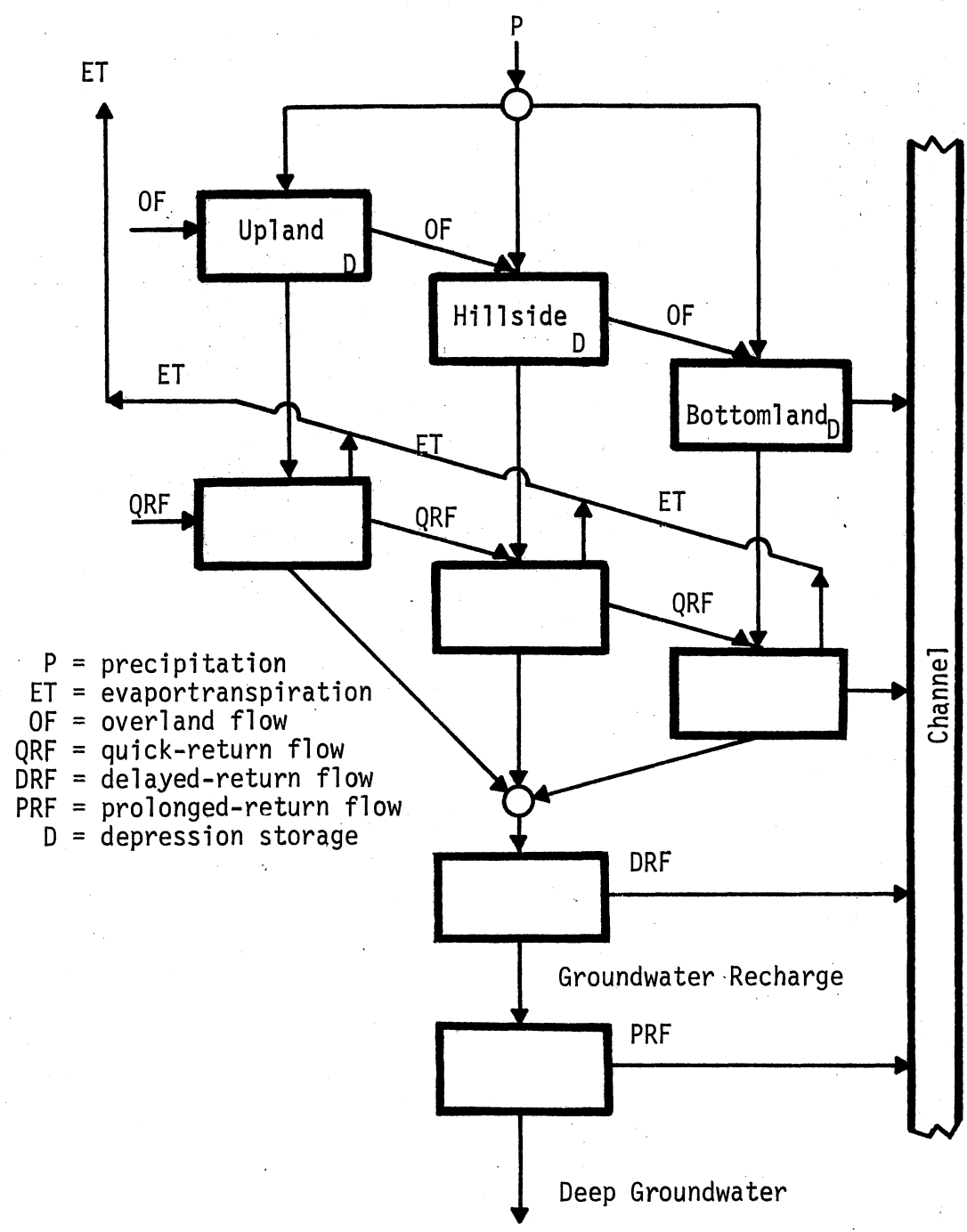


Figure 11. Soil Moisture Flow Chart for the USDAHL Model

while being subject to infiltration and percolation and evapotranspiration at each step along the way. The infiltration rate is limited by an input limit for an impeding horizon. Accretion to groundwater is also limited to times when the available moisture capacity of the surface soil is filled. The DRF and the PRF combine to allow variable groundwater recession rates. Finally the runoff is routed through a linear reservoir which simulates the channel network. The net effect of the model is a routing through nine linear reservoirs of different sizes.

The USDAHL model was designed for very small watersheds, the extent of testing on large watersheds is unknown; nevertheless, it does not seem useful for watersheds of the size normally encountered in forecasting. Lindsley (6) feels it is not particularly adaptable to large watersheds.

U. S. Geological Survey Watershed Model

This model is patterned after the Stanford watershed model, although it is a much simplified version. Its design purpose was to analyze storm peaks. It establishes antecedent soil moisture conditions, utilizes an infiltration equation, a two-level moisture storage system for water balance accounting, and linear storage and translation methods for routing to the basin outflow point. The pilot study for the model was on a 5.41 sq.mi. basin in the Blue Ridge Mountains. Tests have shown that this model has some degree of competence, but extensive testing of it does not appear to have been done. Since its emphasis was on flood peaks, it was designed to only simulate the surface runoff component of the flood hydrograph, and baseflow and seepage were simply not considered.

Since these are the principal components of low flows, this model is not suitable for simulating low flows.

Stanford Watershed Model IV (SWM IV)

A streamflow simulation model that is based on observed physical processes occurring in nature has a distinct advantage over correlation models that do not even attempt to relate to known hydrologic processes. But there is a limit to how detailed the hydrologic cycle can be modeled using existing data collection techniques and standards. The ultimate model would perhaps follow each particle of water from the time it ceased to fall in the atmosphere until the time it left the watershed; that would be the ultimate in moisture accounting. But on any real watershed, that would be a task too immense to even contemplate. It would require such a detailed knowledge of the soil structure and characteristics that it probably could not even be done at the current level of technology.

Certain characteristics for a "good" hydrologic simulation model to be used for daily forecasting are of such importance that they are virtually requirements. First, the model must use for input only those meteorological and hydrological data that are normally observed. It must be capable of continuous simulation for long periods of time, not only for use in calibration in order to fully use all of the data available, but also for generating synthetic streamflow records. As much as possible, parameters should be obtained by measurements, not from the judgement of the person calibrating the model or by iterative procedures. It must be usable on digital computers at a reasonable cost. It must be sufficiently general that it can be used in all climatic

conditions (snow, desert, tropics, etc.) and geographical locations (mountains or plains, etc.). It must be able to output simulated stages and flows on a real-time basis for forecasting as well as continuous records for research. It must be based in the physical processes of the hydrologic cycle, and simulate the entire physical system with sufficient detail and accuracy to sustain confidence in the model.

This is essential for use on ungaged watersheds. This also will contribute to a better understanding of the hydrologic processes occurring in the basin, which is valuable as a training tool for the working forecaster. Since many forecasters have little training other than on-the-job training and perhaps a basic course in hydrology, this can be a feature of considerable importance.

Until the physical processes in the hydrologic cycle can be described in much greater detail than at present, as well as measured, and can be used in hydrologic simulation, it will be necessary to be content to use some judgement parameters in order to calibrate or adjust the model simulation by trial and error against a period of continuous historical data. Our present knowledge of the details of the hydrologic cycle is not adequate to rigorously describe each step of the process, and even if it were, the enormous amount of physical data on the watershed as well as the very small computational increments that would be required for computer simulation would probably make such an exact simulation prohibitive in cost. The result is a model that is sufficiently refined to be reliably accurate, but does not contain unnecessary detail. The parameters will thus be basically lumped parameters in that they represent the average of the physical processes over an area, although they will be distributed parameters in the sense

that they can be used for small sub-areas of the watersheds.

Runoff consists of three components which follow different paths to the channel. First is the surface runoff which is flow over the ground surface into the channel as either sheet or overland flow. The second component is water flowing through the upper soil layers to the channel, and is known as interflow. The exact mechanism of interflow is not well known, but its occurrence is enhanced by the presence of a relatively impermeable horizon in the soil. The third component is groundwater flow, which is water flowing from a groundwater aquifer.

Most runoff relations are designed to predict only the direct runoff (the combination of surface runoff and interflow). Since a flood hydrograph is mostly composed of direct runoff, and it is quite difficult as well as arbitrary to separate the two, groundwater flow is frequently assumed to be rather constant and is just added to the direct runoff to give the storm runoff.

The water balance concept involves maintaining a running account of the water in soil moisture storage by adding the amount of each new rainfall less direct runoff and accretion to groundwater, and subtracting evapotranspiration. The amounts of runoff and groundwater accretion are made functions of the prevailing soil moisture storage.

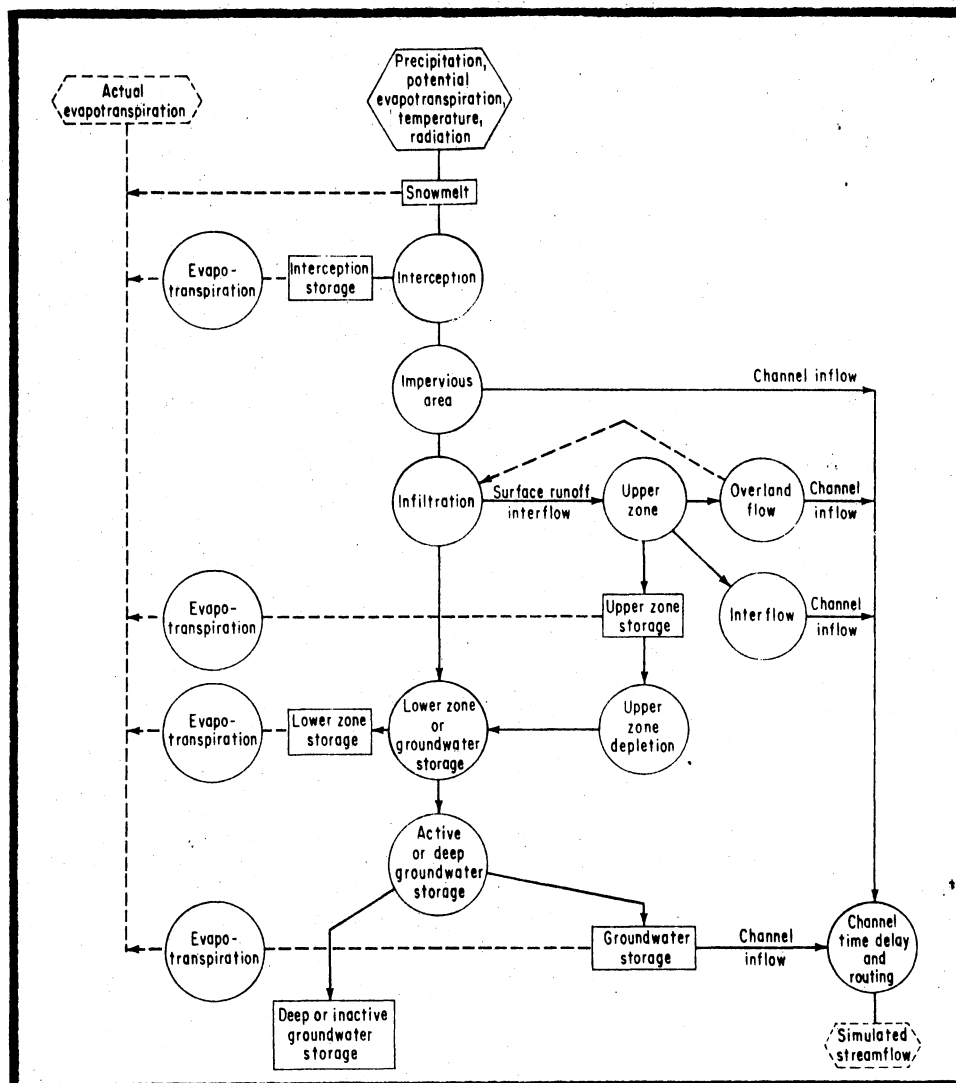
The water balance model is the basis of the SWM IV model. Soil moisture account is through a two-level moisture storage, which uses a small upper storage zone to simulate surface detention and retention in overland flow and the depression storage and soil moisture in a shallow surface layer, plus a lower storage zone that simulates the storage of soil moisture from the surface down to the capillary fringes. Water is accounted for through all storage categories until it leaves the

watershed. Perhaps the best way of describing the SWM IV model is by discussing the structure of the model. Figure 12 is the flowchart of the SWM IV model, and gives the general sequence of operation.

Principal inputs to the model are the hourly precipitation amounts in the form of mean basin precipitation (MBP), and the daily potential evapotranspiration and streamflow data. Additional meteorological inputs (daily maximum and minimum air temperatures and incoming short-wave radiation are necessary if snowfall is significant and the snow routine is used. Hourly and daily precipitation data are readily available on a historical basis from the National Climatic Center (NCC) Environmental Data Service, NOAA, Asheville, North Carolina. However, these data are not readily available on a real time basis, except for a few stations. Except under unusual circumstances, the normal reporting frequency is either every six or twenty-four hours. Potential evapotranspiration is assumed to be equal to the lake evaporation estimated from class A pan records. The actual evapotranspiration is computed by the model as a function of the potential evapotranspiration and the current soil moisture conditions.

Interception

Interception is the initial abstraction from the incident precipitation. It is a function of the watershed cover, and is limited by the current volume in interception storage as well as the preset maximum interception storage amount (EPXM). All incident precipitation is directed to EPXM until that preassigned volume is full. Moisture in interception storage is depleted by evaporation at the potential evapotranspiration rate. Thus, interception can continue throughout a



Flow Chart

Figure 12. Stanford Watershed Model IV

Source: (2), p. 322

storm due to evapotranspiration.

Impervious Area

The impervious areas (A) of a watershed are those areas such as lake or stream surfaces and the adjacent non-permeable surfaces. If rainfall occurs on these areas, it becomes surface runoff immediately. "A" represents a preset percentage of the precipitation that is immediately diverted directly to the channel. It does not include rock outcrops, buildings, or roads that are not immediately adjacent to the streams or which are separated from the stream by previous areas.

Infiltration

Infiltration is a continuously varying function of the soil moisture. First the cumulative watershed infiltration capacity functions determine whether the available moisture infiltrates directly into the soil and into lower zone and groundwater storage or goes to surface detention storage. Water that is directed to surface detention storage is in what is called the upper zone and which is designed to simulate depression storage, soil fissures, and the space around soil particles. The infiltration capacity is divided into two portions (Figure 13); part of the infiltrated water becomes interflow while the rest goes to lower zone and groundwater storage. For a given moisture supply of x inches and a given infiltration capacity, Figure 13 illustrates the division of the available moisture into overland flow, interflow, and lower zone and groundwater storages. Figure 13 also shows the variation of overland flow, interflow, and infiltration as the moisture supply varies.

b = total direct lower zone
 and groundwater infil-
 tration capacity
 $c \cdot b$ = total infiltration capacity

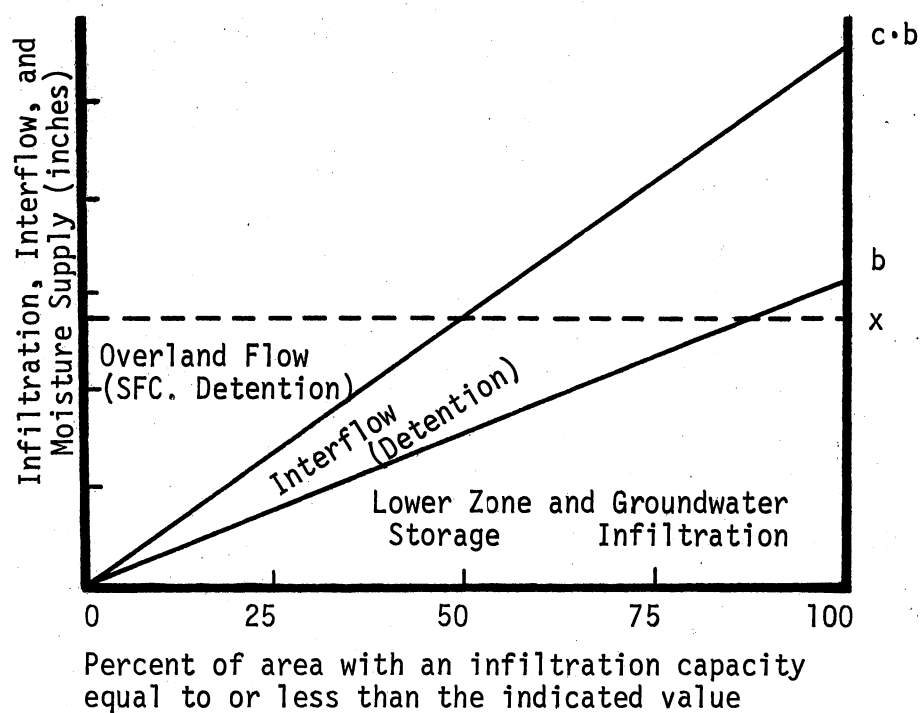


Figure 13. Infiltration Division

Source: (17), p. 33

It is apparent that the variables c and b are extremely important in determining the relative magnitude of each of these flows. c and b are functions of the current lower zone storage ration $LZS/LZSN$ (LZS is the current soil moisture storage in the lower zone, and $LZSN$ is a nominal lower zone storage level that is about equal to the median value of lower zone storage), CB (an infiltration parameter), and CC (the ratio of interflow/overland flow). When $LZS/LZSN < 1.0$

$$b = \frac{CB}{2.0} (4.0 \cdot LZS/LZSN)$$

and when $LZS/LZSN > 1.0$

$$(4.0 + 2.0((LZS/LZSN) - 1.0))$$

$$b = \frac{CB}{2.0} (LZS/LZSN)$$

$$c = CC \cdot 2.0$$

Water that does not infiltrate directly, increases the amount in surface detention storage and will either contribute to overland flow or upper zone storage, and then either evapotranspire (at the potential rate) or infiltrate. The rate of filling of upper zone storage decreases as the upper zone becomes full.

Overland Flow

Overland flow is calculated at fifteen-minute intervals. It is a function of the variable infiltration rate and evaporation. Lindsley (17) believed that the use of rigorous methods for simulating the over-flow (using finite differences techniques for numerical solution of the

governing differential equations: the continuity and momentum equations) were not justified due to the limited accuracy for the basic data. Experimental data indicated that the laminar flow regime could be ignored; therefore, only the equations for the turbulent range were used. The basic approximation equation was derived from Manning's equation, and is used as follows:

$$q = \frac{1.486}{n} y^{5/3} s^{0.5}$$

$$\frac{D_E}{L} = y = \frac{8}{5} D_{E/L}$$

By empirical methods, y was found to be best described by

$$y = \frac{D}{L} \left(1.0 + 0.6 \left(\frac{D}{D_E} \right)^3 \right)$$

$$q = \frac{1.486}{n} s^{0.5} \left(\frac{D}{L} \right)^{5/3} \left(1.0 + 0.6 \left(\frac{D}{D_E} \right)^3 \right)^{5/3}$$

where

- q = overland flow (ft³/sec)
- n = Manning's n
- s = slope (ft/ft)
- D = current detention storage $\frac{FT^3}{FT}$
- D_E = surface detention storage at equilibrium $\frac{FT^3}{FT}$
- L = length of overland flow (ft)
- y = depth of flow (ft)

The overland flow thus determined is used to solve the following continuity equation

$$D_2 = D_1 + \Delta D - \bar{q}\Delta t$$

where

- D_2 = surface detention at the end of the current time

- D_1 = surface detention at the end of the previous time interval
 ΔD = increment added to surface detention time in the interval
 (determined from equations based on Figure 13)
 Δt = time interval used (15 minutes)

Soil Moisture

Briefly, soil moisture is represented by lower zone storage that is filled both by infiltration and percolation from the upper zone, while depleted by evapotranspiration at a rate dependent on the water currently in storage, percolation to deep or inactive groundwater storage and percolation to active groundwater storage (where it either remains or flows to a channel).

Interflow

Interflow storage is principally a function of the infiltration that has occurred, and the infiltration capacity. Its computation is illustrated on Figure 13. Depletion of interflow storage and the movement of interflow is accomplished by a decay or recession function:

$$\text{INTF} = \text{LIRC4} \cdot \text{SRGX}$$

where

- $\text{LIRC4} = 1.0 - (\text{IRC})^{1/96}$
 LIRC4 = the recession coefficient
 INTF = interflow
 SRGX = the amount of water in interflow storage
 IRC = daily recession or depletion coefficient, the ratio of interflow discharge at any time to the interflow discharge twenty-four hours later

Groundwater

Recharge of groundwater storage is by percolation from the lower

zone, and is a function of the amount of water in lower zone storage at that time. The percentage of water that infiltrates (either directly as shown in Figure 13, or as delayed infiltration through upper zone storage) varies as follows:

$$P_g = 100 \left(\frac{LZS}{LZSN} \left(\frac{1.0}{1.0 + LZI} \right) LZI \right)$$

where

$$\frac{LZS}{LZSN} < 1.0 \text{ (if greater, set } \frac{LZS}{LZSN} = 1.0$$

P_g = percentage of water entering groundwater storage
 LZS = amount of water in lower zone storage
 $LZSN$ = lower zone storage level at which fifty percent of all water infiltrated goes to groundwater storage

$$LZI = 1.5 \left(\frac{LZS}{LZSN} - 1.0 \right) + 1.0$$

The relationship of P_g and $LZS/LZSN$ is shown in Figure 14. At a $LZS/LZSN$ of zero there is zero groundwater recharge, when $LZS/LZSN = 1.0$, fifty percent of infiltration is stored in groundwater storage, and as $LZS/LZSN$ approaches 2.5, the percent infiltrated approaches one hundred percent.

Outflow from groundwater storage is to the channel as groundwater flow, by percolation to deep (inactive) groundwater storage, by loss from evapotranspiration. Groundwater flow is based on the simplified model in Figure 15. The flow from this aquifer is proportional to the product of the cross-sectional area of flow and the energy gradient of the flow. The energy gradient is composed of a base gradient plus a variable gradient which depends on groundwater accretion. Groundwater flow is computed by the following equation

$$GWF = LKK4 \cdot (1.0 + KV \cdot GWS) \cdot SGW$$

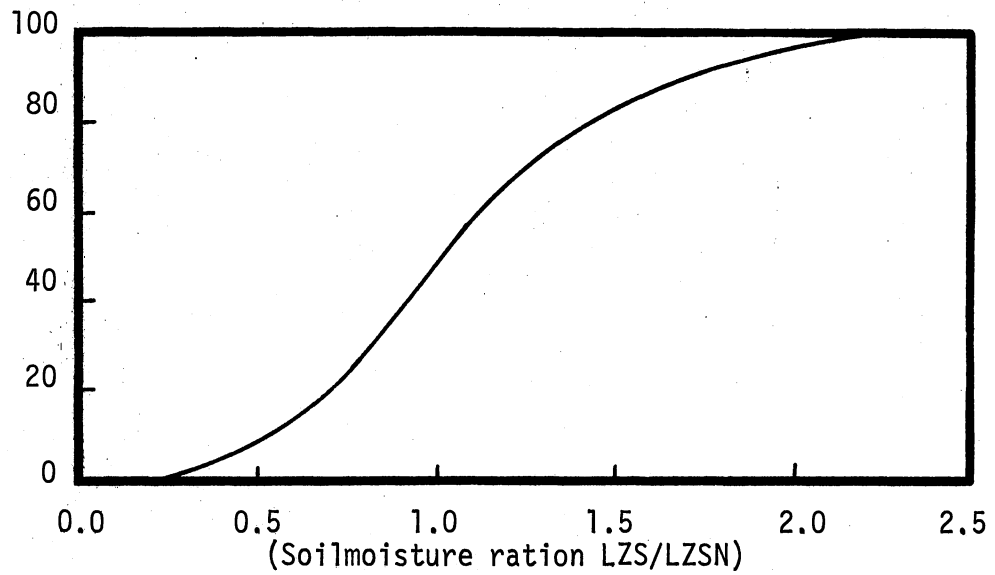


Figure 14. Soil Moisture Ratio (LZS/LZSN) versus Percent of Infiltration Entering Groundwater storage

Source: (17), p. 40

where

- GWF = groundwater flow
 LKK4 = fair weather groundwater recession coefficient
 $= 1.0 - (KK24)^{1/96}$
 KK24 = ratio of current groundwater discharge to the groundwater discharge twenty-four hours earlier (it is the minimum observed daily recession)
 KV = a variable groundwater recession coefficient
 GWS = the antecedent groundwater inflow index
 $= 0.97 (GWS + \text{inflow to groundwater storage})$
 SGW = amount of water in groundwater storage

Percolation to deep (inactive groundwater storage is simulated by shunting a fixed percentage (K24L) of the inflow to groundwater storage directly to inactive storage.

Evapotranspiration

Evapotranspiration is a function of the potential evapotranspiration and the available moisture supply. It occurs from interception storage, upper zone storage, lower zone storage, and groundwater storage. The SWM IV model also includes evaporation from stream surfaces in this category. Hourly potential evapotranspiration is computed from daily or semi-monthly input data. The program attempts to satisfy potential evapotranspiration first from interception storage, and after that, from upper zone storage. If the potential has not been satisfied at that point, the evapotranspiration opportunity (maximum water available for evapotranspiration in a time interval at a point in the basin) from the lower zone is then computed by use of the following equation

$$E = E_p - \frac{E_p^2}{2r}$$

$$r = K3 \frac{LZS}{LZSN}$$

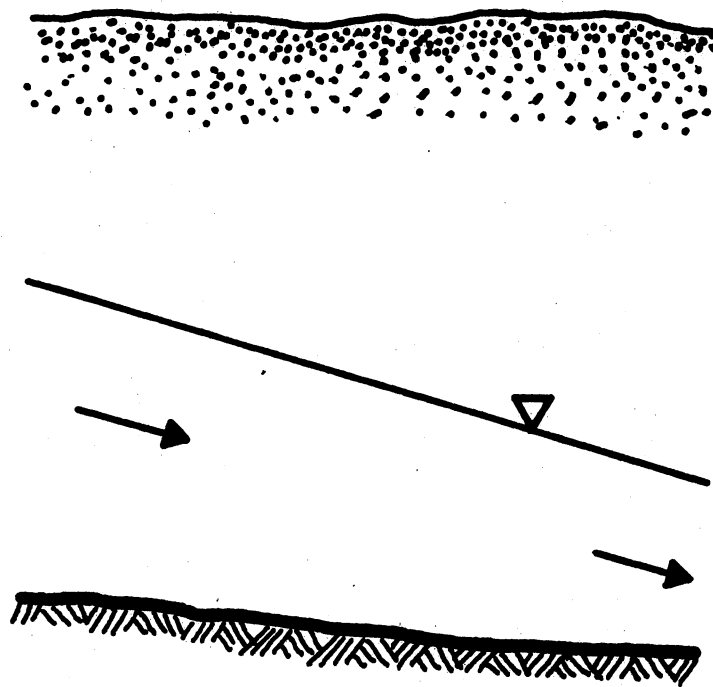


Figure 15. Simplified Model of Outflow From
Groundwater Storage

Source: (17), p. 40

where

E = evapotranspiration from lower zone (inches per day)
 E_p = potential evapotranspiration (inches per day)
 K_3 = variable index to lower zone evapotranspiration

The maximum evapotranspiration for any given lower zone storage level occurs when the potential evapotranspiration equals $n/2$ inches over the watershed.

Channel System

Storage and flow times in the channel system become large compared to those in overland flow as the size of the watershed increases and the channel system becomes the dominate factor in shaping the outflow hydrograph.

Although Linsley (17) stated that the finite differences method for channel routing is the most general physically based method for simulating unsteady open channel flows, the input requirements and long computing times required led to the adoption of an empirical routing method in the model--the channel time-delay histogram. This is a time versus discharge histogram that represents the response of the channel to an inflow with a duration equal to the time increment (Figure 16). Each element of the histogram represents the fraction of the total watershed that contributes to channel flow for a given travel time. Each element of the histogram is thus associated with a particular travel time zone of the watershed. The main advantages to this method are efficient programming and the ability to provide simultaneous output hydrographs at several points in the watershed.

The outflow hydrograph produced from the time-delay histogram is then routed through a linear reservoir at the basin outflow point. The

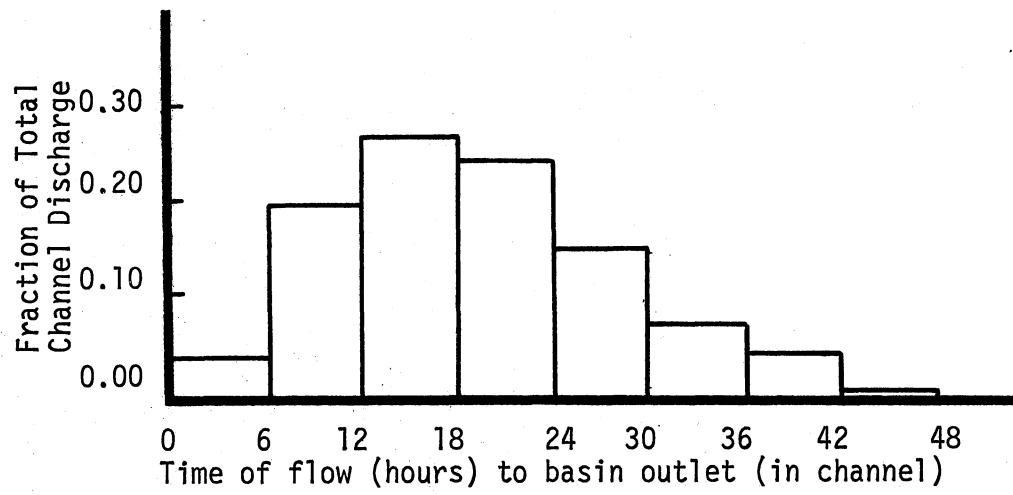


Figure 16. Channel Time-delay Histogram for the Illinois River near Watts, Oklahoma

channel routing equation is

$$O = I - KS1(I - O_1)$$

where

$$KS1 = \frac{(1/k - \Delta t/2)}{(1/k + \Delta t/2)}$$

O = outflow

I = inflow

KS1 = reservoir storage constant

= hourly recession rate for channel runoff

= $\frac{\text{discharge in hour } (t)}{\text{discharge in hour } (t+1)}$

Snowmelt

The model is set up in the sparse data mode and as such requires only daily maximum and minimum temperatures and incoming shortwave radiation. It differentiates between rain and snowfall, maintains the area and depth of the snowpack as well as its water equivalent and density. Albedo is computed as is the melt rate of the pack. Temperature variations with elevation are computed using variable lapse rates that account for diurnal variations as well as for dry and stormy weather conditions.

National Weather Service River Forecast System (NWSRFS)

The acronym NWSRFS stands for National Weather Service River Forecast System, and as used in this report, refers to the system described in NWS HYDRO 14 (9). This system was assembled by the Hydrologic Research Laboratory (HRL) of the National Weather Service's Office of Hydrology, in Silver Spring, Maryland, and includes programs to process data, compute mean basin precipitation (MBP), optimize parameters,

verify model parameters, and produce operational river forecasts.

The heart of this system is the model of the hydrologic cycle. Selection of this portion of the model was based on a statistical analysis of three watershed models: the SSARR model, the Sacramento model, and a version of the Stanford Watershed IV (SWM IV) model as modified by the HRL. The decision of which to choose was narrowed down to a choice between the modified SWM IV and the Sacramento model, and on the basis of statistical analyses completed by August, 1971, the modified SWM IV was chosen. It should be noted that testing performed after that date showed there was no significant difference between the two, and Burnash (15) claims that the latest version of the Sacramento model is considerably better than the one involved in the testing. It is interesting to note that the HRL is now adopting the land phase of the Sacramento model to replace the land phase of the modified SWM IV currently used in the NWSRFS.

Differences From SWM IV

Since the NWSRFS soil moisture accounting is simply a modification of the SWM IV, a detailed description of the land phase of the NWSRFS will not be made. Instead, the major differences will be noted. Many of the changes are a result of the use of precipitation data for six-hour increments instead of for one-hour increments. Outflow from interflow and groundwater storages is now computed every six hours, and percolation is computed daily. Overland flow routing equations of the SWM IV are omitted due to the longer time intervals. Instead, the amount of fast response runoff reaching the channel each hour is computed by the following equation

$$\text{ROST} = \text{SRC1} \cdot \text{RX}$$

where

SRC1 = percent of water in RX that reaches the channel each hour
 RX = surface detention

Three basic types of runoff are considered in this model: fast response (surface runoff), medium response (interflow), and slow response (groundwater flow). The recession coefficient for groundwater flow (GWS) was changed to a variable (KGS) from its fixed value of 0.97

$$\text{GWS} = \text{KGS} \cdot (\text{GWS} + \text{GW inflow})$$

to give additional flexibility needed for some basins. Interception storage is now satisfied after impervious area runoff (Figure 17), instead of the other way around, because it was felt that no interception occurred over impervious areas. The maximum infiltration relation was changed in order to allow more flexibility in shaping the infiltration curve (Figure 18). The new equation is

$$b = \text{CB}/(\text{LZS}/\text{LZSMP})^{\text{POWER}}$$

Evaporation from stream surfaces and evapotranspiration from groundwater are lumped together, instead of being computed separately.

Channel routing also uses the time-delay histogram, but uses constant or variable lag and K routing, which is described in references (2), (3), (8), and (9).

As currently used, there is no snowmelt routine included. However, one is available and is described in NWS-HYDRO-16.

Input data for this model are streamflow and precipitation observations every six or twenty-four hours and daily potential

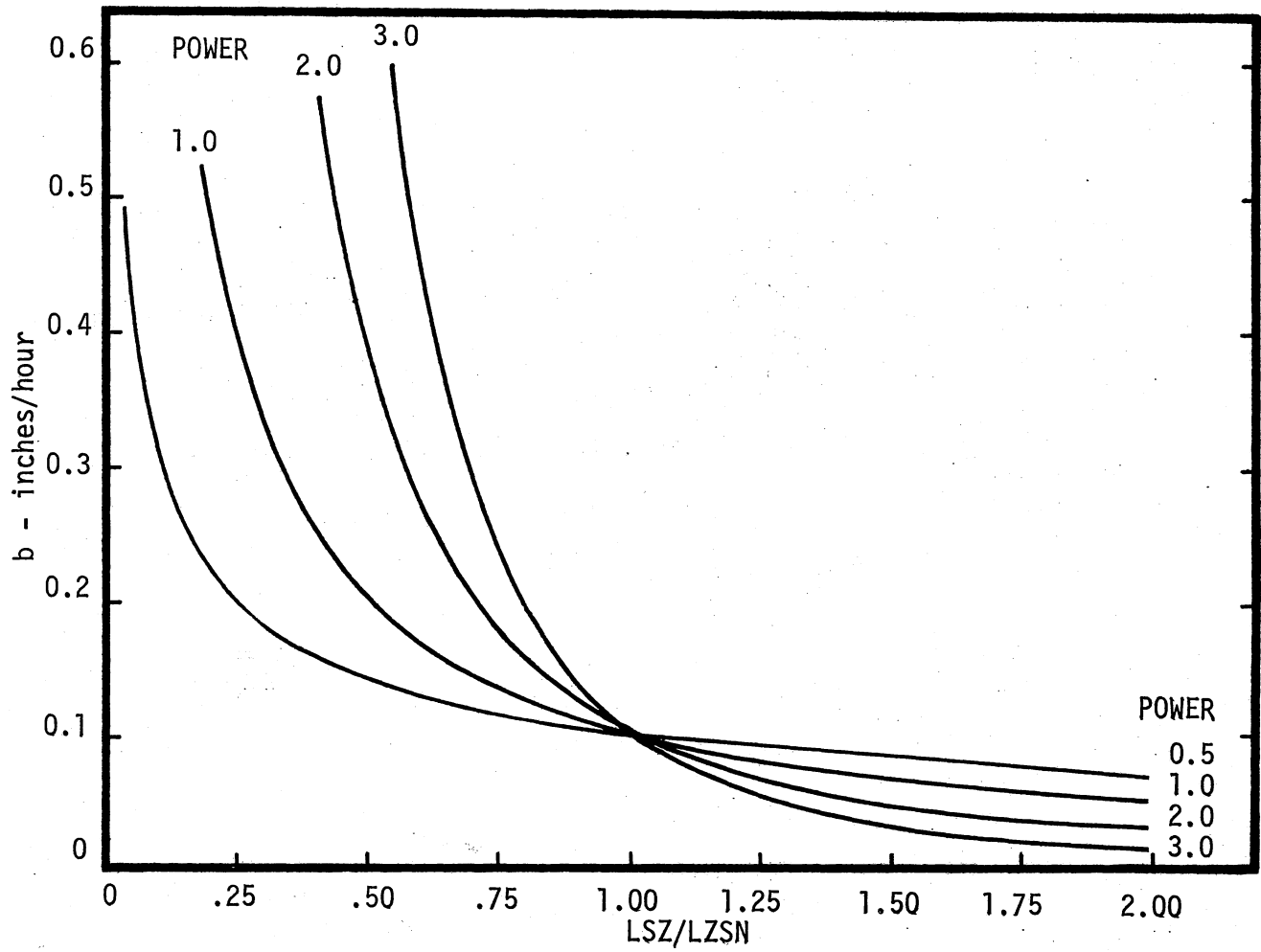


Figure 18. b versus LZS/LZSN for Various Values of POWER for $CB = 0.1$

Source: (9), p. 4-8

evapotranspiration data every twenty-four hours.

The significance of these changes is two-fold:

- 1) additional variables have been added to give additional flexibility to the model, at the expense of making it more complex, and
- 2) the change to longer computational intervals and the resulting deletion of overland flow routing equations may reduce the model's accuracy on very small basins where the overland flow is a significant portion of the total runoff.

Given the normal precipitation and streamflow reporting intervals of six and twenty-four hours, it is apparent that 2) is in fact a concession to reality and is a disadvantage only to research work using historical data which is available on an hourly basis.

If no streamflow data is available, parameters can be estimated from physical basin characteristics or parameters used in nearby and/or hydrologically similar watersheds, and the simulation performed on the basis of those parameters and the available precipitation and potential evapotranspiration (PE) data. The validity of the calibration obviously varies with the accuracy of the estimation of the parameters. Nevertheless, done carefully, this can be a useful tool and provides a valuable method of streamflow simulation under difficult circumstances. If this procedure is continued down to the point where streamflow records are available, the accuracy of the calibration can then be determined and parameter adjustments made. This provides a method of forecasting streamflow or developing streamflow records for ungaged streams.

If precipitation (PE) and streamflow data is available, the NWSRFS can be calibrated to a given basin. Once a basin has been calibrated,

the NWSRFS can be used to extend streamflow records to periods when only meteorological data are available, it can operate in a virtually real-time mode for forecasting use, it can be used with synthetic precipitation data to produce streamflow records for any desired climatological regime, and the parameters in the model can be varied to simulate the effect on the basin of changes to the watershed. The input data required for the NWSRFS is the mean basin precipitation (MBP), streamflow, and potential evapotranspiration (PE).

Mean Basin Precipitation (MBP)

Since precipitation is measured as point values, and these points are usually few in or near a given basin, it is necessary to be able to estimate the precipitation at other points in the basin and finally arrive at average precipitation amounts over given areas. This frequently (although not necessarily) results in the precipitation being averaged over basin-sized areas. Although the concept of area-wide averaging of the precipitation is not too bad when the precipitation is uniformly distributed over a basin, it leaves much to be desired when the precipitation is not uniformly distributed (such as during air-mass thunderstorm activity). Nevertheless, nothing better has been developed, so the NWSRFS provides for the use of three averaging techniques based upon three weighting methods

- 1) Grid Point weights
- 2) Thiessen weights, and
- 3) predetermined weights.

The Grid Point method is based on a basin covered with a fine grid (Figure 19). The precipitation at each of these grid points is

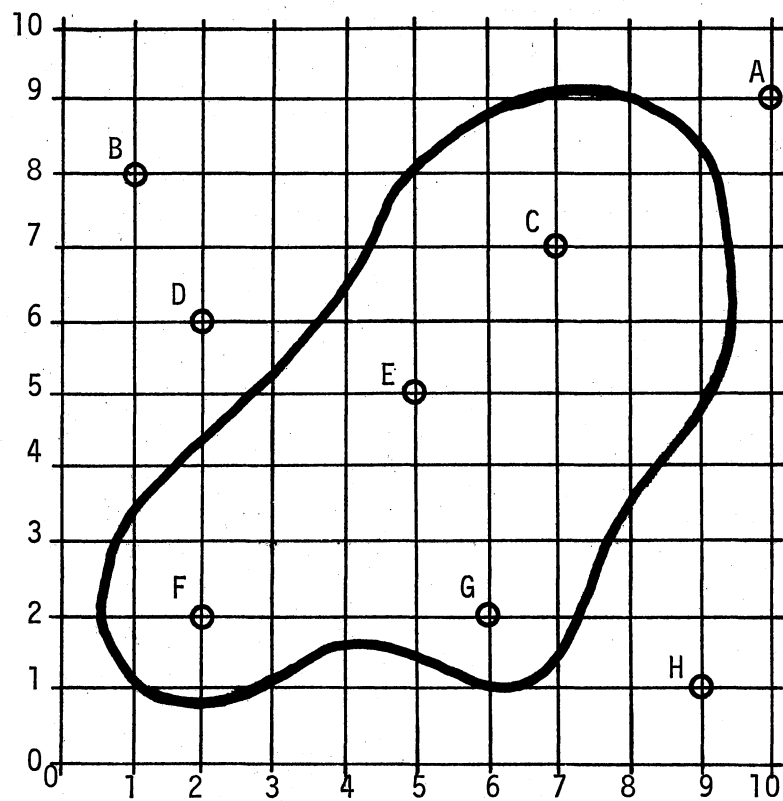


Figure 19. A Grid Superimposed on a Basin

Source: (9), p. 3-5

estimated (using the technique described following the description of the weighting methods) and the MBP is simply the arithmetic average of all of these points. The weights for each grid point are calculated by determining the nearest precipitation station to the grid point in each of the four quadrants around the grid point. Each grid point will then have four weights which are equal to the normalized reciprocal of the squared distance ($1/\text{distance}^2$) to each of the four precipitation stations (sum of the weights = 1.0). Computation of the weights for each of the 47 grid points within the basin (Figure 19) is summarized in Table I. When the grid point coincides with a station, the station is given a weight of 1.000. After this is done for each grid point, the total weight assigned to each station, after being normalized, is its Grid Point weight. Since there are 47 grid points, the sum of the weights is equal to 47.0, which is the total used for normalizing (Table II). Using the basin (Figure 19) as an example, with point precipitation values of A = 1.0, B = 0.2, C = 4.6, D = 1.0, E = 3.2, F = 1.9, G = 2.1, and H = 1.0, and the Grid Point weights in Table II, the MBP was computed to be 2.764 inches. The NWSRFS defines the Thiessen polygon in terms of grid points; the polygon is the boundary of all points which are closer to the subject station than any other station. Table III shows the computed Thiessen weights for this basin. For this example, the Thiessen weights produced an MBP of 3.03 inches, which is close to the 2.764 inches given by the Grid Point method.

Predetermined weights may be entered to compensate for topographical irregularities or unusual aspects such as present in mountains.

The MBP program portion of the NWSRFS has the option of computing and/or using Grid Point weights, Thiessen weights, or predetermined

TABLE I
 NORMALIZED WEIGHTS FOR EACH GRID POINT
 Source: (9), p. 3-6

X	Y	QUAD. I			QUAD. II			QUAD. III			QUAD. IV		
		Sta	D ²	W	Sta	D ²	W	Sta	D ²	W	Sta	D ²	W
1	2	D	17	.056	-	-	-	-	-	-	F	1	.944
1	3	D	10	.167	-	-	-	-	-	-	F	2	.833
2	1	F	1	.980	B	50	.020	-	-	-	-	-	-
2	2	F	0	1.000	-	-	-	-	-	-	-	-	-
2	3	D	9	.092	B	26	.032	F	1	.828	G	17	.048
2	4	D	4	.411	B	17	.096	F	4	.411	G	20	.082
3	1	G	10	.159	F	2	.797	-	-	-	H	36	.044
3	2	E	13	.065	F	1	.842	-	-	-	G	9	.093
3	3	E	8	.094	D	10	.076	F	1	.755	G	10	.075
3	4	E	5	.295	D	5	.295	F	5	.295	G	13	.115
3	5	C	20	.036	D	1	.714	F	10	.071	E	4	.179
4	2	E	10	.166	F	4	.417	-	-	-	G	4	.417
4	3	E	5	.295	D	13	.115	F	5	.295	G	5	.295
4	4	E	1	.727	D	8	.091	F	8	.091	G	8	.091
4	5	C	13	.057	D	5	.148	F	13	.057	E	1	.738
4	6	C	10	.111	D	4	.278	F	20	.056	E	2	.555
5	2	E	9	.091	F	9	.091	-	-	-	G	1	.818
5	3	E	4	.276	D	18	.061	F	10	.111	G	2	.552
5	4	E	1	.738	D	13	.057	F	13	.057	G	5	.148
5	5	E	0	1.000	-	-	-	-	-	-	-	-	-
5	6	C	5	.146	D	9	.081	E	1	.731	G	17	.042
5	7	A	41	.042	B	17	.101	E	4	.429	C	4	.428
5	8	A	26	.094	B	16	.152	E	9	.269	C	5	.485
6	2	G	0	1.000	-	-	-	-	-	-	-	-	-
6	3	C	17	.044	E	5	.150	G	1	.749	H	13	.057
6	4	C	10	.110	E	2	.552	G	4	.276	H	18	.062
6	5	C	5	.148	E	1	.740	G	9	.082	H	25	.030
6	6	C	2	.458	D	16	.057	E	2	.458	H	34	.027
6	7	A	20	.039	B	26	.030	E	5	.155	C	1	.776
6	8	A	17	.084	B	25	.057	E	10	.143	C	2	.716
7	2	C	25	.032	G	1	.806	-	-	-	H	5	.162
7	3	C	16	.077	E	8	.154	G	2	.615	H	8	.154
7	4	C	9	.189	E	5	.340	G	5	.340	H	13	.131
7	5	C	4	.385	E	4	.385	G	10	.154	H	20	.076
7	6	C	1	.785	D	25	.031	E	5	.157	H	29	.027
7	7	C	0	1.000	-	-	-	-	-	-	-	-	-
7	8	A	10	.088	B	36	.024	C	1	.872	H	53	.016
7	9	-	-	-	-	-	-	C	4	.692	A	9	.308
8	4	A	29	.096	C	10	.278	G	8	.348	H	10	.278
8	5	A	20	.130	C	5	.519	G	13	.199	H	17	.152
8	6	A	13	.107	C	2	.699	E	10	.140	H	26	.054
8	7	A	8	.102	C	1	.814	E	13	.062	H	37	.022
8	8	A	5	.270	B	49	.028	C	2	.675	H	50	.027
8	9	-	-	-	-	-	-	C	5	.444	A	4	.556
9	6	A	10	.279	C	5	.557	E	17	.164	-	-	-
9	7	A	5	.400	C	4	.500	E	20	.100	-	-	-
9	8	A	2	.699	B	64	.022	C	5	.279	-	-	-

TABLE II
 GRID POINT WEIGHTS FOR THE VARIOUS STATIONS
 Source: (9), p. 3-7

Station	Sum of Weights	Grid Point Weights
A	3.294	0.0701
B	0.562	0.0119
C	12.312	0.2619
D	2.730	0.0581
E	10.348	0.2202
F	8.931	0.1900
G	7.504	0.1597
H	1.319	0.0281
	47.000	1.0000

TABLE III
 GRID POINT WEIGHTS USED TO COMPUTE THIESSEN WEIGHTS
 Source: (9), p. 3-8

Station	No. of Points	Thiessen Weight
A	2	0.0426
B	0	-
C	16	0.3404
D	3	0.0638
E	10	0.2128
F	9	0.1915
G	7	0.1489
H	0	-

weights, and of producing output MBP for 1, 3, or 6-hour increments. Input to the MBP program consists of hourly (observations each hour) and daily (observations every 24 hours) precipitation for the weighted stations, an 80-by-80 grid map of the basin, and X-Y coordinates of the precipitation stations. More detailed information about the grid map and coordinates is found in Chapter IV.

The basic theory behind estimation of precipitation requires determination of the nearest precipitation station in each of the four quadrants around the point to be estimated (Figure 20). Each of these four stations receives a weight equal to $1/\text{distance}^2$ from the point to that station. The precipitation estimate is then a weighted average of that at the other four points. If there is no precipitation in some of the quadrants, only the quadrants with precipitation are used. A further modification to the operational program as used at the Lower Mississippi River Forecast Center in Slidell, Louisiana, is the option to limit the search for an estimator to a short predetermined distance from the station, when the precipitation is decidedly non-uniform (showers). Stations may be given additional weights if a station gets significantly more precipitation than other stations for a given storm, such as might occur in mountains. This information is called the station's "characteristic."

After the hourly and daily precipitation data have been read into the computer, the MBP program searches the hourly data to estimate missing periods of record and distribute periods for which only an accumulation value is available. It then estimates the missing hourly data by use of the following equation:

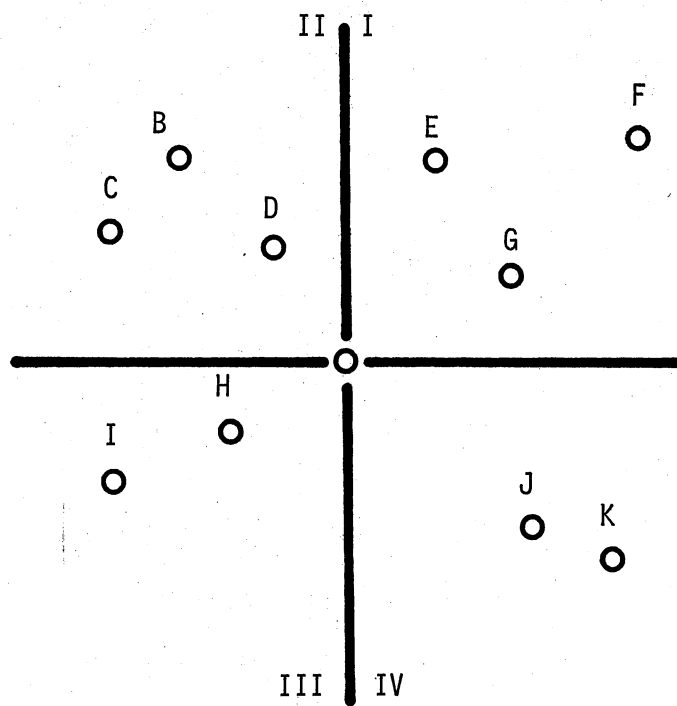


Figure 20. The Four Quadrants Surrounding
Precipitation Station A

Source: (9), p. 3-2

$$A_x = \frac{\sum_{i=1}^{i=n} \left[A_i \cdot \frac{N_x}{N_i} \cdot \frac{1}{(d_{i,x})^2} \right]}{\sum_{i=1}^{i=n} \frac{1}{(d_{i,x})^2}}$$

where

- A_x = the hourly precipitation at the station being estimated
- i = station being used as an estimator
- n = number of estimators
- A_i = hourly precipitation at the estimator station
- N_x = monthly characteristic precipitation at the station being estimated (default = 1)
- N_i = monthly characteristic precipitation at the estimator station (default = 1)
- $d_{i,x}$ = distance from the station being estimated to the estimator station

If only an accumulation value is given, the hourly value is computed by the following equation

$$A_x = \frac{\sum_{i=1}^{i=n} \left[A_i \cdot \frac{T_x}{T_i} \cdot \frac{1}{(d_{i,x})^2} \right]}{\sum_{i=1}^{i=n} \frac{1}{(d_{i,x})^2}}$$

where

- T_x = the accumulative amount at the station being distributed
- T_i = the total precipitation amount for the period of missing time distribution

If no estimator stations are available, that hour is set equal to 0.00, or in the case of an accumulative value, it is left in the last hour. At this point, there is a continuous period of record for all

the hourly precipitation stations which is free of accumulative amount indicators.

Next, the daily precipitation amounts are distributed into hourly amounts by use of the hourly data. This is a two-pass operation. On the first pass, the daily observations are put into hourly amounts except that missing data is ignored. The preceding equation is used with T_x = the daily precipitation amount, and T_j = total precipitation since the last daily observation at the hourly station used to estimate the missing daily amount. The missing periods are then estimated and distributed on the second pass. If there are no estimator stations, the daily amount is set = 0.0. If no stations are available to distribute the precipitation, the undistributed precipitation is left at the time of observation. At this point, the precipitation records are continuous, having no missing data and no accumulative amount indicators.

The MBP is then computed by going through the entire period of record for the area, multiplying the hourly precipitation by the station weight for all stations within the area, and summing these products to give a sequence of MBP values for the period. The MBP values are then written on tape in six-hour increments.

Streamflow

Mean daily flows for the basin outflow point are necessary only as an aid to calibration (so the simulated flow can be compared with the observed flow to assess the accuracy of the simulation and monitor the effect of parameter changes), and as a basis for the generation of six-hour incremental outflows from the basin. For a headwater basin, the NWSRFS can function without streamflow observations. However, for a

reach, the NWSRFS requires inflow to the reach in six-hour increments. The mean daily flows must be input to the program from available records; however, the six-hour incremental flows are generated during a simulation (verification) run and can be put on computer mass storage for use in the downstream reach.

Potential Evapotranspiration (PE)

PE is the water loss that would occur if at no time there is a deficiency of water in the soil for the use of vegetation. Due to the probable error associated with computation of free-water evaporation, the Hydrologic Research Laboratory (HRL) assumed the PE was equal to free-water evaporation (although in theory PE is lower than free-water evaporation). PE can be computed from Class A pan evaporation data using the following equation,

$$PE = E_L = 0.70 \left[E_p + 0.00051PN_p (0.37 + 0.0041U_p)(T_o - T_a)^{0.88} \right]$$

where

- E_L = daily lake evaporation losses (inches/day)
- E_p = daily Class A pan evaporation
- P = atmospheric pressure
- N_p = proportion of advected energy (Class A pan) utilized for evaporation
- U_p = daily wind movement at Class A pan height (six inches above surface)(miles/day)
- T_o = water surface temperature (F)
- T_a = air temperature (F)

If Class A pan data are not available, the PE can be computed from meteorological parameters (air temperature, dew point, daily wind movement, and solar radiation), using the following equation,

$$PE = E_L = \left[e^{(T_a - 212)(0.1024 - 0.01066nR)} - 0.0001 + \right. \\ \left. 0.0105 (E_s - E_a)^{0.88} (0.37 + 0.0041U_p) \right] \cdot \left[0.015 + \right. \\ \left. (T_a + 398.36)^{-2} (6.8554 \times 10^{10}) e^{-7.4826/(T_a + 398.36)} \right]^{-1}$$

where

- E_L = daily lake evaporation losses (inches/day)
- e = Napierian base
- T_a = air temperature (F)
- R = solar radiation in Langleys/day
- E_s = saturation water vapor pressure at T_a
- E_a = atmospheric water vapor pressure at T_a
- U_p = wind movement six inches above Class A pan (miles/day)

Since there are only about 40 solar radiation stations in the United States, it is usually necessary to be able to estimate solar radiation from percent sunshine, where the percent sunshine = (1.0-tenths of sky cover)(100). The program will accept solar radiation either in Langleys or as tenths of sky cover.

The daily wind movement reduced from anemometer height to pan height (two ft) follows the equation:

$$\frac{U_1}{U_2} = \left(\frac{Z_1}{Z_2} \right)^{0.3}$$

where

- U_1 = wind movement at pan height
- U_2 = wind movement at station anemometer height
- Z_1 = height of pan anemometer (two ft)
- Z_2 = height of station anemometer

The PE data is then placed on tape for use by the NWSRFS. This completes the data requirements for the NWSRFS.

Experience with the NWSRFS at the Lower Mississippi River Forecast

Center in Slidell, Louisiana, has shown the NWSRFS is capable of accurate streamflow simulation for normal flood forecasting when the MBP is accurate. However, it has not been tested on low streamflow prior to this time.

Sacramento Model

The model described is level eight of what the model's developers call the Generalized Streamflow Simulation System, which was documented in March, 1973 (15). It attempts to simulate streamflow by simulating all the significant components of the hydrologic cycle in a simplified manner, which is consistent with observed soil moisture profiles. Each variable in the model thus has a recognizable counterpart in the physical world. Data inputs are for twenty-four hour increments, as Burnash (15) felt that the additional costs for smaller increments were not justified for the average size basin (60 - 1200 miles). This model will be described through a description of its various components (see Figure 21 for a simplified flow chart of the soil moisture accounting system of the model).

Incident Surfaces

Rainfall is considered to fall either on

- 1) permeable soil, or
- 2) impervious surfaces or channel connected water surfaces where it contributes direct runoff from any size storm.

The model allows the impervious area to increase as a storm progresses (a set fraction of the basin becomes impervious area when all tension water storages are full).

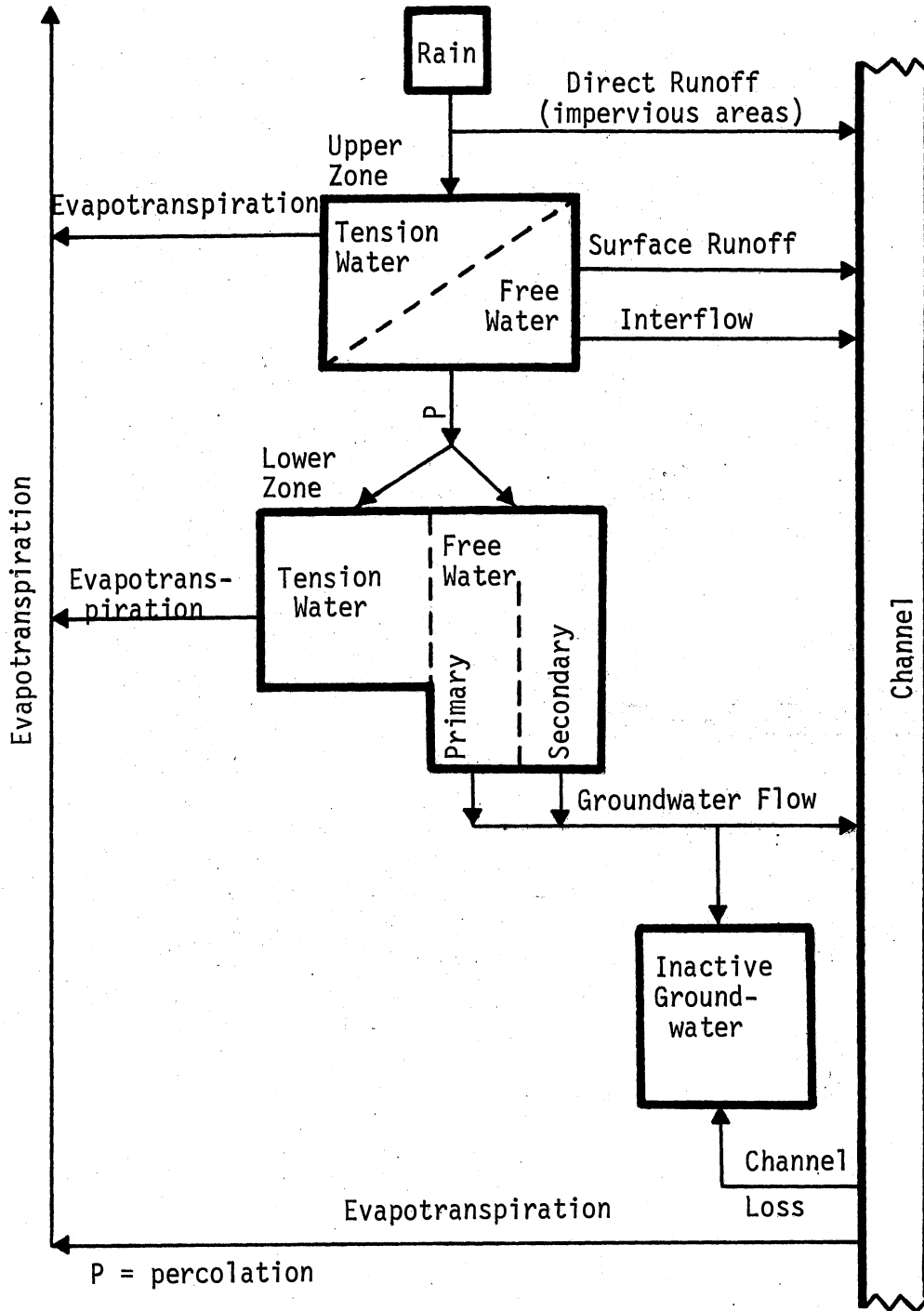


Figure 21. Simplified Flow Chart of the Land Phase of the Sacramento Model

Upper Zone

Precipitation incident upon permeable soil surfaces is used first to satisfy the water requirements of the uppermost storage area, which is called Upper Zone Tension (UZT)(see Figure 22). UZT represents the water that is bound closely to the soil particles which is called tension water, as well as interception storage and surface detention storage. When the UZT storage is full, water accumulates as Upper Zone Free Water (UZFW). This water is not bound to soil particles and it may percolate to lower zones or it may move laterally through the soil as interflow according to the following equation

$$\text{INTERFLOW} = \text{UZK} \cdot \text{UZFWC}$$

where

UZK = UZFW storage depletion coefficient

UZFWC = Upper Zone Free Water Content

Interflow cannot occur until the precipitation rate exceeds the percolation rate downward out of UZFW. Likewise, surface runoff will not occur unless the UZFW storage is full and the precipitation rate exceeds both the percolation rate and the maximum interflow drainage rate. The Upper Zone thus is responsible for direct runoff, surface runoff, and interflow as well as supplying moisture to the Lower Zone.

Lower Zone

The Lower Zone is composed of two tension water storages, Primary and Supplemental, from which water may flow as groundwater flow--either to a channel or to inactive storage. Percolating water goes first to

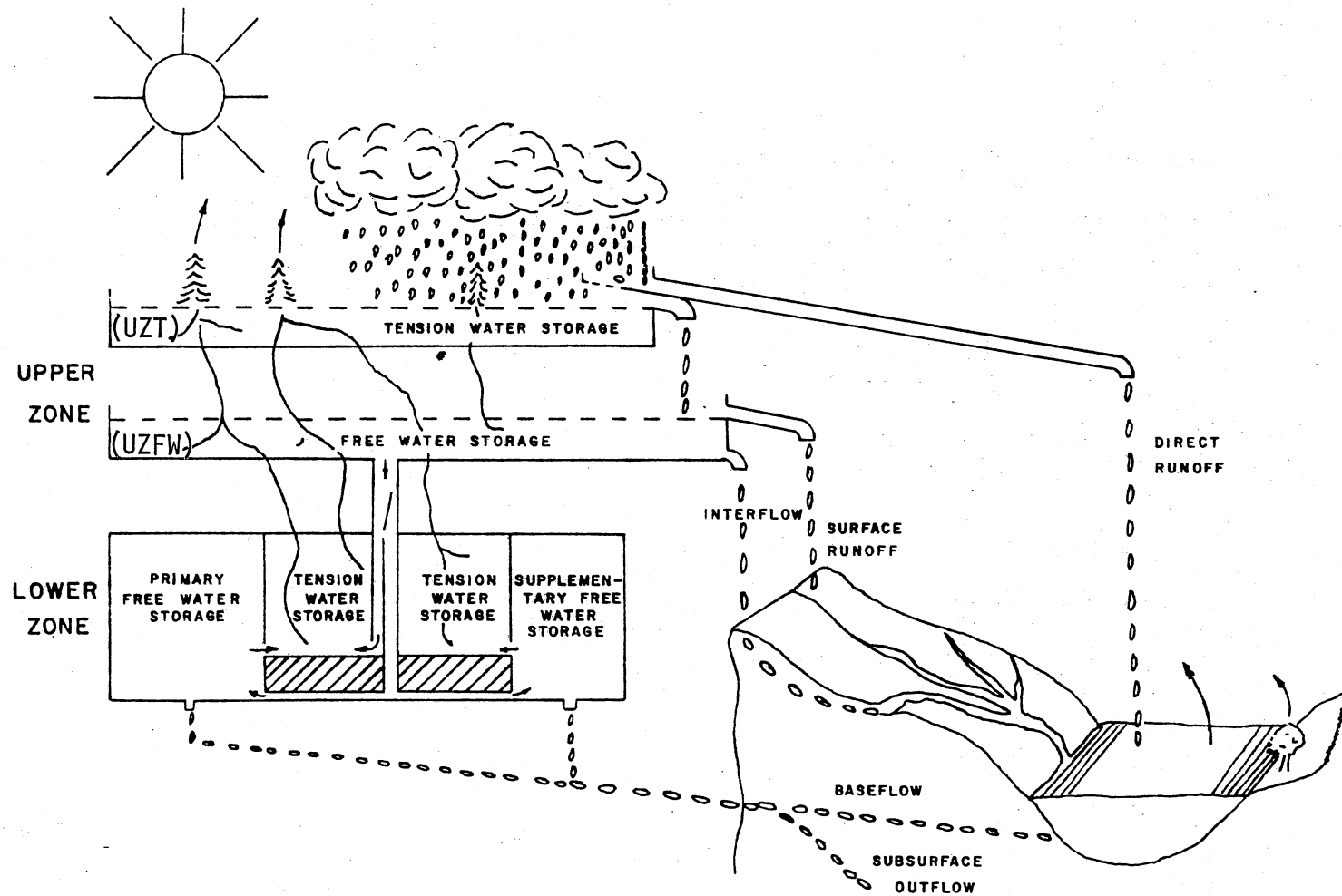


Figure 22. Overall View of the Sacramento Model

Source: (15), p. 12

satisfy tension storage requirements, but a fraction of the water is directed to the free water storages before the tension water storages are completely full. The Primary and Supplemental storages fill simultaneously (although their individual inflow rates are determined by their relative deficiencies), from water which has percolated down from the Upper Zone, but drain independently at different rates in order to provide a variable groundwater recession. When these storages are full, the inflow rate to them is limited to the outflow rate from them. The percolation rate is thus seen to be a function of soil moisture and varies inversely with the soil moisture (within the limits imposed by the available water supply and the soil drainage characteristics). The maximum percolation rate occurs when the Upper Zone is full and the Lower Zone is empty. Thus, the recession is a function of the three Lower Zone storages, and provides a recession similar to that of the USDAHL model (Figure 23).

Evaporation and Evapotranspiration

For the areas covered by surface waters, the evaporation is computed at the potential rate. For the remainder of the basin, the evapotranspiration is a function of the evapotranspiration demand and the water in tension water storage. Evapotranspiration occurs from the Upper Zone at the potential rate multiplied by the proportional loading of the Upper Zone Tension Water Storage. It occurs from the Lower Zone at a rate equal to

$$\left(\begin{array}{l} \text{unsatisfied potential} \\ \text{evapotranspiration} \end{array} \right) \frac{(\text{Lower Zone Tension Water Contents})}{(\text{Total Tension Water Capacity})}$$

Discharge in cfs/sq mi 25.0
Semi-logarithmic Plot - S. Fork Eel River near Miranda, California

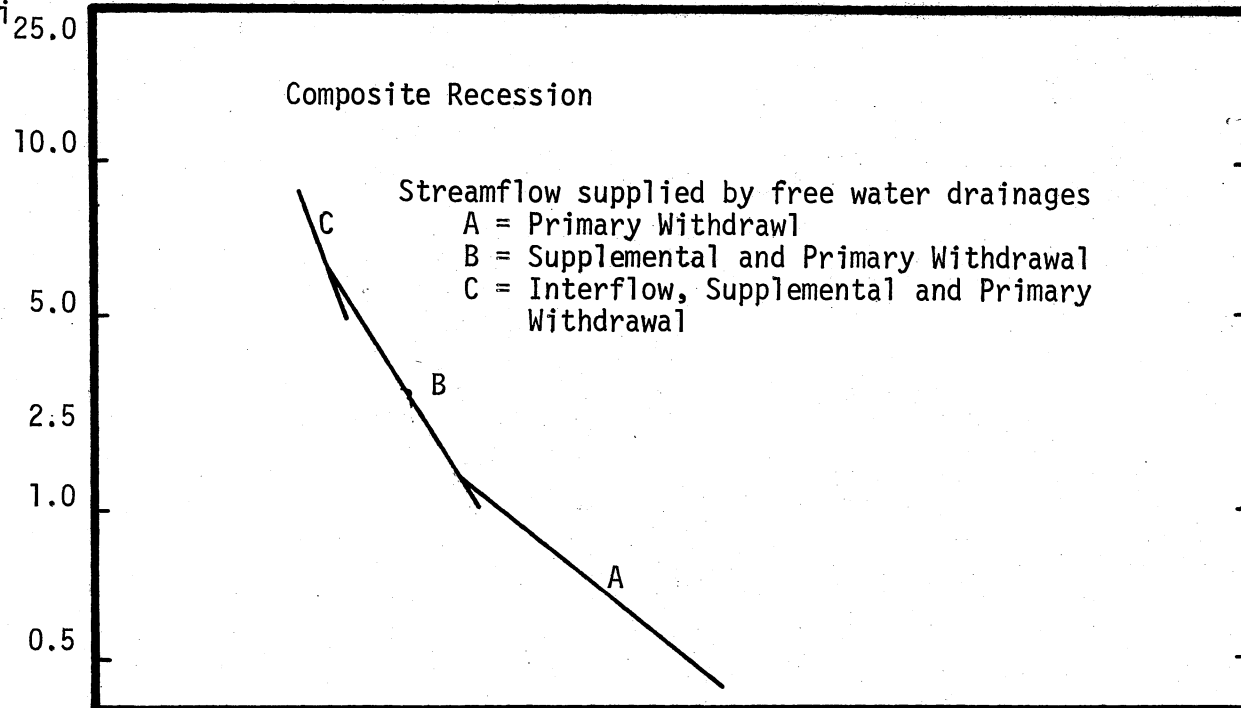


Figure 23. Recession Plot for the Sacramento Model

Source: (18), p. 21

If the ratio

$\frac{\text{Free Water Contents}}{\text{Free Water Capacity}}$ exceeds the ratio $\frac{\text{Tension Water Contents}}{\text{Tension Water Capacity}}$,

water is transferred from free water to tension water and the relative loadings are balanced in order to maintain a consistent soil moisture profile. However, a fraction of the Lower Zone Free Water is not available for such a transfer because it is considered to be below the root zone. To compensate for the discrepancies between observed evaporation data and actual evapotranspiration, twelve values are entered as variables in order to be able to adjust the evapotranspiration curve on a monthly basis.

Routing

Routing to the channel of the direct runoff from impervious areas, surface runoff, and interflow is by use of the unitgraph. Derivation of the unitgraph is found in standard references (2)(3).

Channel Storage

Channel storage routing is by use of the layered Muskingum routing technique (3). The model allows for four layers. This feature was designed to be omitted unless the unitgraph was obviously inadequate.

Model Accuracy

Although virtually no tests of the model are published, it would appear that this model should be capable of reasonably good simulations of flood flows. However, its capabilities for low-flow simulation are not yet established.

CHAPTER III

MODEL SELECTION AND BASIN DESCRIPTION

Model Selection

The state-of-the art indicates that use of any forecasting model that is not based on a simulation of the hydrologic cycle would be a step backward. This restricts the choice to either some version of the Stanford Watershed Model IV or the Sacramento Model. The decision was pragmatic. The author has used the NWSRFS version of the SWM IV for streamflow simulation and daily streamflow forecasting since 1971. Experience has shown it to be an excellent tool, and to give good results when the parameters are properly selected and when the observed data are accurate, and representative of actual conditions. Since the NWSRFS has demonstrated its ability to simulate flood flows, it was decided to test its ability to simulate low flows--leaving the other models for another study.

Basin Description

One approach to selection of the basin to be tested would be to select one which is known to have very good data, and which has given good results after testing. This approach was not used in this study, because this would not be representative of real conditions in the field. Rather, it was decided to use two gage stations on the Illinois

River in Oklahoma, because this exceptionally clean river is threatened with the possibility of degradation due to proposed construction of power and waste treatment plants within its watershed and there has developed the need to be able to project and forecast low flows for this river.

The Illinois River (see Figure 24) begins in the foothills of the Ozark Mountains, and then flows north and then west into Lake Francis, which is 0.8 miles above the Watts gage. The total basin is about 45 percent forests, 0.8 percent cities, and 52.8 percent farm and grazing land. Above Watts there is a considerable amount of farm land, although there are also numerous steep forested slopes, principally in the southern part of the basin. From Watts to Tahlequah, the terrain is mostly rolling hills with steep slopes, mostly forested. The forests are predominantly deciduous trees; the river is rather deeply incised into its flood plain for much of its course.

Illinois River near Watts, Oklahoma

This is a headwater basin of 635 square miles. The average discharge from installation of the gage in 1955 until 1972 was 525 cu ft per second (cfs), which is equivalent to 11.30 inches of runoff or 382,500 acre-feet per year. The maximum discharge was 68,000 cfs (stage was 25.96 feet) on July 25, 1960, and the minimum discharge was 8.6 cfs on October 26, 1955, September 19, 1956, and October 14, 1956. Records were rated as good (within 10 percent) by the U. S. Geological Survey. Low flows are regulated somewhat by Lake Francis Dam, which is 0.8 miles above the gage. The lake is normally full. Siloam Springs, Arkansas, has a small diversion for its municipal water supply in the

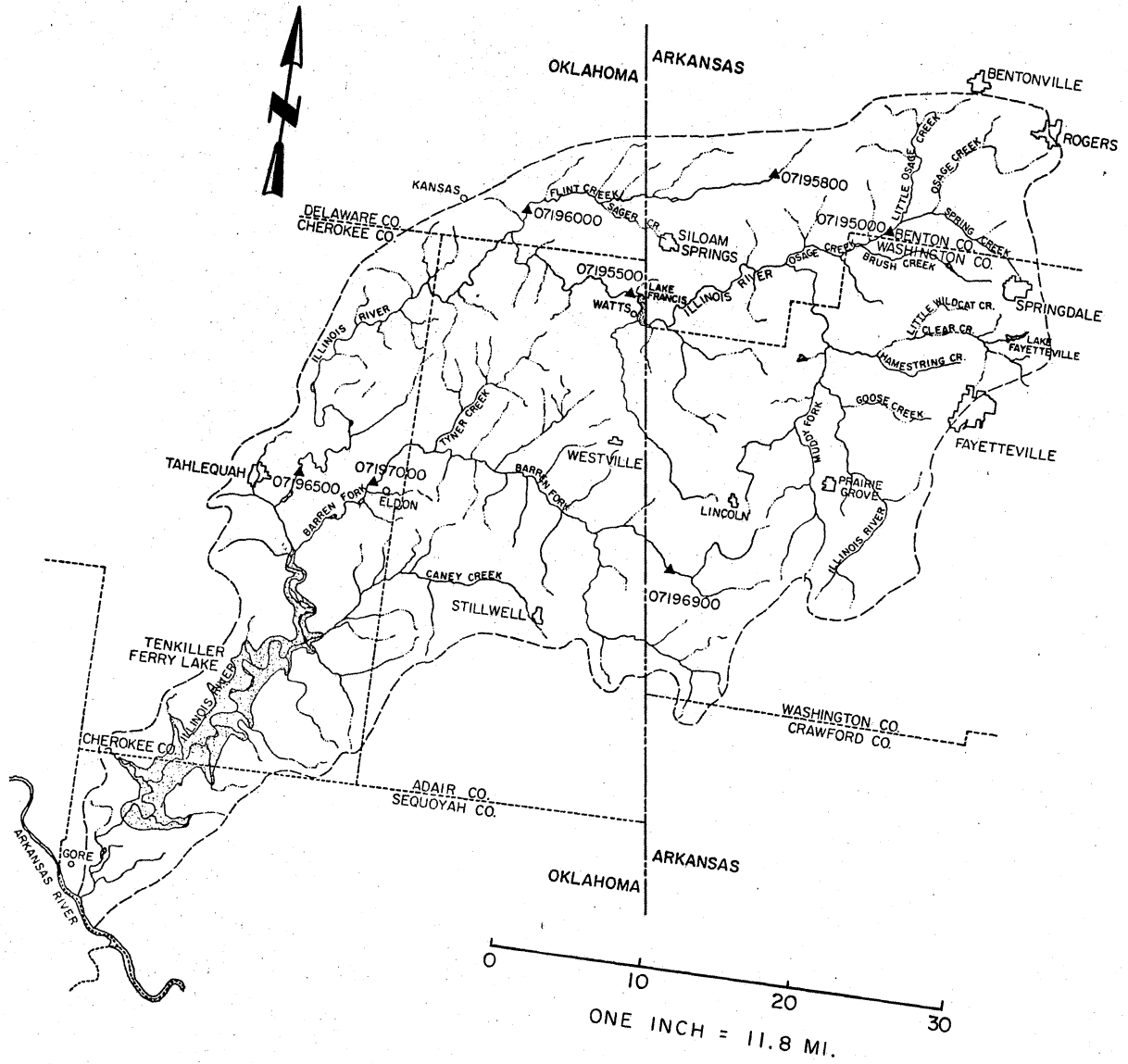


Figure 24. Illinois River Basin

pool near the dam. The dam is not regulated, but has an uncontrolled spillway. The average channel slope is 8.50 ft per mile. Annual precipitation for the basin averages 45.0 inches. The low water control is a gravel riffle, which is about 500 feet below the gage; however, aquatic growth sometimes causes this control to shift seasonally. The channel is straight for 0.5 miles both up and downstream from the gage.

Illinois River near Tahlequah, Oklahoma

The local drainage for Tahlequah is 324 square miles; while total drainage for the reach from Watts to Tahlequah is 959 square miles. Average discharge since gage installation in 1935 was 842 cfs, which is 11.92 inches or 610,000 acre-feet per year, while the maximum discharge was 150,000 cfs (27.94 ft) on May 10, 1950, and the minimum discharge was 0.1 cfs October 10-14, 1956. Records are rated as good. Channel slope averages 5.33 feet per mile. Annual precipitation averages 44.5 inches. The river bed is composed of gravel and rock. The left bank is high and does not overflow. The channel is effective as a control only at high flows, at medium flows control is an island 0.5 miles below the gage (rating is somewhat erratic due to the variable amount of drift getting caught in the trees on the island), and at low flows a gravel riffle which splits around the island is the control. The City of Tahlequah has its water supply intake and pumping plant 0.75 mile below the gage (0.25 mile below the low and medium water controls).

CHAPTER IV

RESULTS AND DISCUSSION

Calibration of the NWSRFS

Calibration (fitting) of a model consists of adjusting all of the model's parameters to give the best match of simulated versus observed flow over a given period of record. A parameter optimizing program using the hill climbing technique has been developed to aid in this process (9)(15) and used with care there are situations in which it can be of use. However, it is really useful only for optimizing the parameters once good values have already been determined by trial and error. If the parameter values that go into the optimizing program are not already good values, the program will proceed to climb the wrong hill and the result will be a worse fit than before. In many cases, the rush to get the model fit to a given basin combined with monetary constraints results in the use of the already "good" parameters. In the operational field, pragmatism is the rule of the day and, although it is desirable to fit a basin to the limits of the accuracy of the model and the data, this may be a somewhat lengthy process, and when the rains come, a basin that is operationally ready, although fit with parameters that are only "good," is certainly preferable to a basin that is not operationally ready. Obtaining good parameter values is also a learning experience for the analyst. As he changes the parameters and sees how the

simulation changes, he gains understanding of the hydrologic characteristics of the basin. So the skill and knowledge of the user also can increase through use of the model. Thus, the process of parameter development is essentially a manual process, although the parameter optimizing program can be useful.

With the larger flows, the rainfall is usually more uniform, the errors are smaller (proportionally), and stages change less for a given discharge increment than for low flows. Low flows are mostly the result of groundwater flow with the addition of some runoff produced by small storms, which by their nature are spatially less uniform. Monitoring low flow processes is also more difficult than high flow processes. These indicate that the problem of fitting a model for low flows may be more difficult than for high flows. Total hydrograph reconstitution takes more work than just fitting the rises, and is a real test of the validity of the model as well as the accuracy of the data.

Since low flows have been of no real concern, they have been of little interest in operational model fitting up to this time. As a result, the tendency has been to obtain a good fit for rises--especially the more significant rises--and not worry too much about low flows. Some have even found it difficult to do otherwise. The approach has sometimes been to fit the larger rises well then quit unless the fit at lower flows was unusually bad. It may be that this is backwards. The small rises--the little events--often tell us more about the hydrologic characteristics of a basin than the large events, where much of the detail is lost. Most simulations have been made using hydrograph plotting scales at which low flow events are hidden, so are not usually noticed. Experience has shown that a basin can be fit with different

sets of parameters, many of which are hydrologically unsound, and that can easily happen if low flow events are ignored.

The calibration of the NWSRFS involves a series of steps that are not rigidly ordered, although it will become obvious that certain steps must precede certain other steps. Although the whole procedure will be discussed as it was applied to the two basins on the Illinois River, the procedures will be applicable to other basins. This section will outline the procedures necessary to make simulation (verification) runs using the NWSRFS. This will be accomplished by discussing the data preparation procedures and the initial selection and modification of parameters required to fit the basins.

Raw Data

The raw hourly (observations every hour) and daily (observations once each 24 hours) precipitation data may be obtained on magnetic tape for each state from the National Climatic Center, Asheville, North Carolina, 28801. This data is available in the Office of Hydrology format, which must be reformatted to a standard tape format by use of the program HRTAPE. Ordering information for the data as well as a listing of the program HRTAPE is found in NWS HYDRO 14 (19) in Appendix B. Raw mean daily discharge records, either on tape or cards, are available for each state from the U. S. Geological Survey, Water Resources Division, Washington, D. C. This data must be converted to the standard tape format by use of the program DAILYF, which is listed in reference (9), Appendix D.

Mean daily PE data is available in the standard format either on tape or cards for 40 stations in the U. S. from the Research and

Development Laboratory, Office of Hydrology, National Weather Service, Silver Springs, Maryland.

Data that is on standard format cards must be converted to standard format tape by use of program NWSRFS2. NWS HYDRO 14 describes the standard format for cards in Appendix A, and gives a listing of NWSRFS2 in Appendix E.1. By obtaining the data from the sources and processing them, the raw data can be made ready for processing by the MBP program and/or combining onto one data tape (as described in the following sections).

MBP Computation Procedure

The method normally used for computation of the average areal precipitation uses the Grid Point weighting system (the MBP program also computes Thiessen weights). The first step in this procedure is to calculate the Grid Point weights for all of the precipitation stations.

Station Weight Computation

Once the basin to be calibrated has been selected, the next step is to outline the basin on a map such as the U. S. Geological Survey 1:250,000 scale topographical charts. Then overlay the outlined basin with a transparent 80 by 80 grid placed so that the 1-1 point is in the upper left corner (Figure 25). If more than one nearby basin is to be calibrated, time may be saved by overlaying up to ten basins at a time. A map of the basin is then prepared by assigning a "1" to every grid intersection that falls within the basin outline, and inputting this map line by line to the program. Each horizontal line is represented by an 80-column computer card, with the "1"s punched at their proper locations.

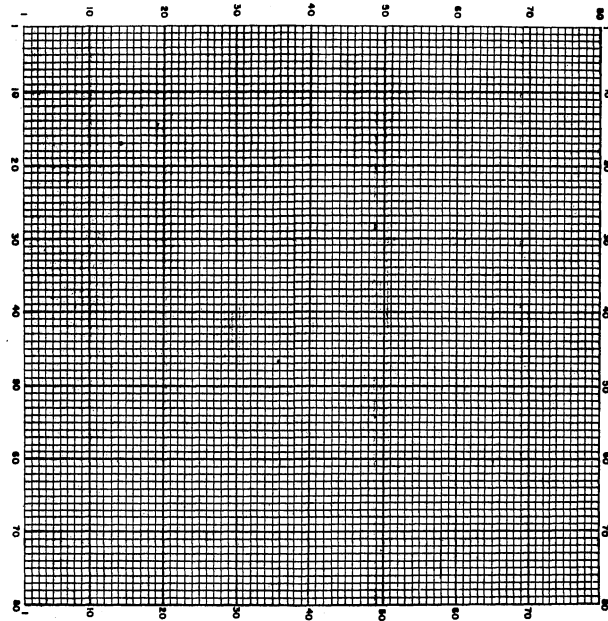


Figure 25. Grid Placement for
Basin Gridding

Eighty such cards are required for each basin (some cards may be blank). The same grid overlay should then be rotated 90 degrees so that the 1-1 point is at the lower left corner (Figure 26). Using this grid arrangement, the X-Y coordinates of each precipitation station can then be determined. The basin grid map and the precipitation station X-Y coordinates are then entered into the MBP program and the Grid Point weights are computed for each of the stations used. A listing of input data instructions, sample input deck, and a sample output listing are contained on pages C-2 through C-15 of NWS HYDRO 14 (9), so this information will not be duplicated in this report. The MBP program as well as all of the programs mentioned in this report can be obtained from the Office of Hydrology, National Weather Service, NOAA, Silver Spring, Maryland, 20910.

MBP Computation for Each Basin

Once the station weights were determined, each station (with a weight greater than 0.0) together with its Grid Point weight and the precipitation data (both hourly and daily) for the desired period of record (in this case, 10/63-9/71) was used as input to the MBP program; then the MBP for the basin was computed and written on magnetic tape in the required format as a continuous record of six-hour incremental MBP.

In order to be able to define the rainfall patterns more precisely, the NWSRFS allows a basin to be divided into sub-areas for MBP computations. According to Morris (16), this can significantly improve the simulation accuracy for non-uniform precipitation events. The Watts and Tahlequah basins were both divided into two basins each, giving a

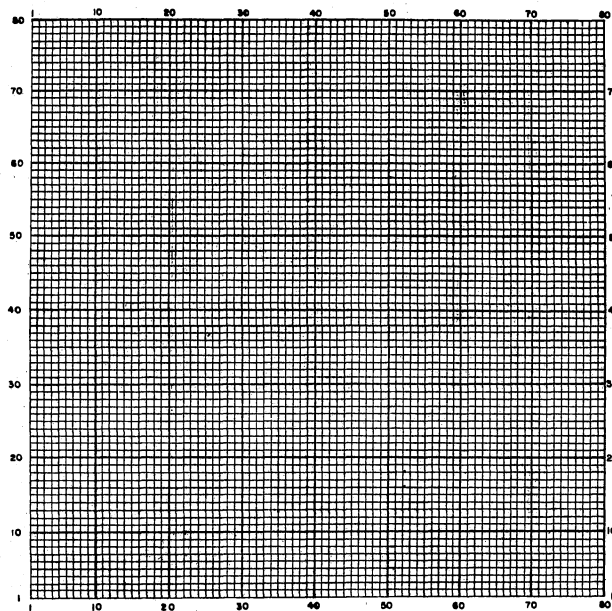


Figure 26. Grid Placement for Precipitation Station Coordinates

total of four MBP areas for the two basins (Figure 27). The weights for each of the four zones are given in Table IV.

TABLE IV
MBP AREA ASSIGNMENTS AND HISTOGRAMS FOR WATTS AND TAHLEQUAH

<u>Illinois River near Watts, Oklahoma</u>								
Histogram Element Number	1	2	3	4	5	6	7	8
Histogram Element (fraction)	.037	.195	.262	.249	.156	.077	.022	.001
MBP Area Assignment	1	1	1	2	2	2	2	2

<u>Illinois River near Tahlequah, Oklahoma</u>								
Histogram Element Number	1	2	3	4	5	6	7	8
Histogram Element (fraction)	.001	.030	.140	.300	.270	.121	.050	.029
MBP Area Assignment	3	3	3	3	4	4	4	4

Histogram Element Number	9	10	11	12	13	14
Histogram Element (fraction)	.022	.018	.013	.003	.002	.001
MBP Area Assignment	4	4	4	4	4	4

Potential Evapotranspiration (PE) Computation

The PE data was obtained on cards from the Fort Worth River Forecast Center in Fort Worth, Texas. The station used was the Class A pan at Fort Gibson Dam, Oklahoma.

Streamflow Computation

The mean daily flows for Watts and Tahlequah were extracted, as discussed under Raw Data, from data tapes obtained from the U. S.

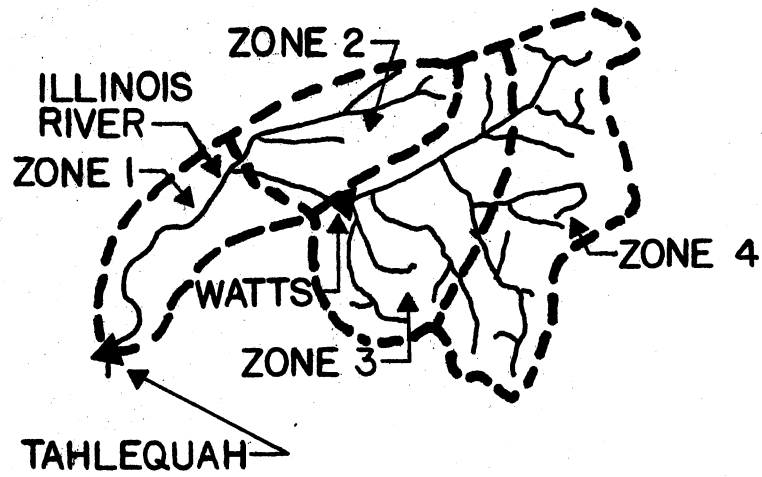


Figure 27. MBP Zones

Geological Survey. The six-hour incremental inflow into the reach below Watts was generated by the simulation run at Watts, placed on temporary disk storage, and used by Tahlequah.

Combined Data Tape

As extracted, the data is on three or four different tapes. In order to reduce the number of tapes, thereby increasing the efficiency of the program, all of the data for the two flow points were put on one data tape by a program called SUPRTP (Appendix E.2 of NWS HYDRO 14 (9) contains a listing of SUPRTP). SUPRTP takes the data on two-four different tapes and combines them on one tape in month-size blocks.

At this point, all of the data required for Watts and Tahlequah, except for the six-hour incremental outflow from Watts, was on one data tape. In this case, both Watts and Tahlequah were simulated sequentially in one computer run, and the six-hour outflow from Watts was generated during each run, placed in temporary storage on disk files, and used when required for the Tahlequah simulation.

Channel Time Delay Histogram

The method used to route flow from the local surface area of a basin to its outflow point is the time delay histogram. This essentially divides the basin into zones of equal travel time (each zone having a different travel time). In Figure 27, the Illinois River basin is divided into four zones, one through four, whose average travel time would be 6-24 hours. The histogram gives the fraction of the flow from each of the four zones. To account for areal variation in runoff, each element of the histogram can have its own separate soil moisture

accounting system (and MBP area). For this study, each of the two basins was divided into two zones (Figure 27). The assignment of the histogram elements for Watts and Tahlequah is given in Table IV. These histogram values were computed by the Tulsa, Oklahoma River Forecast Center staff during initialization of these basins.

The method of developing a histogram is based on the derivation of the unitgraph for that basin. The first step is to derive the unitgraph for the basin [the unitgraph derivation technique is described by Lindsley, Kohler, and Paulhus (2)(3)]. This unitgraph will contain only direct runoff. The histogram ordinates can then be calculated by backrouting the unitgraph by using the following mathematical relationship

$$\bar{I} = \frac{O_i + 1 - \frac{K-3}{K+3}}{1 - \frac{K-3}{K+3}}$$

where

\bar{I} = histogram ordinate

O_i = instantaneous outflow at the time, i

K = six-hour storage constant (the normal range of K is from six to twelve hours, with nine hours being the normal first guess. K must be greater than 3.0)

The histogram elements used in the NWSRFS are simply normalized values of \bar{I} . This procedure has been computerized at the Lower Mississippi River Forecast Center, Slidell, Louisiana.

Selection of Initial Parameter and Soil Moisture
Values and the Effect of Changes Leading
to the Final Values

The initial as well as the final parameters and soil moisture values are found in Table V. The final 1 parameters were developed mostly by the Tulsa River Forecast Center, while the Final 2 parameters resulted from this study. Both are presented in order to illustrate that different parameter sets can give similar results (both good); however, only the Final 2 values will be discussed. Values for the Illinois River near Watts and Tahlequah, Oklahoma, will be identified by the names Watts and Tahlequah, respectively.

Each of the parameters required for the model will be discussed in alphabetical order. The initial values for each of these parameters were determined by one of four methods:

- 1) calculation using equations derived from observable watershed hydrologic characteristics
- 2) parameters transferred from a nearby basin which was already calibrated
- 3) knowledge of the hydrologic response of the basin, and
- 4) parameters taken from a set of typical values (Table VI).

Discussion of initial parameter derivation will be limited to those that can be calculated.

Parameter A

"A" is the percent of the total watershed area covered by lakes, streams, and impervious areas (excluding areas such as isolated rock

TABLE V
INITIAL AND FINAL PARAMETER VALUES

Parameter	Illinois River near Watts, Oklahoma		Illinois River near Tahlequah, Oklahoma		
	Initial Value	Initial Value	Initial Value	Final 1 Value	Final 2 Value
K1	1.000	1.000	1.000	1.000	1.000
A	0.000	0.002	0.000	0.000	0.001
EPXM	0.350	0.200	0.840	0.620	0.850
UZSN	0.330	0.380	0.900	0.782	0.800
LZSN	8.500	7.500	10.000	8.398	9.000
CB	0.990	0.120	0.106	0.103	0.150
POWER	1.388	2.500	0.450	1.654	0.450
CC	0.857	1.400	1.200	1.386	1.000
K24L	0.070	0.000	0.100	0.201	0.000
K3	0.473	0.300	0.300	0.317	0.280
GAGEPE	1.000	1.000	1.000	1.000	1.000
E-HIGH	0.930	1.500	1.250	1.005	1.300
E-LOW	0.202	0.080	0.300	0.126	0.150
K24EL	0.000	0.000	0.000	0.014	0.007
SRC1	0.900	0.900	0.900	0.846	0.900
LIRC6	0.060	0.060	0.080	0.051	0.080
LKK6	0.007	0.010	0.014	0.149	0.010
KV	0.439	0.439	2.176	3.015	2.176
KGS	0.993	0.820	0.937	0.9012	0.8370
STHIGH	171	171	171	162	171
NDUR	40	40	40	16	40
STLOW	46	46	46	46	46
NEP	0	0	0	0	0
KS1	9.00	9.00	9.0	0.00	0.00

The histograms and lag curve were unchanged from initial to final run

Histogram - Watts: 0.037, 0.195, 0.262, 0.249, 0.156, 0.077
0.022, 0.001

Histogram - Tahlequah: 0.001, 0.030, 0.140, 0.300, 0.270, 0.121,
0.050, 0.029, 0.022, 0.018, 0.013, 0.002,
0.001

Tahlequah LAG and K:

Variable Lag (hours) - Final 1: 44.0 33.0 18.0 18.0

- Final 2: 56.0 33.0 18.0 18.0

Flow (cfs) - Both: 0.0 500.0 1000.0 2000.0

Variable K (hours) - Both: 12.0 9.0 9.0 120 12.0

Flow (cfs) - Both: 0.0 1500.0 7100.0 10000.0 25000.0

TABLE VI
TYPICAL INITIAL PARAMETER VALUES AND RANGES

No.	Name	Typical Value	Normal Range	Calculation Procedure
1	A	0.003	0.001 - 0.005	
2	CB	0.150	0.050 - 0.350	
3	CC	1.100	0.500 - 1.500	
4	CSSR	0.350	0.250 - 0.750	From histogram program: $CSSR = \frac{KS1-3}{KS1+3}$
5	EHIGH	1.150	0.900 - 1.500	
6	ELOW	0.400	0.200 - 0.900	
7	EPXM	0.170	0.100 - 0.500	See Table
8	GAGEPE (PEADJ)	1.000	1.000 - 1.000	
9	GWSI	0.000	0.000 - 0.000	Start run during dry weather
10	HWARP	N/A	0.400 - 2.000	
11	KGS	0.910	0.820 - 0.990	See Table
12	KS1	9.000	6.000 - 12.000	$KS1 = 3(1+CSSR)/(1-CSSR)$
13	KV	2.500	0.700 - 12.000	
14	K1	1.000	1.00 - 1.000	
15	K24EL	0.000	0.001 - 0.010	80% of "A"
16	K24L	0.000	0.000 - 0.250	
17	K3	0.280	0.200 - 0.350	See Table
18	L1RC6	0.100	0.050 - 0.150	
19	LKK6	0.010	0.003 - 0.150	$LKK6 = 1.0$ (daily recession) ^{0.25}
20	LZSI	COMPUTE	2.000 - 6.000	$LZSN = 0.5(LZSN)$
21	LZSN	8.500	4.000 - 12.000	
22	NEP	0.000	0.0 - -60.0	
23	NDUR	40.0	0.0 - -60.0	
24	PEADJ (GAGEPE)	1.000	1.000 - 1.000	
25	POWER	2.000	0.500 - 3.000	
26	RESI	0.000	0.000 - 0.000	Start run during dry weather
27	SCEPI	0.000	0.000 - 0.000	Start run during dry weather
28	SGWI	COMPUTE	0.100 - 0.500	$SGWI = \frac{GWF \text{ for first day of run}}{(LKK6)(107.7)(\text{basin area})}$
29	SRC1	0.900	0.800 - 0.950	
30	SRGXI	0.000	0.000 - 0.000	Start run during dry weather
31	STHIGH	150.0	100.0 - 200.0	
32	STLOW	46.0	30.0 - 55.0	
33	UZSI	0.000	0.000 - 0.000	Start run during dry weather
34	UZSN	0.250	0.050 - 0.400	
35	VWARP	N/A	0.700 - 2.000	

outcrops, building, or roads). Runoff from this area reaches the stream almost immediately (within one hour). It is a sensitive parameter both in respect to volume as well as hydrograph response, but its effects are primarily on small rises and the initial portions of larger rises (when "A" is increased, the small rises increase). "A" for Watts and Tahlequah was increased from 0.000 to 0.001 and 0.002, respectively, because some impervious area is present in all basins, without exception, and is needed to simulate the small rises properly. As a minimum, "A" must represent the stream surfaces themselves. Above 0.002, the smaller rises become excessive on the Illinois River, so "A" was finalized at 0.002.

CB

"CB" is the index to infiltration. It is the one-hour infiltration rate (inches/hour) when Lower Zone Storage (LZS) is at its nominal capacity (LZSN). It is a very sensitive parameter; small changes of CB produce large hydrograph changes as well as moderate annual volume changes. Decreasing CB increases the wave amplitude and causes the peaks to occur earlier and higher due to the increased fast response flow. The initial values of CB for Watts (0.99) and Tahlequah (0.106) were increased to 0.120 and 0.150, respectively, in order to reduce excessively high peak flows. Table VII gives initial CB values based on soil permeability.

TABLE VII
INITIAL CB VALUES

Soil Permeability	CB(inches/hour)
low	0.05
medium	0.10 - 0.20
high	0.25 - 0.50

CC

"CC" is the ratio $\frac{\text{interflow}}{\text{surface runoff}}$. It influences the time distribution of the flow, not the volume. It is only moderately sensitive. If CC is decreased, the proportion of surface runoff increases and the hydrograph peaks become higher, sharper, and slightly earlier; however, only the storm hydrograph is affected, not dry weather flow. The initial value of CC for Watts (0.857) was increased to 1.400 because there was a need for more interflow during the falling limb of the hydrograph, while Tahlequah (1.200) was reduced to 1.000 due to excessive interflow.

EHIGH

"EHIGH" is the maximum value of the annual evapotranspiration (ET) curve (Figure 28). EHIGH is reached after the number of days given by STHIGH, and it remains there for the number of days given by NDUR. As EHIGH is increased, the ET losses increase. Its effect is seasonal, and its reaction is usually only moderately sensitive, although there are times when the ET curve is at EHIGH when the storm simulation becomes markedly sensitive to EHIGH changes. All ET curve parameters should be similar for a given region. All initial values for Watts (0.930) and Tahlequah (1.250) were increased to 1.500 and 1.300, respectively, because the initial ET losses were too low during the summer.

ELOW

"ELOW" is the minimum value of the annual ET curve (Figure 28). ELOW is reached after the number of days given by STLOW, and it remains

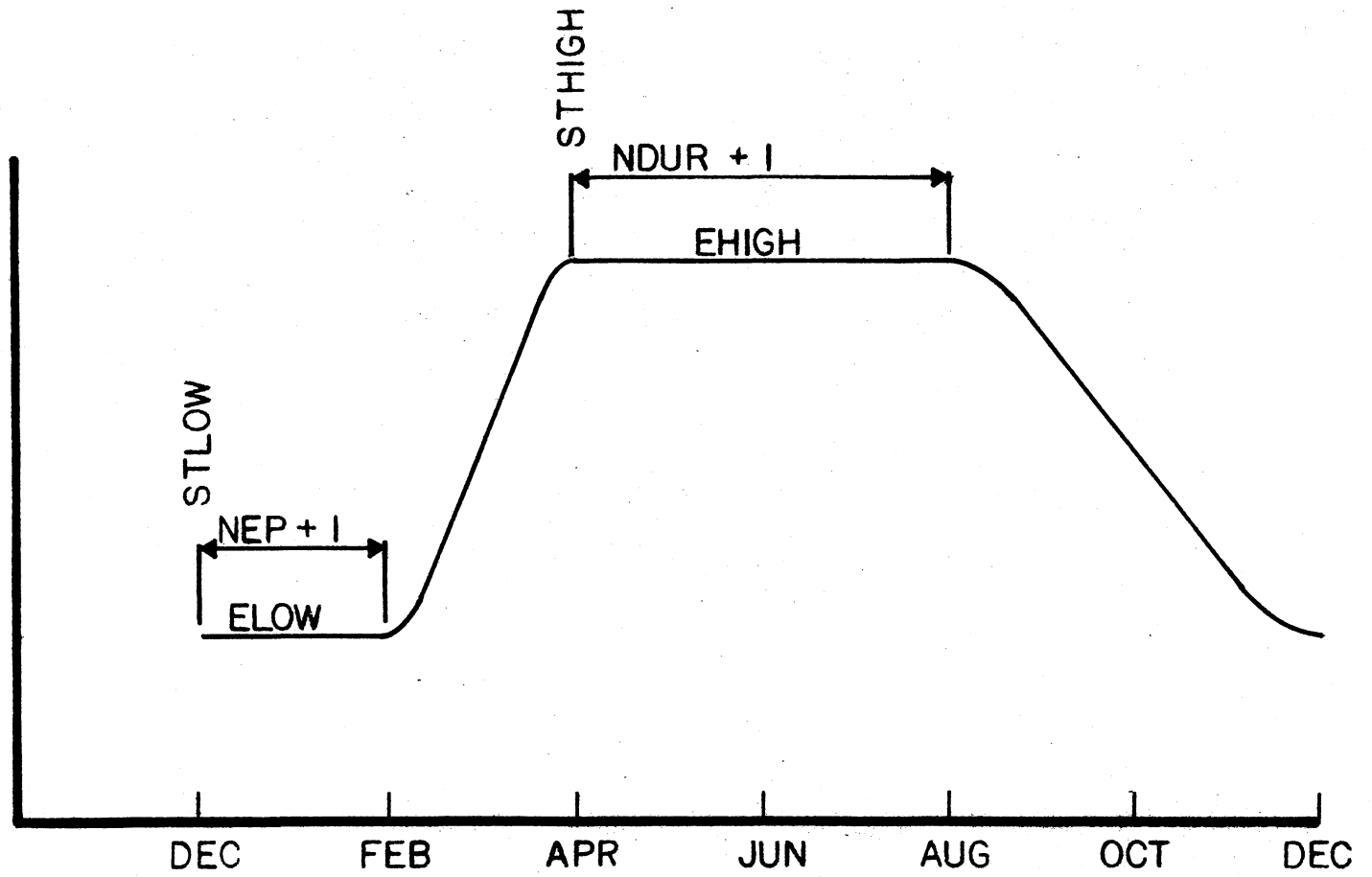


Figure 28. Evapotranspiration Curve

there for the number of days given by NEP. As ELOW is decreased, the ET losses decrease during the period of ELOW, but it is only moderately sensitive. Initial values of ELOW can be taken from Table VIII.

TABLE VIII
INITIAL ELOW VALUES

Area	ELOW
Southern	0.60
Mid-latitude	0.30
Northern	0.00

The initial values for Watts (0.20 and Tahlequah (0.300) were reduced to 0.080 and 0.150, respectively, because the ET was too high during winter.

EPXM

"EPXM" is the maximum interception storage (inches). It is moderately sensitive for small rises, but has relatively little effect on large rises. Increasing EPXM reduces the small rises. When the small rises are more predominant during one period of the year, EPXM exerts a seasonal effect. It has little effect on the annual flow volume. Table IX gives initial values for EPXM based on basin characteristics. Table IX illustrates the greater effect that EPXM has on lower flows than higher flows. Table IX shows the seasonal effect of EPXM changes. The initial EPXM value for Watts (0.350) was reduced to 0.200 to increase the small rises, while Tahlequah (0.840) was not changed significantly (0.850).

TABLE IX
INITIAL EPXM VALUES

Vegetation	EXPM (inches)
Grassland	0.10
Moderate Forest	0.020-0.130
Heavy forest	0.15 - 0.20
Exceptions	
Many farm ponds	1.50
Many natural ponds	0.30 or greater

TABLE X
EXAMPLE OF CHANGE IN LAYER BIAS DUE TO INCREASE IN EPXM

Flow Interval (cfs)	Percent Bias EXPM = .100	Percent Bias EXPM = .500	Percent Change
29-177	+23.7	-21.3	-45.0
177-645	+16.8	-15.3	-32.1
645-1761	+2.8	-14.4	-17.2
1761-4000	-4.3	-15.6	-14.3
4000-8003	-9.8	-17.3	-7.5
8003-14595	-.3	-5.1	-4.8

TABLE XI
 EXAMPLE OF CHANGE IN MONTHLY BIAS DUE TO INCREASE IN EPXM

Month	Percent Bias EXPM = .100	Percent Bias EXPM = .500	Percent Change
Oct	+21.2	-30.8	-52.0
Nov	-39.7	-52.2	-12.5
Dec	-15.2	-36.5	21.3
Jan	-.3	-21.2	-20.9
Feb	+.1	-6.7	-6.8
Mar	-.5	-21.3	-20.8
Apr	-2.1	-24.8	-22.7
May	-4.6	-15.7	-11.1
Jun	+39.9	-4.3	-44.2
Jul	+34.8	-5.8	-40.6
Aug	+11.1	-17.7	-28.8
Sep	+18.6	-12.5	-31.1

GAGEPE

"GAGEPE" moves the entire ET curve higher or lower. It should be used only if there is a significant bias in the Potential Evapotranspiration (PE) data. Normally, GAGEPE is left at 1.000, as it was for Watts and Tahlequah. This is an extremely sensitive parameter; small changes produce large hydrograph and annual volume changes. Increasing GAGEPE increased the ET, thereby decreasing the flow.

GWSI

"GWSI" is the initial groundwater slope. It is normally assumed to be 0.000 because the run is normally begun during dry weather (as was done with Watts and Tahlequah).

KGS

"KGS" is the six-hour groundwater carryover. It is one of the parameters allowing variable groundwater recession. It is an index to the time required to reach fair weather recession. Initial KGS values should be set according to Table XII.

TABLE XII
INITIAL KGS VALUES

Time to Reach Fair Weather Recession	KGS
1 - 2 months	0.97 - 0.98
1 month	0.94 - 0.96
short	0.90 - 0.93
very short	0.85 - 0.90

The initial value for Watts (0.993) was reduced to 0.820 in order to reduce the rate of groundwater recession. Tahlequah, at 0.837, was not changed.

KS1

"KS1" is the channel storage recession parameter. It represents the

histogram lag, and is normally between 6.0 and 9.0 hours, having a minimum value of 3.0 and a normal maximum of 12.0 (if greater than 12.0, the histogram should be revised). It is computed from the CSSR value (obtained from the histogram computation program) by use of the following equation

$$KS1 = 3(1.0 + CSSR)/(1.0 - CSSR)$$

or a starting value of 9.0 is assumed (as was done for Watts). Watts KS1 was not changed from 9.0 during the run. Tahlequah's KS1 was set and left at 0.0 due to use of variable K for that basin.

KV

"KV" is the major parameter allowing a variable recession for the groundwater flow (other parameters are KGS and IKK6). The larger KV is, the steeper the recession is. KV has little effect on volume, and only a moderate effect on the hydrograph shape. The initial values for Watts (0.439) and Tahlequah (2.176) were not changed.

K1

"K1" is the adjustment factor for MBP that is uniformly too high or too low. Raising K1 increases the amount of MBP along with the annual flow volume. This is a very sensitive parameter that is normally set to 1.00 (as was done for Watts and Tahlequah).

K24EL

"K24EL" is the fraction of the total watershed area from which ET occurs at the potential rate. It is the percent of the watershed with

shallow groundwater that is within reach of vegetation.

Initial values of K24EL are usually set at 0.000, as was done for Watts and Tahlequah. Only Tahlequah was changed (to 0.007 to reduce the groundwater flow in the summer).

K24L

"K24L" is the percent of groundwater inflow that percolates to deep (inactive) groundwater storage. It is the percent of groundwater recharge assigned to deep percolation. An increase of K24L decreases flow, but the annual losses are normally small compared with rainfall. It is a moderately sensitive parameter. It provides a way of reducing the groundwater flow in a relative uniform manner. The initial values for Watts (0.070) and Tahlequah (0.100) were reduced to 0.000 to reduce excessive groundwater losses.

K3

"K3" is the index to the actual ET losses. It is a sensitive parameter that has considerable effect on flow volumes as well as hydrograph shape. Initial values should be either selected from Table XIII or set using a similar basin.

TABLE XIII
INITIAL K3 VALUES

Watershed Cover	K3
Open Land	0.20
Grassland	0.23
Light Forest	0.28
Heavy Forest	0.30

The initial values for Watts (0.473) and Tahlequah (0.300) produced too high ET losses, so were reduced to 0.300 and 0.280, respectively.

LIRC6

"LIRC6" is the interflow (medium response runoff) routing coefficient; it is the percent of interflow detention storage reaching the channel each six hours. It is normally set at 0.900 and not varied during calibration, its effect being compensated for by other parameters--mainly CC. Other work, however, indicated other values for these basins. Watts and Tahlequah were set to 0.060 and 0.080, respectively, and not changed.

LKK6

"LKK6" is the complement of the six-hour fair weather groundwater recession coefficient. It is the percent of groundwater storage that reaches the channel each six hours when $KV = 0.0$. The initial value for LKK6 is normally computed by the equation

$$LKK6 = 1.0 - (KK24)^{\frac{1}{4}}$$

where

KK24 is the 24-hour recession coefficient = today's flow/yesterday's flow. If LKK6 is reduced, groundwater flow recession will be slowed, resulting in flatter, higher recession hydrographs. The initial values for Watts (0.007) and Tahlequah (0.014) were both changed to 0.010--Watts because the groundwater recession was too rapid, and Tahlequah because the recession was not rapid enough.

LZSI

"LZSI" is the initial amount (inches) of water held in lower zone storage (LZS). It is normally set equal to 0.5(LZSN) due to beginning the run during dry weather; however, Table XIV gives values for other conditions. Since LZSI simply provides a starting place for LZS, a LZSI of the proper magnitude will suffice. By the end of the first 30-60 days, its effect will be minimal.

TABLE XIV
INITIAL LZSI VALUES

Moisture Supply	
Dry Weather	0.50 (LZSN)
Little Precipitation	0.75 (LZSN)
Normal Precipitation	1.00 (LZSN)
Above Normal Precipitation	1.25 (LZSN)

LZSN

"LZSN" is the nominal lower zone storage capacity (inches). It is about one-half of maximum LZ capacity. It is a sensitive parameter that has a major effect on the volume. If LZSN is decreased, the annual flow volume increases, hydrograph peaks become sharper and higher, recession becomes more rapid, and infiltration is decreased. The initial values for both Watts (8.500) and Tahlequah (10.00) were reduced to 7.500 and 9.000, respectively, in order to obtain more fast response runoff and thereby raise the crests of rises.

NEP

"NEP" is the number of days the ET curve remains at ELOW. It is normally set equal to zero and changed only if an analysis of seasonal bias indicates a need for an adjustment. The initial values of zero for both Watts and Tahlequah were unchanged.

NDUR

"NDUR" is the number of days that the ET curve remains at EHIGH. It represents the average duration of the maximum or near maximum growing activity. It is normally set by use of a nearby basin, and changed after analysis of the simulation for seasonal bias. All ET curve parameters should be similar for adjacent basins. Both Watts and Tahlequah were not changed from their initial value of 46.0.

POWER

"POWER" determines the slope of the infiltration curve; the larger POWER is the faster infiltration. Rates change as the wetness ratio (LZS/LZSN) changes (Figure 18). It is moderately sensitive in respect to hydrograph shape, but has little effect on the annual flow volume. The initial value for Watts (1.388) was increased to 2.500 in order to give more infiltration during dry conditions and less during wet conditions. Tahlequah was not changed from 0.450.

RESI

"RESI" is the initial surface detention storage in inches. It is normally set equal to 0.000 because the run is started during dry

weather. Watts and Tahlequah were both set equal to 0.000.

SCEPI

"SCEPI" is the initial interception storage in inches. Since the run is normally started during dry weather, SCEPI is normally set equal to 0.000, as was done for Watts and Tahlequah.

SGWI

"SGWI" is the initial groundwater storage in inches. It is computed from the following equation:

$$SGWI = \frac{\text{groundwater flow for the first day of the run}}{(LKK6)(107.7)(\text{Basin Area})}$$

SRC1

"SRC1" is the fast response (surface detention) flow routing coefficient; it is the percent of calculated potential fast response (surface detention) flow that reaches the channel each hour. It was set at 0.900 for both Watts and Tahlequah and not changed.

SRGXI

"SRGXI" is the initial interflow detention storage in inches. It is normally set equal to 0.000, because the run starts during dry weather, as was done for Watts and Tahlequah.

STHIGH

"STHIGH" is the Julian date on which the ET curve reaches EHIGH, which is the date when the watershed vegetation reaches its maximum.

growing activity (about April 1 for southern basins, and about May 15 for northern basins). It is usually set according to nearby basins and changed after analysis of the simulation run for seasonal bias. The initial and final values for Watts and Tahlequah were 171 days.

STLOW

"STLOW" is the Julian date on which the ET curve reaches ELOW. It is normally set according to nearby basins (the most common date is 46), and changed after analysis of the data for seasonal bias. The initial and final dates for Watts and Tahlequah were 46 days.

UZSI

"UZSI" is the initial upper zone storage in inches. It is normally set equal to 0.000, since the run usually starts during dry weather. Watts and Tahlequah were both set to 0.000.

UZSN

"UZSN" is the nominal upper zone storage capacity; it is about equal to 1/3 of the maximum storage capacity. It includes both surface depression storage as well as storage in the soil profile near the soil surface. It is a very sensitive parameter that has a major effect on the annual flow volume, as well as small rises. Decreasing UZSN increases smaller rises and the beginning of larger rises. UZSN is normally larger than EPXM. If there is a deep litter layer, UZSN varies from 0.75-1.00. If the soil is permeable, UZSN varies from 0.10-0.25. The initial value for Watts (0.330) was increased slightly to 0.380 to decrease the amplitude of small rises, while Tahlequah (.900)

was decreased to .800 to increase the magnitude of the small rises.

LAG

"LAG" is the amount of constant lag for the reach from Watts to Tahlequah. It was set to 0.00 because all of the lag was accounted for by the variable lag (Table V).

The NWSRFS was calibrated for Watts and Tahlequah using an eight-year period of record--Water Years (October through September) 1964-1971. This period of record includes dry, wet, as well as average years. In the Appendix will be found a one-year sample of the output hydrographs, the actual computed (simulated) and observed mean daily flows (cfs), and the mean basin precipitation for each day. The period of record displayed was chosen to include a period with low flow values; these are not necessarily the years in which the fit was optimum. In fact, the simulation for Watts for that period is not extremely good but it does illustrate problems such as non-representative mean basin precipitation and streamflow measurements as well as the fact that there is some degree of regulation of low flows resulting from the dam and waterfall upstream at Lake Francis. Data for the whole period of record, however, does show that the overall fit for Watts is reasonably good. Seasonal bias is also quite in evidence for that year, which suggests that a more flexible method of defining the seasonal potential evapotranspiration would be useful in obtaining a better fit. More work would enable a better fit at Watts. The simulation for Tahlequah, however, is noticeably better than for Watts. Low flow simulation inadequacies for Tahlequah are due primarily to inadequate mean basin precipitation. Peak flows are not optimum for Tahlequah for this year, but

they are better during years with higher flows. The need for better seasonal potential evapotranspiration definition is also apparent for Tahlequah. The output for Tahlequah begins in November rather than in October, because Water Year 1964 was the first year of the run, and the soil moisture balance had not yet stabilized during October.

With the model calibrated for both Watts and Tahlequah, the NWSRFS may now be used for forecasting streamflow, for developing additional periods of records, and for examining the hydrologic effects of changes to the watersheds. As there is much interest in developing records of extreme values of streamflow for these basins, it should be noted that this can now be done by simply running the model using synthetic data. For a synthetic record of low flows, mean basin precipitation and potential evapotranspiration data reflecting drought conditions can be generated for as long a period as desired and used with the NWSRFS to produce the desired low flow records. In fact, synthetic streamflow records of any desired length for any desired climatic conditions can be generated simply by using the appropriate mean basin and potential evapotranspiration data. Watershed changes can also now be examined by changing some of the parameters and running the model. For example, extensive deforestation could be simulated by reducing EPXM, and extensive creation of impervious areas could be simulated by increasing A. Various combinations can be created by thoughtful variation of the parameters which will cover most changes possible to a watershed, both for past periods of record as well as for generated future records.

Discussion of the Calibration

The process of calibrating a model to a basin can be a long, tedious process that has no clear-out ending point. Normally, the analyst must establish criteria that will tell him when to stop. The criteria are usually time, money, or goodness-of-fit. The limiting resource for this study was time. The results are given in Tables XV and XVI.

TABLE XV
MODEL FIT BY FLOW INTERVALS FOR TAHLEQUAH
WATER YEARS 1964-1971

Flow Interval (cfs)	Number of Observed Cases	Observed Mean Flow (cfs)	Simulated Mean Flow (cfs)		Percent Bias	
			(1)	(2)	(1)	(2)
0-33	6	32	35	35	9.4	9.4
33-88	199	69	72	70	4.3	1.4
88-200	891	136	130	125	4.4	8.1
200-399	573	287	287	278	0.0	3.1
399-727	487	552	549	536	0.5	2.9
727-1234	370	943	885	873	6.2	7.4
1234-1983	201	1518	1473	1955	3.0	3.0
Above 1983	195	4287	4205	4116	1.9	4.0

TABLE XVI
 MODEL FIT BY FLOW INTERVAL FOR WATTS
 WATER YEARS 1964-1971

Flow Interval (cfs)	Number of Observed Cases	Observed Mean Flow (cfs)	Simulated Mean Flow (cfs)	Percent Bias
0-88	522	67	66	-1.4
88-200	911	135	144	6.3
200-399	545	286	336	14.9
399-727	508	535	552	3.2
727-1234	226	921	855	-7.2
1234-1983	105	1528	1419	-7.1
Above 1983	105	4206	2990	-28.1

The U. S. Geological Survey rates the accuracy of measurements taken at the two stations as "good," which represents an accuracy within ten percent. Accordingly, it was decided that a fit that yielded biases less than ten percent would be acceptable. Inspection of Tables XV and XVI shows that the fit obtained for Tahlequah is thus acceptable, while the fit for Watts is outside the limits for flows from 200-399 cu ft per second (cfs) and above 1983 cfs. The reasons that better results were not obtained at Watts are inaccurate data, insufficient data, and deficiencies in the model itself. Experience with other basins has shown it is common to have difficulties fitting a headwater basin accurately. Inspection of the data disclosed numerous occasions where the

river stage at Watts rose, although no precipitation had been recorded in the basin. Obviously, rain had fallen in places other than in the rain gages. With thunderstorm activity especially, it is not surprising that the rain often misses the eight-inch rain gages, although it may fall nearby. With most of the precipitation stations reporting on a daily basis and the others every six hours, there is ample room for error also in the precipitation timing. Averaging the precipitation over the basin can sometimes erroneously spread precipitation over areas where it did not fall, as well as reduce the intensity over the area where it did fall. The rating of a gage can also change due to channel configuration changes as well as vegetative growth and accumulation of debris. The rating at Watts is known to occasionally vary seasonally due to aquatic growth. In basins such as these, where most of the trees are deciduous, the surface area available for interception storage varies widely both during the course of a year as well as from year to year, depending on meteorological conditions. However, the model cannot account for year to year changes except by parameter changes to give some sort of average fit for each year, and the only way of controlling seasonal changes is through changes in the evapotranspiration curve, which is only an indirect method, and not really satisfactory for an area in which interception is as important as it is in these basins.

The model fit for Tahlequah is obviously much better than the fit for Watts. Experience with numerous other basins has shown that this is normal; reaches are usually fit more accurately and easily than headwater basins. The reason for this is that a reach has a known inflow, while a headwater or even the local area of a reach does not.

The implication here is that the model does a better job of routing flow than it does of hydrologic simulation. Although this implication is probably true, it is also probably true that this is a result of the model being data bound, and as Linsley (6) stated, there is no point in trying to make a simulation model with greater accuracy than the stream gaging. His comment is just as applicable to precipitation measurements as to streamflow measurements. Still, it is apparent that the model needs to be refined still further to enable it to more closely match watershed responses. Further refinement, however, may lead to an increase in the number of parameters the analyst has to be concerned with, which would not be good. In its present state, there are more than enough parameters available to make the task of fitting a basin a complex matter. There is also a great degree of interaction among the various parameters. A given hydrograph can be reconstituted using many different parameter value sets--a good fit does not imply a unique set of parameters. These factors require considerable experience and ability on the part of the analyst to achieve a good fit.

Since both engineering and forecasting activities are primarily interested in results, the most desirable solution for the model fitting problem is a computer based parameter optimizing model. HYDRO 14 (9) describes such a currently available model, but it is only a step in the right direction. It requires a good fit prior to using it, and is not controllable as to how the model is fit (low flows, high flows, or seasons). The ideal parameter optimizing model would accept rough parameter values and would have adjustable fitting criteria, so that the analyst can emphasize that segment of the hydrograph or time of year

that needs to be refined. Since fitting errors are frequently systematic, and can be located in terms of flow intervals and/or time of year, the ability to work only on specific problems would be helpful. This approach would also cut down on the costs of using such a program.

CHAPTER V

CONCLUSIONS

Based on the results of this study of using a digital conceptual hydrologic model for simulating streamflow, the following conclusions can be drawn:

- 1) The NWSRFS can be used to simulate accurately low flows in addition to high flows, using as data only mean basin precipitation, potential evapotranspiration and, if the basin is a reach, the inflow to the reach.
- 2) It is more difficult to fit a headwater basin than a reach.
- 3) The limiting factors in model calibration are data and parametric complexities.
- 4) There are variations in a basin from one year to another, such as amount of vegetation and moisture conditions that cannot be accounted for by the model.
- 5) Once the NWSRFS has been calibrated for a given basin, it may be used to predict future streamflow, if synthetic mean basin precipitation, potential evapotranspiration and, if the basin is a reach, inflow to the reach.

CHAPTER VI

SUGGESTIONS FOR FUTURE STUDY

Based upon the findings of this investigation, the following suggestions are made for future work involving digital hydrologic simulation models:

- 1) Develop a parameter calibration model that can accept poor initial values, be susceptible to varying the optimizing criteria in order to concentrate on specific portions of the hydrograph (specified flow intervals and/or time of year), and be inexpensive to use.

- 2) Conduct comparison tests using the Sacramento model and the NWSRFS for low flows.

- 3) Modify the NWSRFS/SWM IV model to account for observable seasonal basin changes such as loss of leaves from deciduous trees, as well as relate the parameters better to physically observable features of the watershed.

A SELECTED BIBLIOGRAPHY

1. 92nd Congress, S. 2770, Public Law 92-500 (1972).
2. Lindsley, R. K., Kohler, M. A., and Paulhus, J. L. H. Applied Hydrology. New York: McGraw-Hill (1949).
3. Lindsley, R. K., Kohler, M. A., and Paulhus, J. L. H. Hydrology for Engineers. New York: McGraw-Hill (1974).
4. Neal, J. H., "The Effect of the Degree of Slope and Rainfall Characteristics on Runoff and Soil Erosion." University of Missouri Research Bulletin 280 (1930).
5. Ross, G. A., "The Stanford Watershed Model: The Correlation of Parameter Values Selected by a Computerized Procedure With Measurable Physical Characteristics of the Watershed." University of Kentucky Water Resources Institute Research Report No. 35 (1970).
6. Linsley, R. L., "A Critical Review of Currently Available Hydrologic Models for Analysis of Urban Stormwater Runoff." Hydrocomp International (1972).
7. Ligon, J. T., Law, A. G., and Higgins, D. H., "Evaluation and Application of a Digital Hydrologic Simulation Model." WRRRI, Clemson University (1969).
8. Richards, M. M., and Strahl, J. A., "Elements of River Forecasting." ESSA Technical Memorandum WBTM HYDRO 9, Dept. of Commerce (1969).
9. "National Weather Service River Forecast System Forecast Procedures." NOAA Technical Memorandum NWS HYDRO 14. Dept. of Commerce (1972).
10. U. S. Army Engineer District, Tulsa Corps of Engineers, "Appendix I to Technical Report No. 1 - Low-Flow Frequency Analysis." Civil Works Investigation Project CW-154 Minimum Volume Studies (1964).
11. Onstad, C. A., and Jamieson, J., "Subsurface Flow Regimes of a Hydrologic Watershed Model." Proceedings Second Seepage Symposium. U. S. Dept. of Agriculture ARS 41-147 (1968).

12. Lichty, R. W., Dawdy, D. R., and Bergmann, J. M., "Rainfall-Runoff Model for Small Basin Flood Hydrograph Simulation." The Use of Analog and Digital Computers in Hydrology, IASH/AIHS-UNESCO, Vol. 2, pp 356-367 (1969).
13. Rockwood, D. M., "Application of Streamflow Synthesis and Reservoir Regulation--"SSARR"--Program to the Lower Mekong River." The Use of Analog and Digital Computers in Hydrology, IASH/AIHS-UNESCO, Vol. 1, pp 329-344 (1969).
14. Schermerhorn, V. P., and Kuehl, D. W., "Operational Streamflow Forecasting with the SSARR Model." The Use of Analog and Digital Computers in Hydrology, IASH/AIHS-UNESCO, Vol. 1, pp 317-322 (1969).
15. Burnash, R. J. C., Ferral, R. L, and McGuire, R. A., "A Generalized Streamflow Simulation System." U. S. Dept. of Commerce and State of California Dept. of Water Resources (1973).
16. Morris, David G., "The Use of a Multi-Zone Hydrologic Model With Distributed Rainfall and Distributed Parameters in the National Weather Service River Forecast System." Unpublished Manuscript (1974).
17. Crawford, N. H., and Linsley, R. K., "Digital Simulation in Hydrology: Stanford Watershed Model IV." Technical Report No. 39, Stanford University (1966).

APPENDIX

MEAN DAILY FLOW PLOTS

Nov	25.8	258.0	2580.0	Simulated	Observed	Precip
1	73.5	44.0	0.00	73.5	44.0	0.00
2	64.0	52.0	0.00	64.0	52.0	0.00
3	56.9	56.0	.14	56.9	56.0	.14
4	55.5	52.0	.00	55.5	52.0	.00
5	62.8	50.0	.05	62.8	50.0	.05
6	64.9	56.0	0.00	64.9	56.0	0.00
7	63.9	56.0	0.00	63.9	56.0	0.00
8	65.1	58.0	0.00	65.1	58.0	0.00
9	64.8	60.0	0.00	64.8	60.0	0.00
10	65.0	64.0	0.00	65.0	64.0	0.00
11	63.2	64.0	.00	63.2	64.0	.00
12	62.9	66.0	.01	62.9	66.0	.01
13	61.4	66.0	0.00	61.4	66.0	0.00
14	60.7	66.0	0.00	60.7	66.0	0.00
15	60.0	66.0	0.00	60.0	66.0	0.00
16	62.0	66.0	0.00	62.0	66.0	0.00
17	75.4	68.0	0.00	75.4	68.0	0.00
18	81.9	76.0	0.00	81.9	76.0	0.00
19	62.9	86.0	1.05	62.9	86.0	1.05
20	53.6	86.0	0.00	53.6	86.0	0.00
21	69.5	82.0	.01	69.5	82.0	.01
22	108.9	96.0	.31	108.9	96.0	.31
23	127.1	110.0	0.00	127.1	110.0	0.00
24	120.8	116.0	0.00	120.8	116.0	0.00
25	116.7	108.0	0.00	116.7	108.0	0.00
26	113.7	106.0	0.00	113.7	106.0	0.00
27	105.6	102.0	0.00	105.6	102.0	0.00
28	99.1	98.0	0.00	99.1	98.0	0.00
29	93.7	94.0	0.00	93.7	94.0	0.00
30	88.0	90.0	0.00	88.0	90.0	0.00

Mean Daily Flow Plot (cfs) Illinois River
near Tahlequah, Oklahoma, November, 1963
* = simulated
+ = observed

Dec - Jan	25.8	258.0	2580.0	SIMULATED	OBSERVED	PRECIP
1	86.4	86.4	86.4	*	*	0.00
2	84.4	84.4	84.4	*	*	0.00
3	84.8	84.8	84.8	*	*	0.00
4	79.0	79.0	79.0	*	*	0.00
5	78.9	78.9	78.9	*	*	0.00
6	78.7	78.7	78.7	*	*	0.00
7	78.8	78.8	78.8	*	*	0.00
8	79.7	79.7	79.7	*	*	0.00
9	81.4	81.4	81.4	*	*	0.00
10	75.4	75.4	75.4	*	*	0.63
11	73.3	73.3	73.3	*	*	0.45
12	76.2	76.2	76.2	*	*	0.00
13	103.3	103.3	103.3	*	*	0.00
14	132.9	132.9	132.9	*	*	0.00
15	134.1	134.1	134.1	*	*	0.00
16	126.8	126.8	126.8	*	*	0.00
17	118.5	118.5	118.5	*	*	0.00
18	110.5	110.5	110.5	*	*	0.00
19	104.8	104.8	104.8	*	*	0.00
20	99.4	99.4	99.4	*	*	0.00
21	97.9	97.9	97.9	*	*	0.00
22	94.0	94.0	94.0	*	*	0.30
23	92.0	92.0	92.0	*	*	0.00
24	98.2	98.2	98.2	*	*	0.00
25	106.1	106.1	106.1	*	*	0.00
26	105.9	105.9	105.9	*	*	0.00
27	104.6	104.6	104.6	*	*	0.00
28	103.3	103.3	103.3	*	*	0.00
29	104.3	104.3	104.3	*	*	0.00
30	104.4	104.4	104.4	*	*	0.00
31	102.0	102.0	102.0	*	*	0.00
1	100.1	100.1	100.1	*	*	0.00
2	98.0	98.0	98.0	*	*	0.00
3	96.6	96.6	96.6	*	*	0.00
4	94.9	94.9	94.9	*	*	0.00
5	91.5	91.5	91.5	*	*	0.00
6	91.8	91.8	91.8	*	*	0.00
7	93.9	93.9	93.9	*	*	0.00
8	94.8	94.8	94.8	*	*	0.00
9	102.1	102.1	102.1	*	*	0.06
10	85.5	85.5	85.5	*	*	0.00
11	74.6	74.6	74.6	*	*	0.00
12	84.8	84.8	84.8	*	*	0.12
13	77.1	77.1	77.1	*	*	0.00
14	66.4	66.4	66.4	*	*	0.00
15	65.4	65.4	65.4	*	*	0.00
16	67.6	67.6	67.6	*	*	0.00
17	72.4	72.4	72.4	*	*	0.00
18	76.5	76.5	76.5	*	*	0.00
19	74.6	74.6	74.6	*	*	0.00
20	70.4	70.4	70.4	*	*	0.00
21	68.0	68.0	68.0	*	*	0.00
22	66.3	66.3	66.3	*	*	0.00
23	66.5	66.5	66.5	*	*	0.00
24	65.9	65.9	65.9	*	*	0.01
25	66.1	66.1	66.1	*	*	0.00
26	57.1	57.1	57.1	*	*	0.00
27	58.2	58.2	58.2	*	*	0.00
28	61.0	61.0	61.0	*	*	0.00
29	59.7	59.7	59.7	*	*	0.00
30	59.1	59.1	59.1	*	*	0.45
31	58.7	58.7	58.7	*	*	0.03

Mean Daily Flow Plot (cfs) Illinois River near Tahlequah, Oklahoma, December, 1963-January, 1964. * = simulated + = observed

Feb	Mar	258.0	2580.0	SIMULATED	OBSERVED	PRECIP
1	.	.	.	58.0	94.0	.00
2	.	.	.	75.2	98.0	0.00
3	.	.	.	89.7	100.0	0.00
4	.	.	.	100.7	102.0	.40
5	.	.	.	92.1	122.0	1.03
6	.	.	.	76.7	128.0	.00
7	.	.	.	131.9	138.0	0.00
8	.	.	.	228.2	145.0	0.00
9	.	.	.	239.8	148.0	0.00
10	.	.	.	222.3	145.0	0.00
11	.	.	.	196.8	138.0	0.00
12	.	.	.	176.4	130.0	.30
13	.	.	.	175.1	132.0	.00
14	.	.	.	160.5	130.0	0.00
15	.	.	.	156.7	118.0	.07
16	.	.	.	167.9	116.0	.05
17	.	.	.	160.6	114.0	0.00
18	.	.	.	158.5	110.0	.04
19	.	.	.	157.0	108.0	.01
20	.	.	.	147.1	104.0	.00
21	.	.	.	141.0	100.0	.00
22	.	.	.	135.3	100.0	0.00
23	.	.	.	129.7	100.0	0.00
24	.	.	.	124.9	95.0	0.00
25	.	.	.	120.4	95.0	0.00
26	.	.	.	117.1	94.0	0.00
27	.	.	.	112.5	92.0	0.00
28	.	.	.	105.8	90.0	0.00
29	.	.	.	103.6	90.0	0.00
1	.	.	.	104.2	90.0	0.00
2	.	.	.	114.6	94.0	0.00
3	.	.	.	99.2	98.0	0.00
4	.	.	.	95.4	98.0	.53
5	.	.	.	103.1	112.0	0.00
6	.	.	.	93.7	116.0	.01
7	.	.	.	129.9	116.0	.26
8	.	.	.	166.3	138.0	.71
9	.	.	.	136.1	181.0	1.53
10	.	.	.	175.5	218.0	.01
11	.	.	.	827.9	357.0	0.00
12	.	.	.	951.7	477.0	0.00
13	.	.	.	856.2	530.0	0.00
14	.	.	.	764.5	535.0	0.00
15	.	.	.	642.5	464.0	0.00
16	.	.	.	538.8	405.0	0.00
17	.	.	.	486.6	352.0	0.00
18	.	.	.	425.0	316.0	.15
19	.	.	.	374.1	320.0	1.21
20	.	.	.	367.1	374.0	.00
21	.	.	.	922.8	446.0	.02
22	.	.	.	890.6	486.0	0.00
23	.	.	.	745.2	477.0	0.00
24	.	.	.	633.8	441.0	0.00
25	.	.	.	546.6	392.0	.00
26	.	.	.	496.0	348.0	0.00
27	.	.	.	446.9	320.0	0.00
28	.	.	.	406.3	296.0	.00
29	.	.	.	371.2	273.0	0.00
30	.	.	.	328.5	248.0	.03
31	.	.	.	302.1	238.0	0.00

Mean Daily Flow Plot (cfs) Illinois River near Tahlequah, Oklahoma, February -
 March, 1964.
 * = simulated
 + = observed

Mean Daily Flow Plot (cfs) Illinois River near Tahlequah, Oklahoma, April - May, 1964. * = simulated
 + = observed

Apr-May	258.0	2580.0	SIMULATED	OBSERVED	PRECIP
1	.	.	280.1	234.0	.01
2	.	.	260.4	224.0	.03
3	.	.	255.9	220.0	.11
4	.	.	242.8	231.0	1.99
5	.	.	209.8	518.0	.42
6	.	.	2309.6	1560.0	0.00
7	.	.	3060.5	2070.0	0.00
8	.	.	1903.8	1600.0	0.00
9	.	.	1374.5	1260.0	0.00
10	.	.	1111.4	1020.0	0.00
11	.	.	964.9	833.0	.04
12	.	.	837.6	710.0	.26
13	.	.	740.6	628.0	.02
14	.	.	641.1	530.0	0.00
15	.	.	568.3	477.0	0.00
16	.	.	518.5	441.0	0.00
17	.	.	488.1	396.0	0.00
18	.	.	445.0	374.0	0.00
19	.	.	399.6	340.0	0.00
20	.	.	361.8	320.0	.15
21	.	.	342.4	336.0	.52
22	.	.	323.6	328.0	0.00
23	.	.	310.5	324.0	.00
24	.	.	337.1	340.0	.16
25	.	.	319.6	328.0	.00
26	.	.	310.7	340.0	.57
27	.	.	308.1	387.0	.00
28	.	.	291.9	364.0	.01
29	.	.	277.7	340.0	0.00
30	.	.	261.0	328.0	0.00
1	.	.	245.0	312.0	.02
2	.	.	232.0	296.0	0.00
3	.	.	220.9	276.0	0.00
4	.	.	212.1	262.0	0.00
5	.	.	207.3	252.0	.01
6	.	.	189.4	238.0	.21
7	.	.	181.9	234.0	.04
8	.	.	167.4	231.0	.55
9	.	.	157.2	220.0	.10
10	.	.	159.7	231.0	1.50
11	.	.	173.3	345.0	.21
12	.	.	1548.0	1800.0	.00
13	.	.	2043.0	2100.0	.00
14	.	.	1277.5	1420.0	0.00
15	.	.	931.5	1080.0	.05
16	.	.	721.0	847.0	0.00
17	.	.	586.8	680.0	0.00
18	.	.	510.8	570.0	0.00
19	.	.	460.4	490.0	0.00
20	.	.	400.9	423.0	.00
21	.	.	343.9	374.0	0.00
22	.	.	303.9	332.0	0.00
23	.	.	273.0	292.0	0.00
24	.	.	247.7	262.0	.00
25	.	.	219.7	245.0	.00
26	.	.	196.0	220.0	0.00
27	.	.	188.1	207.0	.12
28	.	.	178.3	192.0	.00
29	.	.	168.9	186.0	.00
30	.	.	158.6	186.0	.72
31	.	.	152.1	180.0	0.00

Mean Daily Flow Plot (cfs) Illinois River near Tahlequah, Oklahoma, August -
 September, 1967. * = simulated
 + = observed

Aug - Sep	258.0	2560.0	SIMULATED	OBSERVED	PRECIP
1	.	.	47.1	38.0	0.00
2	.	.	43.5	37.0	0.00
3	.	.	41.2	36.0	0.00
4	.	.	39.7	35.0	0.00
5	.	.	38.0	35.0	0.00
6	.	.	37.5	34.0	.01
7	.	.	36.6	33.0	.00
8	.	.	35.1	32.0	.00
9	.	.	33.9	30.0	0.00
10	.	.	33.3	30.0	1.38
11	.	.	32.4	33.0	.01
12	.	.	40.0	32.0	.00
13	.	.	57.2	48.0	0.00
14	.	.	77.2	70.0	1.23
15	.	.	81.8	99.0	.34
16	.	.	79.4	103.0	0.00
17	.	.	101.4	111.0	0.00
18	.	.	123.9	119.0	.00
19	.	.	124.7	121.0	.00
20	.	.	108.8	113.0	0.00
21	.	.	98.2	105.0	.87
22	.	.	95.2	101.0	0.00
23	.	.	85.4	103.0	0.00
24	.	.	128.9	120.0	.00
25	.	.	194.0	188.0	.74
26	.	.	168.7	259.0	1.85
27	.	.	187.4	329.0	0.00
28	.	.	470.9	911.0	1.71
29	.	.	764.4	1230.0	.07
30	.	.	1139.2	1760.0	1.36
1	.	.	1183.6	1520.0	.01
2	.	.	1211.8	1520.0	.03
3	.	.	923.5	1160.0	0.00
4	.	.	694.0	840.0	0.00
5	.	.	564.7	639.0	0.00
6	.	.	497.2	510.0	.03
7	.	.	441.8	428.0	0.00
8	.	.	392.4	360.0	0.00
9	.	.	354.0	316.0	0.00
10	.	.	320.9	273.0	0.00
11	.	.	284.1	242.0	0.00
12	.	.	258.3	217.0	.03
13	.	.	231.1	192.0	0.00
14	.	.	210.3	177.0	0.00
15	.	.	193.7	162.0	0.00
16	.	.	173.9	153.0	.00
17	.	.	149.8	145.0	.09
18	.	.	135.6	142.0	.09
19	.	.	137.6	138.0	.01
20	.	.	143.6	132.0	0.00
21	.	.	149.8	135.0	.54
22	.	.	135.1	162.0	.74
23	.	.	126.7	196.0	.93
24	.	.	323.5	350.0	0.00
25	.	.	944.9	1220.0	0.00
26	.	.	870.3	1060.0	0.00
27	.	.	608.0	700.0	.41
28	.	.	491.1	525.0	.18
29	.	.	411.3	432.0	0.00
30	.	.	395.2	400.0	0.00
1	.	.	408.6	396.0	.00

OCT-NOV	170.7	1707.0	SIMULATED	OBSERVED	PRECIP
1	.	.	204.7	404.0	0.00
2	.	.	196.2	618.0	0.00
3	.	.	188.3	586.0	0.00
4	.	.	180.9	469.0	0.00
5	.	.	173.7	367.0	0.00
6	.	.	166.9	140.0	0.00
7	.	.	160.3	86.0	0.00
8	.	.	154.0	166.0	0.00
9	.	.	147.9	142.0	0.00
10	.	.	142.1	111.0	0.00
11	.	.	136.5	106.0	0.00
12	.	.	134.5	104.0	.34
13	.	.	138.0	101.0	.00
14	.	.	129.3	99.0	0.00
15	.	.	123.1	97.0	0.00
16	.	.	118.1	93.0	0.00
17	.	.	113.4	86.0	0.00
18	.	.	108.9	84.0	0.00
19	.	.	104.6	78.0	0.00
20	.	.	100.5	71.0	0.00
21	.	.	96.6	70.0	0.00
22	.	.	92.7	71.0	0.00
23	.	.	89.1	74.0	0.00
24	.	.	85.6	75.0	0.00
25	.	.	82.2	77.0	0.00
26	.	.	88.8	113.0	.65
27	.	.	99.0	148.0	0.00
28	.	.	88.3	123.0	.01
29	.	.	83.3	110.0	0.00
30	.	.	79.7	102.0	0.00
31	.	.	76.5	97.0	0.00
1	.	.	73.5	92.0	0.00
2	.	.	70.6	89.0	0.00
3	.	.	67.8	86.0	0.00
4	.	.	65.1	84.0	0.00
5	.	.	62.6	83.0	0.00
6	.	.	68.9	95.0	1.06
7	.	.	98.6	124.0	0.00
8	.	.	88.5	154.0	.04
9	.	.	82.1	146.0	0.00
10	.	.	78.1	134.0	0.00
11	.	.	74.8	123.0	0.00
12	.	.	71.8	117.0	.01
13	.	.	69.1	111.0	0.00
14	.	.	66.4	108.0	.00
15	.	.	63.7	104.0	.04
16	.	.	63.0	99.0	.10
17	.	.	70.3	108.0	.57
18	.	.	86.2	121.0	.72
19	.	.	139.3	299.0	.94
20	.	.	189.5	500.0	.00
21	.	.	171.2	534.0	0.00
22	.	.	161.0	534.0	0.00
23	.	.	153.5	500.0	0.00
24	.	.	146.8	469.0	0.00
25	.	.	140.6	439.0	0.00
26	.	.	134.9	409.0	0.00
27	.	.	129.5	367.0	.01
28	.	.	124.8	294.0	.02
29	.	.	120.1	223.0	0.00
30	.	.	114.8	193.0	0.00

Mean Daily Flow Plots (cfs) Illinois River near Watts, Oklahoma, October -
 November, 1964. * = simulated
 + = observed

Mean Daily Flow Plots (cfs) Illinois River near Watts, Oklahoma, December, 1963 -
 January, 1974. * = simulated
 + = observed

DEC-JAN	170.7	1707.0	SIMULATED	OBSERVED	PRECIP
1	.	.	110.2	177.0	0.00
2	.	.	105.9	169.0	0.00
3	.	.	102.3	162.0	.08
4	.	.	99.4	156.0	.01
5	.	.	94.3	148.0	0.00
6	.	.	90.3	144.0	0.00
7	.	.	86.6	134.0	0.00
8	.	.	83.2	130.0	0.00
9	.	.	79.9	142.0	.03
10	.	.	87.6	142.0	.41
11	.	.	100.5	142.0	.02
12	.	.	94.8	136.0	0.00
13	.	.	90.2	130.0	0.00
14	.	.	86.5	117.0	0.00
15	.	.	83.0	110.0	0.00
16	.	.	79.7	108.0	0.00
17	.	.	76.5	104.0	0.00
18	.	.	73.5	102.0	0.00
19	.	.	70.7	97.0	.01
20	.	.	68.0	89.0	0.00
21	.	.	65.2	89.0	0.00
22	.	.	62.6	89.0	0.00
23	.	.	60.1	89.0	0.00
24	.	.	57.8	91.0	.00
25	.	.	56.3	91.0	.06
26	.	.	54.4	89.0	.00
27	.	.	51.3	84.0	0.00
28	.	.	49.2	80.0	0.00
29	.	.	47.3	80.0	.00
30	.	.	45.4	78.0	0.00
31	.	.	46.0	80.0	.31
1	.	.	55.4	87.0	.42
2	.	.	98.7	324.0	.58
3	.	.	152.5	517.0	0.00
4	.	.	144.0	606.0	0.00
5	.	.	136.2	644.0	0.00
6	.	.	129.9	685.0	.00
7	.	.	124.4	644.0	.00
8	.	.	122.4	586.0	.43
9	.	.	154.4	517.0	.32
10	.	.	186.4	469.0	0.00
11	.	.	198.4	439.0	0.00
12	.	.	188.8	424.0	.01
13	.	.	180.1	409.0	0.00
14	.	.	172.3	409.0	0.00
15	.	.	165.2	394.0	.00
16	.	.	158.5	380.0	.00
17	.	.	152.1	354.0	0.00
18	.	.	146.0	308.0	0.00
19	.	.	140.3	251.0	0.00
20	.	.	134.7	210.0	0.00
21	.	.	129.5	197.0	.15
22	.	.	151.0	195.0	.57
23	.	.	225.7	265.0	.06
24	.	.	235.9	337.0	0.00
25	.	.	229.4	354.0	0.00
26	.	.	218.5	337.0	0.00
27	.	.	208.6	316.0	0.00
28	.	.	199.8	294.0	0.00
29	.	.	191.6	258.0	0.00
30	.	.	183.9	228.0	0.00
31	.	.	176.5	208.0	0.00

Mean Daily Flow Plots (cfs) Illinois River near Watts, Oklahoma, February - March, 1964.
 * = simulated
 + = observed

FEB-MAR	170.7	1707.0	SIMULATED	OBSERVED	PRECIP.
1	.	.	169.5	147.0	0.00
2	+	.	162.8	30.0	0.00
3	+	.	156.4	31.0	0.00
4	+	.	150.2	32.0	0.00
5	+	.	144.3	33.0	.00
6	+	.	139.7	34.0	.09
7	+	.	137.5	34.0	.08
8	+	.	142.6	35.0	.30
9	+	.	260.1	39.0	.96
10	.	.	469.5	1180.0	0.00
11	.	.	419.0	940.0	.04
12	.	.	383.1	748.0	0.00
13	.	.	358.1	606.0	0.00
14	.	.	337.4	517.0	0.00
15	.	.	319.8	454.0	0.00
16	.	.	304.3	394.0	0.00
17	.	.	290.3	367.0	0.00
18	.	.	277.3	337.0	0.00
19	.	.	265.2	313.0	0.00
20	.	.	253.9	299.0	0.00
21	.	.	243.3	272.0	.00
22	.	.	233.2	275.0	0.00
23	.	.	231.4	234.0	.87
24	.	.	638.9	260.0	.04
25	.	.	646.4	394.0	.04
26	.	.	498.9	367.0	0.00
27	.	.	449.6	517.0	0.00
28	.	.	413.0	625.0	.26
1	.	.	647.5	1110.0	.54
2	.	.	875.5	1780.0	.02
3	.	.	704.6	1300.0	.00
4	.	.	620.1	940.0	.05
5	.	.	572.3	794.0	.04
6	.	.	549.7	685.0	0.00
7	.	.	513.3	625.0	.01
8	.	.	481.0	550.0	0.00
9	.	.	452.9	484.0	0.00
10	.	.	428.5	469.0	.02
11	.	.	411.9	439.0	.35
12	.	.	529.4	424.0	.01
13	.	.	538.6	424.0	.00
14	.	.	487.1	424.0	0.00
15	.	.	455.6	366.0	0.00
16	.	.	430.6	234.0	0.00
17	.	.	409.0	284.0	.00
18	.	.	389.8	301.0	0.00
19	.	.	372.3	289.0	0.00
20	.	.	356.2	277.0	0.00
21	.	.	341.3	272.0	0.00
22	.	.	327.2	260.0	0.00
23	.	.	313.7	232.0	0.00
24	.	.	301.7	234.0	.17
25	.	.	324.4	239.0	.25
26	.	.	388.5	246.0	.05
27	.	.	366.7	260.0	0.00
28	.	.	345.0	291.0	.01
29	.	.	326.7	291.0	.03
30	.	.	311.0	287.0	0.00
31	.	.	296.2	275.0	0.00

Mean Daily Flow Plots (cfs) Illinois River near Watts, Oklahoma, April - May, 1964.
 * = simulated
 + = observed

APR-MAY	170.7	1707.0	SIMULATED	OBSERVED	PRECIP	
1	.	.	.	283.0	260.0	0.00
2	.	.	.	711.8	352.0	1.74
3	.	.	.	4486.0	5000.0	.53
4	.	.	.	3017.5	3000.0	.07
5	.	.	.	2387.0	3500.0	1.42
6	.	.	.	5311.8	6950.0	.00
7	.	.	.	3494.3	3530.0	.06
8	.	.	.	2919.3	2620.0	.49
9	.	.	.	2723.1	2470.0	.01
10	.	.	.	2097.1	1710.0	.07
11	.	.	.	1750.8	1420.0	.13
12	.	.	.	1493.9	1240.0	0.00
13	.	.	.	1288.7	1020.0	.22
14	.	.	.	1257.6	915.0	1.14
15	.	.	.	2470.9	2660.0	.28
16	.	.	.	2296.6	2020.0	0.00
17	.	.	.	1722.7	1330.0	0.00
18	.	.	.	1462.5	1070.0	0.00
19	.	.	.	1281.5	915.0	0.00
20	.	.	.	1140.1	794.0	0.00
21	.	.	.	1026.2	727.0	0.00
22	.	.	.	932.8	498.0	0.00
23	.	.	.	855.1	550.0	0.00
24	.	.	.	789.7	517.0	.09
25	.	.	.	736.9	484.0	.09
26	.	.	.	688.6	500.0	.12
27	.	.	.	646.3	469.0	0.00
28	.	.	.	606.9	439.0	.00
29	.	.	.	573.3	409.0	0.00
30	.	.	.	543.5	380.0	0.00
1	.	.	.	516.5	367.0	0.00
2	.	.	.	491.8	354.0	0.00
3	.	.	.	469.0	329.0	0.00
4	.	.	.	447.9	277.0	0.00
5	.	.	.	428.2	260.0	.02
6	.	.	.	410.9	282.0	.11
7	.	.	.	394.8	277.0	0.00
8	.	.	.	376.4	279.0	.45
9	.	.	.	406.4	367.0	1.41
10	.	.	.	633.3	898.0	.04
11	.	.	.	686.3	816.0	.00
12	.	.	.	629.8	606.0	0.00
13	.	.	.	586.5	500.0	0.00
14	.	.	.	571.5	586.0	.37
15	.	.	.	580.6	360.0	.06
16	.	.	.	556.4	223.0	.11
17	.	.	.	530.0	294.0	0.00
18	.	.	.	505.3	270.0	.41
19	.	.	.	511.4	294.0	.01
20	.	.	.	518.5	299.0	.02
21	.	.	.	494.5	277.0	0.00
22	.	.	.	471.5	246.0	0.00
23	.	.	.	451.4	226.0	0.00
24	.	.	.	433.1	230.0	.03
25	.	.	.	416.3	186.0	.02
26	.	.	.	426.4	232.0	1.06
27	.	.	.	508.8	255.0	0.00
28	.	.	.	487.9	253.0	.08
29	.	.	.	459.6	228.0	0.00
30	.	.	.	435.8	204.0	0.00
31	.	.	.	416.4	193.0	.02

JUN-JUL	170.7	1707.0	SIMULATED	OBSERVED	PRECIP
1	.	.	399.4	182.0	.00
2	.	.	382.7	169.0	.01
3	.	.	367.1	160.0	0.00
4	.	.	352.2	164.0	.00
5	.	.	338.2	158.0	.01
6	.	.	324.8	148.0	0.00
7	.	.	311.9	146.0	.03
8	.	.	311.1	146.0	.67
9	.	.	336.1	146.0	0.00
10	.	.	323.6	150.0	.49
11	.	.	332.5	205.0	.13
12	.	.	327.3	154.0	.43
13	.	.	334.4	290.0	.41
14	.	.	352.5	240.0	.40
15	.	.	347.3	898.0	.27
16	.	.	352.5	606.0	.00
17	.	.	335.8	367.0	0.00
18	.	.	320.4	313.0	0.00
19	.	.	306.8	253.0	0.00
20	.	.	294.3	228.0	0.00
21	.	.	296.4	204.0	.68
22	.	.	310.4	186.0	.52
23	.	.	325.7	204.0	.20
24	.	.	331.5	728.0	.29
25	.	.	336.1	706.0	.00
26	.	.	318.8	409.0	.00
27	.	.	304.2	282.0	0.00
28	.	.	291.3	275.0	0.00
29	.	.	279.4	251.0	0.00
30	.	.	268.3	199.0	0.00
1	.	.	257.6	182.0	0.00
2	.	.	247.4	177.0	0.00
3	.	.	237.7	156.0	0.00
4	.	.	228.8	154.0	.07
5	.	.	220.8	144.0	0.00
6	.	.	210.9	136.0	.08
7	.	.	204.9	128.0	.26
8	.	.	200.1	128.0	0.00
9	.	.	192.7	140.0	.12
10	.	.	183.3	140.0	0.00
11	.	.	174.6	130.0	.00
12	.	.	167.8	111.0	.10
13	.	.	162.5	106.0	0.00
14	.	.	156.2	97.0	.34
15	.	.	158.5	97.0	0.00
16	.	.	147.8	95.0	0.00
17	.	.	140.6	89.0	0.00
18	.	.	134.9	87.0	.13
19	.	.	131.8	86.0	.05
20	.	.	128.2	99.0	.00
21	.	.	120.7	108.0	.00
22	.	.	115.7	102.0	.01
23	.	.	111.2	95.0	0.00
24	.	.	106.6	87.0	0.00
25	.	.	104.2	101.0	.74
26	.	.	120.7	111.0	0.00
27	.	.	109.6	99.0	.21
28	.	.	109.5	130.0	.30
29	.	.	109.4	148.0	0.00
30	.	.	99.2	126.0	0.00
31	.	.	94.6	115.0	0.00

Mean Daily Flow Plots (cfs) Illinois River near Watts, Oklahoma, June - July, 1964. * = simulated + = observed

Mean Daily Flow Plots (cfs) Illinois River near Watts, Oklahoma, August -
 September, 1964. * = simulated
 + = observed

AUG-SEP	170.7	1707.0	SIMULATED	OBSERVED	PRECIP.
1	.	.	90.7	104.0	0.00
2	.	.	87.1	92.0	0.00
3	.	.	83.7	83.0	0.00
4	.	.	80.4	81.0	0.00
5	.	.	77.2	78.0	0.00
6	.	.	74.2	74.0	0.00
7	.	.	72.3	68.0	.08
8	.	.	72.2	73.0	.22
9	.	.	69.4	68.0	0.00
10	.	.	65.1	62.0	0.00
11	.	.	60.8	59.0	0.00
12	.	.	58.3	58.0	0.00
13	.	.	56.0	56.0	0.00
14	.	.	53.8	58.0	0.00
15	.	.	51.8	60.0	.37
16	.	.	57.7	62.0	.46
17	.	.	67.0	63.0	0.00
18	.	.	56.0	68.0	.00
19	.	.	50.4	67.0	.00
20	.	.	48.9	70.0	.08
21	.	.	49.2	77.0	.12
22	.	.	46.9	81.0	.02
23	.	.	48.7	77.0	.35
24	.	.	48.8	77.0	.01
25	.	.	41.8	68.0	0.00
26	.	.	39.5	63.0	0.00
27	.	.	41.2	96.0	1.59
28	.	.	81.4	1090.0	0.00
29	.	.	64.6	370.0	0.00
30	.	.	51.5	223.0	0.00
31	.	.	70.8	456.0	2.39
1	.	.	142.5	1080.0	0.00
2	.	.	134.5	620.0	0.00
3	.	.	118.7	394.0	0.00
4	.	.	112.5	308.0	.01
5	.	.	108.0	253.0	.06
6	.	.	105.1	226.0	.05
7	.	.	100.6	195.0	0.00
8	.	.	95.4	171.0	0.00
9	.	.	91.5	158.0	0.00
10	.	.	87.8	142.0	0.00
11	.	.	84.4	115.0	0.00
12	.	.	81.1	119.0	0.00
13	.	.	77.9	121.0	.00
14	.	.	75.8	113.0	.15
15	.	.	75.2	111.0	.04
16	.	.	71.0	121.0	.03
17	.	.	67.1	91.0	0.00
18	.	.	64.1	86.0	0.00
19	.	.	61.3	86.0	.22
20	.	.	63.1	92.0	0.00
21	.	.	69.3	83.0	1.32
22	.	.	110.3	130.0	.69
23	.	.	121.2	173.0	0.00
24	.	.	102.9	162.0	0.00
25	.	.	96.9	146.0	0.00
26	.	.	92.8	130.0	.00
27	.	.	89.0	126.0	0.00
28	.	.	85.4	123.0	0.00
29	.	.	82.0	124.0	0.00
30	.	.	78.9	111.0	.01

2
VITA

Ronald Creighton Martin

Candidate for the Degree of

Master of Science

Thesis: LOW FLOW SIMULATION OF THE ILLINOIS RIVER USING A CONCEPTUAL HYDROLOGIC MODEL

Major Field: Bioenvironmental Engineering

Biographical:

Personal Data: Born on December 3, 1940, in Huntington, West Virginia, son of W. Marshall Martin and Helyne E. Martin.

Education: Graduated from Zanesville High School, Zanesville, Ohio, in June, 1958; received the Bachelor of Arts degree from Ohio State University, Columbus, Ohio, in August, 1964; attended Texas A & M University from January, 1965, to January, 1966; completed requirements for Bachelor of Science degree in Meteorology except for a three-hour course in Texas history; completed requirements for Master of Science degree in Bioenvironmental Engineering at Oklahoma State University, Stillwater, Oklahoma, in May, 1975.

Professional Experience: Weather Officer, U. S. Air Force, 1965-1969; air pollution research meteorologist for GCA Corporation, 1969-1970; meteorologist for National Weather Service, 1970-1971; hydrologist for National Weather Service, 1971-1975.

Membership in Honorary Societies: Chi Epsilon.